CHARACTERIZING THE ROLE OF MITOCHONDRIA IN THE TOXICITY OF TRICHOTHECENES PRODUCED BY *FUSARIUM GRAMINEARUM*

by

MOHAMED ANWAR BIN UMER

A Dissertation submitted to the

Graduate School-New Brunswick

Rutgers, The State University of New Jersey

and

The Graduate School of Biomedical Sciences

University of Medicine and Dentistry of New Jersey

in partial fulfillment of the requirements

for the degree of

Doctor of Philosophy

Graduate Program in Microbiology and Molecular Genetics

written under the direction of

Nilgun E. Tumer, Ph.D.

and approved by

_____

_____

_____

_____

New Brunswick, New Jersey

January, 2014

ABSTRACT OF THE DISSERTATION

CHARACTERIZING THE ROLE OF MITOCHONDRIA IN THE TOXICITY OF TRICHOTHECENES PRODUCED BY *FUSARIUM GRAMINEARUM*

by

MOHAMED ANWAR BIN UMER

Dissertation Director:

Nilgun E. Tumer, Ph.D.

Fusarium graminearum is a toxigenic fungal pathogen infecting economically significant cereal crops. Trichothecenes are a large family of low molecular weight sesquiterpenoid mycotoxins synthesized by *F. graminearum* and other fungi and are among the most toxic compounds known to man. These mycotoxins and their producers are encountered worldwide in the environment as natural contaminants of cereal grains presenting a high food safety risk for humans and cattle and threaten the global food supply. Trichothecene mycotoxicosis was primarily associated with their inhibitory effects on translation. However, these highly stable toxins also inhibit other cellular processes which contribute to their toxicity. In this work, using yeast as a model organism, a genome wide approach

has been applied to obtain a comprehensive understanding of the molecular mechanism of the type A and B trichothecene toxicity. Due to their prevalence and impact, T-2 toxin and diacetoxyscirpenol (DAS) are used as representative type A toxins while trichothecin (Tcin) and deoxynivalenol (DON) are used as representative type B toxins. The yeast knockout collection of nonessential genes was initially used to identify mutant strains that exhibited increased resistance or susceptibility to trichothecenes. This screening led to identification of the role of mitochondria during trichothecene toxicity. The largest group of mutants exhibiting resistance was affected in their mitochondrial functions. Mitochondrial translation was directly inhibited, independent of total translation, and the trichothecene-treated cells exhibited severe fragmentation of mitochondrial membrane. Furthermore, actively respiring cells with functional mitochondria were essential for trichothecene cytotoxicity suggesting a critical role for mitochondria. A large fraction of the highly susceptible strains exhibited very high levels of reactive oxygen species (ROS) upon trichothecene treatment. Antioxidants increased cell survival and reduced mitochondrial membrane damage in trichothecene-treated cells. The direct role for ROS in mediating trichothecene cytotoxicity was confirmed when two novel Arabidopsis nonspecific lipid transfer proteins that mediated resistance to trichothecenes in *A. thaliana* exhibited antioxidant property and rescued trichothecene-treated yeast cells. Rapamycin-induced mitophagy reduced ROS levels and increased survival in trichothecene-treated cells suggesting mitophagy as a novel prosurvival cellular mechanism during oxidative stress in trichothecene-treated cells.

ACKNOWLEDGEMENTS

"He who does not thank people is ungrateful to God" is a saying attributed to the blessed Prophet in Islamic tradition. I express my utmost praise to my Lord, the Most Merciful to whom I attribute every success in my life. I am also grateful to Him for blessing my life with the many people to whom I am indebted during my years as a doctoral student. First and foremost, I would like to express my sincere gratitude to my thesis advisor, Dr. Nilgun Tumer, for accepting me as a member of her lab. Her work ethics and her tireless pursuit of investigating novel and complex scientific ideas have truly inspired me. I am truly grateful that she granted me enough freedom to explore different research ideas and encouraged me to publish and present my findings at national and international scientific meetings. I shall never forget her support and mentorship throughout my studies. I am also grateful to Dr. John McLaughlin who mentored me during my initial days in the Tumer lab and my time spent under his mentorship piqued my interests in learning about trichothecene toxicity and the larger problems associated with these toxins. I shall not forget the time we spent discussing various topics and our travel to the different meetings. His conduct and character is awe-inspiring and I am grateful to him for his support as a mentor and a friend. I would also like to acknowledge Dr. Susan McCormick from USDA who generously supplied the lab with the different trichothecenes without which such a large undertaking would not have been logistically possible. I am also grateful to the current and former senior members of the Tumer lab including Dr. Xiaoping Li, Dr. Rong Di, Dr. Kerrie May, Dr. Mike Pierce and Dr. Przemek Grela. I will truly miss the intriguing conversations about mystery novels and politics during coffee breaks with Dr. Jennifer Kahn. Time spent in the Tumer lab was truly momentous

and fun and it wouldn't have been possible without Debaleena, Matthew, Qing, Maria, Jiachi, Natasha, and Yijun. They are a truly wonderful group of friends and colleagues from whom I have benefited immensely. I would also like to acknowledge the support of the administrators particularly Karen Yudin, Diane Murano, and Carolyn Ambrose for being patient, supportive and accessible.

I am truly grateful and blessed for being part of the wider Muslim community in NJ particularly the Muslim American Society whose members have become very dear to me over the years. Their companionship and embrace never made me miss home or my family during my studies. I owe a lot to them for my personal and spiritual development into a God conscious citizen of the society. Over the years I have met some amazing people and have shared some special moments that I shall cherish for the rest of my life.

Finally, I owe every moment of success in my life to my parents and siblings who have been always there for me. Thank you for your love and support and I couldn't have done it without you. I once again express my gratitude to my Lord for blessing my life with all these wonderful people and for bestowing your mercy during my studies.

DEDICATION

To my loving parents K. Ummer and Jameela Umer and my many teachers.

TABLE OF CONTENTS

LIST OF TABLES

LIST OF FIGURES

CHAPTER 1.

INTRODUCTION

1.1 A moldy history of sacrificial rituals, witchcraft and wars

Man's dueling encounter with molds predates biblical times when the ancient Romans established the festival of "Robigalia" which was celebrated on the 25th day of April, a time most likely for crops to be attacked by rust, mildew or other phytopathogenic fungi (Peraica et al., 1999). During the festival Robigus, who the Romans believed to be the protector of grains and trees, was honored with a procession through the city and ended with a sacrifice to pacify their deity and protect their crops. Today the Venetians celebrate it as St. Mark's Day (Peraica et al., 1999). The earliest recorded instance of mold poisoning (mycotoxicosis) dates back to 600 B.C. based on descriptions found on an Assyrian cuneiform tablet which read "noxious pustule in the ear of grain" and we now know that this mycotoxicosis was caused by the ergot mold which also caused St. Anthony's Fire (van Dongen and de Groot, 1995). Interestingly those accused of bewitchment during the Salem witch trials of 1692 in Massachusetts, when scores of people were hung or condemned, were all reported to show convulsive and psychological symptoms that resemble those afflicted with ergot poisoning (ergotism) (Caporael, 1976).

While Europe in the Middle Ages was frequented by large-scale epidemics of different mycotoxicoses, mostly from eating mold-contaminated food, post Renaissance era they were largely replaced by famine and war-related mycotoxicoses. The earliest such documented instance was during the spring months post World War II in USSR which saw the outbreak of a hemorrhagic disease resulting from consumption of bread prepared from grains that remained in the field until the snow thawed. Later this outbreak

was found to be a case of mycotoxicosis caused by a group of mycotoxins called trichothecenes which are produced by Fusarium molds and the disease was alimentary toxic aleukia (ATA) (Gajdusek, 1953). Other cases of mycotoxicoses were also reported in Eastern India during which 65,000 Japanese soldiers and millions of civilians were poisoned after consumption of food made from moldy grains (Tainsh, 1981).

Although not war-related the first outbreak associated with trichothecene mycotoxicoses was recorded in East Siberia in 1913 and later in Western Siberia in 1942 during which more than 10% of the population was affected and had a 60% mortality rate (Gajdusek, 1953). In several of these instances trichothecene mycotoxioses was caused by a single ingestion of bread made from moldy grains (Wang et al., 1993). Hence due to its high toxicity and potential as a weapon of mass destruction (WMD) some reports have identified the alleged use of trichothecenes as a chemical warfare agent because of the unusually high amount of trichothecenes found in samples collected after the "yellow rain" attack on the Hmong people in South-East Asia during the Cold War (Mirocha et al., 1983). In present times we can only speculate whether particular disease outbreaks of the past were caused by mycotoxins since we mostly rely on descriptions of symptoms. While lack of proper control of grain storage and food production have been attributed to most of these mycotoxicoses, despite current advances in the field of food safety and control, mycotoxins continue to contaminate cereal grains to this day and pose a major threat to humans, cattle and plants and also resulting in severe economic loses.

1.2 Trichothecenes: A highly toxic group of mycotoxins

Mycotoxins are secondary metabolites, which, unlike primary metabolites, are largely considered nonessential for the growth and development of fungi (Bu'Lock, 1980). They are synthesized largely by enzymes with low specificity, which however allows for relative plasticity in their regulation resulting in chemically diverse compounds (Betina, 1989). While a variety of these fungal metabolites were originally discovered as antibiotics and later characterized as mycotoxins others were initially identified as mycotoxins and their antimicrobial and antiviral properties were found later (Betina, 1983). The toxic effects of mycotoxins are manifold which can be acute, chronic or both, depending on the dose and length of exposure, and have been characterized to be carcinogenic, mutagenic, teratogenic, immunosuppressive, antimicrobial, insecticidal and phytotoxic (Betina, 1989).

Trichothecenes are among the most toxic compounds known to man, posing a threat to humans and animals (Grovey, 2007). Many of them are also associated with devastating plant diseases such as Fusarium Head Blight (FHB) in which they are a major determinant of fungal spread and disease development and severity (Langevin et al., 2004).They are a unique class of mycotoxins because they are produced by a number of genera of taxonomically unrelated fungi such as *Fusarium*, *Trichoderma*, *Trichothecium*, *Cephalosporium*, *Stachybotrys* and *Verticimonosporium* (Ueno, 1983). They exhibit a wide spectrum of biological activity (antibacterial, antifungal, antiviral and insecticidal) and are characterized by their 12, 13-epoxy-trichothec-9-ene structure (also known as trichothecane) after which they are named (Fig. 1.1) (Ueno, 1983).

The first compound in this group to be isolated was trichothecin (Tcin) from *Trichothecium roseum* in 1949 by Freeman et al. (Freeman and Morrison, 1948). Although several mold poisonings in the past have been attributed to trichothecenes including the red mold poisoning in Japan and ATA in the former USSR (Ueno, 1983) it was, however, not until 1971 their role as etiological agents in mycotoxicoses was demonstrated when T-2 toxin, a trichothecene, was identified in moldy corn that killed dairy cows (Ichinoe and Kurata, 1983). Since then trichothecenes have been identified as the causative agent of several deadly diseases. Furthermore, since trichothecene-producing fungi are common and widespread in nature they have also significantly contributed to food and feed contamination and pose grave risks to human health and security. For instance, one epidemiological survey pointed to high incidence of esophageal cancer in South Africa associated with high levels of trichothecenes in the locally produced corn which was the staple diet in the surveyed region (Ueno, 1983). In light of these and other findings trichothecenes have since become the focus of much interest in several investigations and the FDA has established several rigid regulatory policies for food and feeds that may contain trichothecenes (Murphy et al., 2006).

1.3 *Fusarium spp.* – Phytopathogenic and toxigenic trichothecene-producers with the highest impact on health, environment and economy

Trichothecene producers particularly *Fusarium spp*. are encountered all over the world as a natural contaminant and associated with different diseases affecting

economically significant plants that are as diverse as maize, wheat, bananas and tomatoes (Summerell and Leslie, 2011). Thus *Fusarium spp.* are the most significant producers of trichothecenes which also contribute to the increased presence of these mycotoxins in the food supply. One of the first *Fusarium* members to be isolated was *Fusarium sporotrichioides* which produces the trichothecene T-2 toxin, in 1971 in Wisconsin, from moldy corn which caused death of dairy cows (Ichinoe and Kurata, 1983). *F. graminearum,* which produces the trichothecene deoxynivalenol (DON) was first found in infected barley, in 1972 in Japan, while investigating red mold poisoning in humans and animals and later in the U.S, in 1973 in Ohio, in infected corn (Ichinoe and Kurata, 1983). Soon after *Fusarium* producers of other trichothecenes such as diacteoxyscirpenol (DAS) and nivalenol (NIV) were also found. DAS was in fact the first *Fusarium* trichothecene to be isolated (Ueno, 1983).

1.4 *F. graminearum* and FHB: A serious threat to the world's breadbasket

Plant diseases caused by Fusarium species are not restricted to a particular region or to one climate and symptoms include vascular wilts (wilting due to blocking of water flow from obstruction of vascular bundles by the pathogen), head and seed blights (sudden chlorosis and necrosis of plant tissues), stem rot, and root and crown rots with some species causing multiple or overlapping diseases (Foroud and Eudes, 2009). Many of these diseases affect largely cereal crops resulting in yield loss, stunted growth and accumulation of trichothecenes in cereal grains rendering them unsuitable for

consumption. Of the different plant diseases, Fusarium Head Blight (FHB) is one of the most destructive cereal crop diseases impacting worldwide food supply and causing significant economic losses. FHB outbreak was first documented in England in 1884 and has since been reported in increasing numbers across the world with the outbreak in the U.S. during the late 1990s alone costing nearly 3 billion dollars (Summerell and Leslie, 2011). Diseased spikelets exhibit bleaching which progresses throughout with pathogen spread (Fig. 1.2). Necrotic lesions appear in the advanced stages of infection with the grain appearing shriveled and discolored (Goswami and Kistler, 2004). FHB is caused by different Fusarium species particularly *F. graminearum* which is also the most relevant economically. In fact the most abundant source of trichothecene contamination is FHB, which is often (but not necessarily) recognized by the shriveled and discolored appearance of infected grains (Goswami and Kistler, 2004). As a result of the global reemergence of FHB in the last decade *F. graminearum* has become one of the most studied fungal plant pathogens.

F. graminearum feeds on plant debris as a saprophytic mycelia which during the warm moist spring weather develops and matures producing ascospores that are forcibly discharged and dispersed by natural factors (wind, insect or rain) to the host plant (Goswami and Kistler, 2004) . Following deposition of the spores on the spikelets the infection process is initiated and the fungal hyphae, rather than penetrate directly through the epidermis, develops and grows towards susceptible sites within the inflorescence. It then spreads from one spikelet to another through the vascular bundles leading to their partial dysfunction and premature death of the spikelet (Bushnell et al., 2003). Thus the

brief biotrophic relationship of the fungus with the host (marked by minimal colonization) soon switches to a necrotrophic one which is characterized by significant increases in colonization leading to death of the host plant (Goswami and Kistler, 2004).

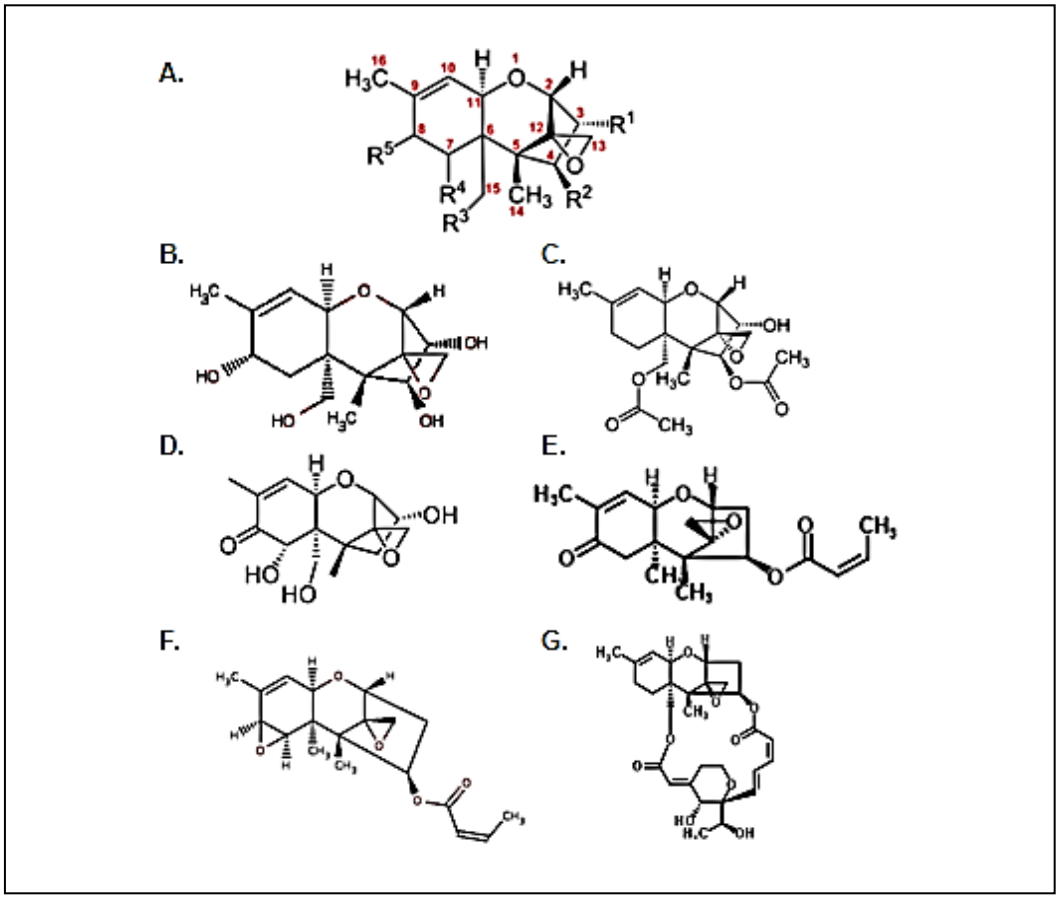

Figure 1.1. Structural classification of trichothecenes. The basic trichothecene structure containing the 12, 13-epoxy-trichotec-9-ene structure is shown (A). Type A T-2 toxin (B), DAS (C), type B DON (D), Tcin (E), the type C crotocin (F) and the type D satratoxin H (G) are also shown as representative trichothecenes from each group. Image credits: Modified using images deposited in Wikimedia (http://commons.wikimedia.org)

Figure 1.2. Inflorescence from uninfected and FHB wheat. The left panel shows the image of healthy wheat while the right panel is the image of Fusarium-infected wheat inflorescence with spikelets showing the dark purplish necrotic lesions (scab) and tissue bleaching (blight) that are characteristic symptoms of FHB. Image credits: Jacki Morrison, USDA ARS Cereal Disease Laboratory (Goswami and Kistler, 2004).

Some trichothecenes also contribute to the fungal spread by inhibiting callose deposition and cell wall thickening which form a barrier of defense raised by the host against the fungal pathogen (Merhej et al., 2011). While trichothecenes serve as virulence factors and contribute to the aggressiveness of the pathogen, environmental factors such as low temperature and high moisture, also significantly increase fungal proliferation on grains during storage (Peraica et al., 1999). FHB can destroy a potentially high-yielding crop within a few weeks of harvest and disease symptoms, for instance in wheat, include dark necrotic lesions on the exterior surface of florets (referred to as scab) and bleaching of tissues of the inflorescence (referred to as blight). However, symptoms are not always

readily apparent and appearances may differ from one host plant to another. The threat posed by F. graminearum is therefore manifold because it causes significant losses in yield and quality which in turn makes it logistically and financially prohibitive for processing these grains. Furthermore, FHB outbreaks also lead to trichothecene-contaminated cereal grains. Consumption of food produced from Fusarium-infected cereal crops or trichothecene-contaminated grains leads to different mycotoxicoses resulting in ATA, vomiting, diarrhea, emesis, immunosuppression and opportunistic infections, and retarded growth (Ueno, 1983). For instance, in the late 1990s 1700 children were hospitalized in the U.S. with vomiting, nausea, headache & abdominal cramps from eating burritos made from trichothecene-contaminated grains (Sherif et al., 2009).

Recently different FHB-management strategies, targeting inoculum source, host susceptibility and favorable environmental conditions, have been employed to minimize financial loss and health risks associated with this disease. These include (i) better agronomic practices like crop-rotation that reduces the amount of contaminated crop debris, (ii) use of FHB-resistant cultivars, and (iii) scheduled spraying for effective chemical control. The latter has resulted in the most progress towards FHB control since neither environmental factors or the aggressiveness of the Fusarium strain seem to impact disease outcomes, underlying the importance of developing resistant cultivars (Foroud and Eudes, 2009).

1.5 Biosynthesis of Fusarium trichothecenes

Due to their significance and detrimental impact much focus has been put on how *Fusarium spp.* synthesize trichothecenes. As a result the biosynthetic pathway of trichothecene has been well characterized. The pathway involves species-specific sequence of chemical modifications leading to different types of trichothecenes. The enzymes and regulators of this pathway are encoded by 15 trichothecene biosynthetic genes (Tri) clustered at three different loci on different chromosomes: (i) a 12-gene core Tri cluster, (ii) a 2-gene Tri1-Tri6 cluster, and (iii) the Tri101 locus. Two of these genes have been attributed to self-defense mechanisms with the Tri12 product mediating the specific extrusion of trichothecenes and the Tri101-encoded 3α-acetyltransferase esterifying the trichothecenes and significantly diminishing their toxicity (Grovey, 2007). Briefly the trichothecene biosynthetic pathway begins with the steroid biosynthesis pathway intermediate, farnesyl pyrophosphate (FPP), undergoing a cyclization step catalyzed by the Tri5 gene product, trichodiene synthase, to form the first intermediate called trichodiene. Following a series of nine reactions catalyzed by different enzymes encoded by the Tri genes, calonectrin, which contains the basic trichothecane skeleton, is formed. The reaction then proceeds with further biochemical modifications catalyzed by species-specific enzymes, encoded by Tri genes, leading to the formation of different trichothecenes such as T-2 toxin, NIV and DON (Merhej et al., 2011).

1.6 Structural classification of trichothecenes

Since Tcin was isolated from *T. roseum* from bitter tasting apples more than two hundred trichothecenes have been isolated (Ueno, 1983). Structurally they all contain a sesquiterpenoid skeleton containing two features crucial for their toxicity, namely a double bond at C-9,10 and the epoxide ring at C-12,13 position (Grovey, 2007). Broadly they can be classified into macrocyclic and simple trichothecenes with the latter making up over 60% of all naturally occurring trichothecenes (Grovey, 2007; McCormick et al., 2011). Simple trichothecenes can be further divided based on the functional group at C8 position with type A containing a non-ketone group (hydroxyl, ester or no oxygen substitution), type B containing a ketone group and type C containing a C7-C8 epoxide ring (Fig. 1.1). Examples of simple trichothecenes include the type A T-2 toxin and diacetoxyscirpenol (DAS), the type B trichothecin (Tcin), deoxynivalenol (DON), and nivalenol (NIV) and the type C crotocin and baccharin. The macrocyclic trichothecenes are characterized by an additional ring linking C-4 and C-15 positions and include satratoxin H and roridin A. In addition some structural features of trichothecenes are producer-specific (McCormick et al., 2011). Hence all trichothecenes produced by *Fusarium spp.* have a hydroxyl or acetyl group at C3 position and the type B *Fusarium* trichothecenes, in addition, have a hydroxyl group at C7 position (Table 1.1).

These differences in structural features also contribute to their toxicity with increasing oxygenation of the trichothecane skeleton rendering them more cytotoxic (Grovey, 2007; McCormick et al., 2011). While the degree of toxicity does not correlate with the above mentioned structural classification, however, in general macrocyclic

trichothecenes are more toxic than simple trichothecenes and within the latter group members of type A are often more toxic than type B, with type C showing the lowest toxicity (McCormick et al., 2011).

Trichothecenes		**R1**	**R2**	**R3**	**R4**	**R5**
HT-2		OH	OH	OAc	H	$OCOCH_2CH(CH_3)_2$
T-2		OH	OAc	OAc	H	$OCOCH_2CH(CH_3)_2$
Diacetoxyscirpenol (DAS)		OH	OAc	OAc	H	H
Trichothecin (Tcin)		H	$OCO(CH)_2CH_3$	H	H	O
Deoxynivalenol (DON)		OH	H	OH	OH	O
Nivalenol (NIV)		OH	OH	OH	OH	O

Table 1. 1. Differences in the functional groups on the trichothecene skeletal structure of type A and type B trichothecenes. R4 represents the functional group at C7position and R5 is the functional group at C8 position.

1.7 Toxicology of trichothecenes

One of the major challenges dealing with trichothecenes is their stability as they are not degraded by autoclaving and remain toxic even after normal food processing. Furthermore, they are stable at acidic pH and hence not hydrolyzed in the stomach following ingestion (Yazar and Omurtag, 2008). A second challenge is that, unlike other mycotoxins, trichothecenes do not require metabolic activation to exert their toxic effects (Wannemacher and Wiener, 1997). This is evident from the immediate skin irritation upon direct dermal application.

Various toxicological effects of trichothecenes in livestock and experimental animals have been previously reported (Fig. 1.3) (Ueno, 1983). While toxicity is not strictly determined by the structural classification these toxicological surveys suggest that toxicity decreases in the following order: type D, type A, type B and then type C. Thus we find verrucarin A (type D) exhibiting the highest acute toxicity while crotocin (type C) is the least toxic. The most characteristic of symptoms in cattle fed on trichothecene-contaminated feed is reduced feed intake or feed refusal and emesis. The emetic effect of DON was so pronounced that it was originally called vomitoxin. In animals, they are more toxic when exposed via lungs than any other routes (Ueno, 1985).

Figure 1.3. Trichothecene toxicosis in farm animals. Excessive vomiting in pigs fed on DON-contaminated animal feed (left panel). Growth retardation in broiler chicken fed with low levels of T-2 toxin (middle panel). Image credits: www.apsnet.org (Schmale and Munkvold, 2009) Necrosis and lesions in piglets poisoned with DON (right panel). Image credits: www.biomin.net

1.8 Trichothecene mycotoxicoses

Toxicological effects include gastric and intestinal lesions, immunosuppressive effects leading to CNS toxicity, vascular effects, suppression of reproductive functions, multi-organ failure and in some cases death (Rocha et al., 2005). The most frequent symptoms include vomiting, diarrhea, severe dermatitis, and bleeding (Goswami and Kistler, 2004). Teratogenic effects of trichothecenes were observed when vertebral malformations were detected in the fetus of T-2 treated pregnant mice (Ueno, 1983). Despite the varying genotoxic effects observed in trichothecene-administered animals, the majority of studies suggest that trichothecenes are most likely not carcinogenic.

Chronic exposure to trichothecenes will also cause Alimentary Toxic Aleukia (ATA) in humans. It is characterized by severely decreased leukocytes, severe pain, bleeding from the nose and throat etc. In addition affected individuals are highly susceptible to secondary infections (Etzel, 2002). Two examples of trichothecene-related human mycotoxicoses are the ATA outbreak in Russia in the 1940s that killed more than 100,000 people (Foroud and Eudes, 2009) and the trichothecene poisoning outbreak in China in 1991 (Murphy et al., 2006) during which approximately 130,000 people were affected by gastrointestinal disorders. Affected individuals in these and other incidents were reported to experience severe gastrointestinal symptoms lasting several days followed by simultaneous development of anemia, thrombocytopenia and leukopenia over a period of several weeks. In cases where dietary exposure to trichothecenes continued, necrotic lesions in the airways and gastrointestinal tract were observed accompanied by infectious and hemorrhagic complications (Sudakin, 2003). Trichothecenes are deemed as unavoidable natural contaminants. Low levels of

trichothecenes continue to be reported in cereal grains worldwide. While not acutely toxic at these very low doses, the prolonged dietary exposure to trichothecenes is, however, a serious threat to human health due to their chronic toxicity.

1.9 Cellular toxicity of trichothecenes

The potent and varied effects of trichothecene toxicosis have been largely attributed to their inhibitory effects on multiple targets in the cell. Fundamentally, trichothecenes are known for their potent inhibition of protein synthesis in eukaryotes with the peptidyl transferase center (PTC) as their key target (Ehrlich and Daigle, 1987). In fact, trichothecene-producing fungi have an altered ribosomal protein in the 60S subunit, which renders them resistant to these toxic metabolites (Schindler et al., 1974). Moreover, the first isolated trichothecene-resistant yeast mutant was the ribosomal protein L3 (Rpl3) mutant, *tcm1*, which conferred resistance to trichodermin (Fried and Warner, 1981). Although trichothecenes inhibit protein synthesis, there are differences in their mechanisms of inhibition. For instance, T-2, NIV and verrucarin inhibit the initiation step while DON, Tcin, and trichodermol inhibit the elongation-termination step (Cundliffe and Davies, 1977).

Recently, some studies have, however, suggested that trichothecene toxicosis might not be the result of a simple translation arrest but rather involved complex signaling pathways involving mitogen-activated protein kinases (MAPKs) in response to the inhibitory effects on the ribosome (Bae et al., 2009). This signaling cascade, referred

to as the ribotoxic stress response, has been identified to be triggered by trichothecenes to rapidly induce apoptosis (Shifrin and Anderson, 1999). However, the exact mechanisms by which trichothecenes induce ribotoxic stress response including all the downstream targets are not yet well understood. During ribotoxic stress, 28S rRNA is damaged by translation inhibitors, which is followed by MAPK activation and the resulting signaling cascade (proapoptotic) ends with the death of the cell (Iordanov et al., 1997). Cleavage of the α-sarcin/ricin (S/R) loop in the 28S rRNA is a trademark feature of ribotoxic stressors such as the type 2 ribosome inactive protein (RIP) ricin, which possess the required N-glycosidase activity (Hartley and Lord, 2004). Although trichothecenes do not have this activity, they nevertheless did promote cleavage of the 28S rRNA in DON and T-2-treated murine macrophages. Interestingly, unlike ricin, this cleavage by the two trichothecenes was not observed under cell-free conditions suggesting that they might be promoting activation of endogenous RNAses (Li and Pestka, 2008) to facilitate 28S rRNA cleavage.

The amphophilic nature of trichothecenes allows them to cross the cell membrane and interact with different cellular organelles such as mitochondria, the ER or the chloroplasts. Hence they are also known to target nucleotide metabolism, membrane integrity, mitochondrial functions, signal transduction, cell division and induce programmed cell death (Rocha et al., 2005). However, these inhibitory effects were largely regarded as secondary effects of translation inhibition. Hence most trichothecene-related studies have traditionally focused on inhibitory effects on translation and the resulting consequences to the health of the poisoned organism.

Plant colonization by *F. oxysporum* was recently shown to require a mitochondrial carrier protein, which is not essential for growth but significantly enhances virulence (Inoue et al., 2002). While the role of mitochondria in the pathogenicity of Fusarium is a relatively unexplored topic, trichothecenes, however, have been shown to target mitochondria in both plants and animals (Rocha et al., 2005). For instance, T-2 toxin inhibited mitochondrial activity in bovine kidney cells and DON localized to mitochondria in infected wheat spikes and kernels. Within mitochondria, in rat liver cells, *in vitro* experiments have shown T-2 toxin to inhibit translation and oxidative phosphorylation. DON treatment in macrophages caused BAX translocation to the mitochondria, caspase-3 activation and subsequent DNA fragmentation. Surprisingly, in the same cells DON also initiated antiapoptotic survival pathways (Zhou et al., 2005a). Of the eight type A and D trichothecenes studied in *S. cerevisiae*, verrucarin A (type D) exhibited the highest toxicity towards mitochondria (Schappert et al., 1986). In addition, T-2 inhibited yeast growth when grown in glycerol media and yeast strains lacking a functional mitochondria (petite) exhibited resistance when compared to the wild type cells (Schappert and Khachatourians, 1986). In lymphocytes, type B trichothecenes induced cytotoxicity via apoptotic pathway while exposure to type A trichothecenes at 1000-fold lower concentration significantly reduced mitochondrial activity and resulted in necrosis (Nasri et al., 2006). Recently it was also shown that during the mitochondrial-dependent apoptotic pathway in T2-mediated hepatotoxicity the toxin seems to target the inner membrane ADP/ATP carrier and thereby induce the opening of the mitochondrial permeability transition pore complex (PTPC) and the subsequent loss of mitochondrial

membrane potential (MMP). The Bcl-2 family members have been suggested to mediate T-2 toxicity with the apoptotic protein Bax promoting toxicity while the antiapoptotic protein Bcl-x_L prevented it (Bouaziz et al., 2009). The more recently identified caspase-2, which is required for stress-mediated apoptosis, was shown to be activated in T-2-mediated apoptotic death of leukocytes in which mitochondria amplifies signaling rather than regulating apoptosis (Huang et al., 2007). Furthermore, transcriptome profiling of T-2 toxin-treated yeast cells revealed genes associated with membrane and mitochondrial integrity to be key targets in mediating toxicity (Iwahashi et al., 2008). Interestingly no gene deletions in the caspase-dependent apoptotic pathway conferred resistance to the type B trichothecene, Tcin, upon screening the yeast deletion library (McLaughlin et al., 2009).

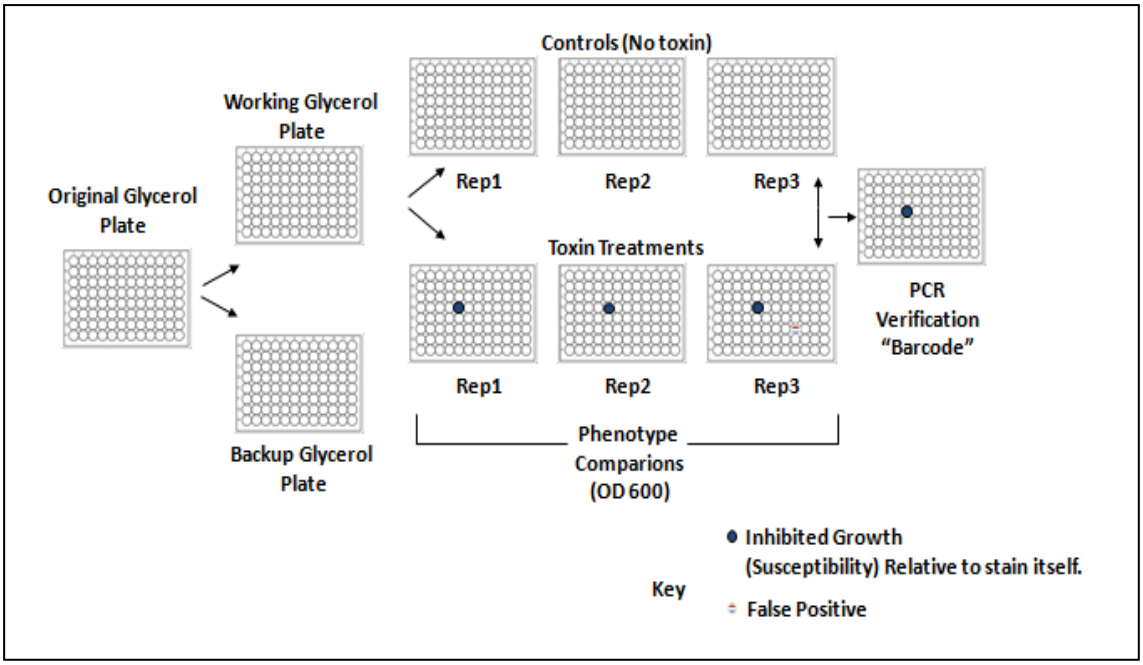

Figure 1.4. Schematic used for the high throughput screening. For the resistance screening the treatments were carried out in liquid media whereas for the sensitivity screening the treatments were carried out on solid media.

1.10 Yeast as a model to study trichothecenes

Although some of the earlier investigations used the model organism *Saccharomyces cerevisiae*, most of the current studies have focused primarily on higher eukaryotes. One possible reason could be the relative insensitivity of yeast to several of these trichothecenes, especially DON. However, when compared to other systems, yeast provides a very powerful tool to study trichothecenes with a fully sequenced genome, plethora of investigational tools and its powerful genome manipulation and mutant selection systems. With highly conserved protein sequences, findings from yeast studies can be easily translated into mammalian and plant systems. Moreover, higher eukaryotic systems, unlike yeast, do not allow investigating genome wide perturbations caused by trichothecenes. This comprehensive approach is more important when studying toxins with multiple inhibitory effects like the trichothecenes. Also, the role of mitochondria during trichothecene toxicity can be extensively studied in yeast because mitochondrial respiration is dispensable for yeast growth in fermentable media. Furthermore the effects of trichothecenes can be studied at the single cell level which is generally not the case with higher eukaryotes. In light of these and other factors, using yeast to study trichothecene toxicity should facilitate rapid progress in this area of research.

1.11 Overview of the research presented in this work

This work has used yeast as a model to study toxicity of trichothecenes. While yeast is highly tolerant to increasing concentrations of DON, Tcin on the other hand is highly toxic and therefore this DON congener was used for the initial study. This work begins with a genome wide approach which is used to identify the different cellular targets that mediate trichothecene toxicity. The yeast nonessential gene deletion library was screened to identify genes whose deletions rendered the mutants either resistant or sensitive to trichothecenes based on the schematic represented in figure 1.4. Analysis of the resistance screening revealed mitochondria to be a critical target for trichothecenes, particularly processes that regulate mitochondrial translation and membrane dynamics. Mutant analysis also shed new light on other inhibitory targets. Results from the genome wide screening was then used to explore the mechanism of action of type A (T-2 and DAS) and type B (DON and Tcin) trichothecenes. This work showed mitochondrial translation to be inhibited directly and upstream of cytosolic translation and independent of mitochondrial membrane defects. In later work, based on analysis of the sensitivity screening, trichothecene-induced oxidative stress was investigated to reveal that toxicity of trichothecenes correlates with levels of mitochondrial reactive oxygen species (mtROS) and this requires fully functional mitochondria. This study then further explores the ROS results to show that enhancing removal of ROS-producing damaged mitochondria alleviates trichothecene cytotoxicity and thereby linking, for the first time, mitophagy with trichothecene toxicity and thereby proposing a new alternative mechanism of cellular defense. Finally the mechanism of protection of two novel genes,

identified from an Arabidopsis screening for trichothecene resistance, which encode lipid transfer proteins, are shown to confer resistance to trichothecenes in yeast by protecting mitochondrial translation and membrane integrity by alleviating trichothecene-induced oxidative stress.

CHAPTER 2

Genome wide screening in yeast reveals a critical role for mitochondria in trichothecene toxicity.

Acknowledgement: Experiments in this chapter was performed along with Dr. John McLaughlin, a Research Associate in the lab. For the screening experiment the author was assisted by Dr. John McLaughlin, Andrew Tortora (lab technician) and Natasha Mendez (pre-doctoral student). Dr. McLaughlin also helped with the *in vivo* total and mitochondrial translation assays. Results and partial sections of this chapter have been previously published in the article (cited below) coauthored by Dr. John McLaughlin and the thesis author. This chapter has modified and expanded this publication to include later findings as well as include more detailed explanations which was not possible in the original publication due to page limit restrictions.

Publication Citation: McLaughlin, J.E., Bin-Umer, M.A., Tortora, A., Mendez, N., McCormick, S., and Tumer, N.E. (2009). A genome-wide screen in *Saccharomyces cerevisiae* reveals a critical role for the mitochondria in the toxicity of a trichothecene mycotoxin. Proceedings of the National Academy of Sciences *106*, 21883-21888.

Abstract:

Trichothecene mycotoxins synthesized by *Fusarium* species are potent inhibitors of eukaryotic translation. They are encountered in the environment and in food posing a threat to human and animal health. They have diverse roles in the cell that are not limited to the inhibition of protein synthesis. To understand the trichothecene mechanism of action, we screened the yeast knockout library to identify genes whose deletion confers resistance to trichothecin (Tcin). The largest group of resistant strains affected mitochondrial function, suggesting a role for fully active mitochondria in trichothecene toxicity. Tcin inhibited mitochondrial translation in the wild type strain to a greater extent than in the most resistant strains, implicating mitochondrial translation as a previously unrecognized site of action. The Tcin-resistant strains were cross-resistant to anisomycin and chloramphenicol, suggesting that Tcin targets the peptidyltransferase center of mitochondrial ribosomes. Tcin induced cell death was partially rescued by mutants that regulate mitochondrial fusion and maintenance of the tubular morphology of mitochondria. Treatment of yeast cells with Tcin led to the fragmentation of the tubular mitochondrial network, supporting a role for Tcin in disruption of mitochondrial membrane morphology. These results provide genome-wide insight into the mode of action of trichothecene mycotoxins and uncover a critical role for mitochondrial translation and membrane maintenance in their toxicity.

2.1 Introduction

Trichothecenes were first identified as potent inhibitors of translation that target the peptidyl transfer center (McLaughlin et al., 1977). In trichothecene-treated cells inhibition of DNA synthesis is preceded by inhibition of protein synthesis (Cundliffe et al., 1974; Iglesias and Ballesta, 1994). *In vitro* assays using rabbit reticulocytes indicated that different trichothecenes inhibited different steps of translation (Iglesias and Ballesta, 1994). Furthermore, polysome profiling showed trichothecenes caused breakdown of polysomes with type A trichothecenes T-2 and DAS inhibiting polypeptide chain initiation while type B trichothecenes Tcin and trichodermin inhibited the elongation step (Cundliffe et al., 1974). However, later reports suggested that toxicity of trichothecenes might not be a simple function of translational arrest and that they may have multiple mechanisms of toxicity. The mode of action of trichothecenes, including the mechanism of translation inhibition (Cannon et al., 1976; Ueno, 1985) and different signaling pathways that lead to cytotoxicity and apoptosis (Bae et al., 2009; Bouaziz et al., 2009) were also reported to show differences. These early studies have implicated DNA synthesis (Rocha et al., 2005), respiration (Pace et al., 1988), mitochondrial protein synthesis (Pace et al., 1988) and membrane structure and integrity (Schappert and Khachatourians, 1984) in the cytotoxicity of trichothecenes. The molecular mechanisms of their toxicity are therefore not well understood and the proteins targeted by trichothecenes other than ribosomal protein L3 have not yet been identified. Since multiple cellular processes are targeted by trichothecenes, a genome wide approach is

likely to provide a better insight into their mechanism of action. We therefore proposed a chemical genomics approach to study trichothecene toxicity in yeast.

The yeast deletion collections are powerful resources to identify drug targets in the cell. Since growth rate is one of the easiest phenotype to measure, fitness profiling has been used in several investigations to identify relationships between genes as well as uncover novel functions of characterized and uncharacterized genes (Hoon et al., 2008). More importantly chemical genomics approach has been successfully used in uncovering the mode of action of various compounds. Fitness profiling is a forward screening methodology that includes haploinsufficiency profiling, multicopy-suppression profiling, and homozygous profiling. We have used homozygous profiling for our screening in which viable homozygous diploid yeast knockouts are screened against the toxin and their fitness levels measured. This allows identifying genes that interact with the target of the toxin and also infer the mechanism of action of the toxin based on the functional clustering of the identified genes (Hoon et al., 2008). Here we have identified genes, in yeast, which when deleted confer resistance to trichothecin (Tcin), the type B trichothecene and a DON congener. Our results provide a genome-wide insight into the mechanisms of toxicity of a trichothecene mycotoxin and uncover a primary role for the mitochondria in trichothecene induced cell death.

2.2 Results

2.2.1 Tcin-resistant mutants have disrupted mitochondrial functions

To identify the genes involved in mediating sensitivity to trichothecenes, we carried out a systematic screen of the 4720 viable *Saccharomyces cerevisiae* diploid gene deletion collection for Tcin resistance. The screen was carried out using 4 µM Tcin, which severely inhibited the growth of the parental strain, BY4743 (>90%) with an IC_{50} of 2.5 µM in liquid YPD media (Fig. 2.1). We identified 138 deletion strains as resistant to 4 µM Tcin from three independent experiments (Table 2.1). The largest group of deletions (89/138 or 64%) that showed resistance to 4 µM Tcin encoded proteins associated with the mitochondria or affected mitochondrial function (Fig. 2.2A). Strains associated with mitochondrial ribosomes constituted the largest group (43%) within the mitochondria category (Fig. 2.2B). About 25% (35/138) of the Tcin-resistant strains that were associated with the mitochondria had abnormal mitochondrial morphology based on the *Saccharomyces* Genome Database (SGD) (http://www.yeastgenome.org/).

To determine if any of the strains that showed resistance to 4 µM Tcin had mitochondrial defects, the 138 resistant strains were grown on YPDG plates containing 3% glycerol and 0.2% dextrose. A large fraction (62%) of the strains that showed resistance to 4 µM Tcin was confirmed to be *petite*, consistent with their classification in the SGD (Table 2.1). Only four (*ndi1*Δ, *ups1*Δ, *ydc1*Δ, *cir2*Δ) deletion strains resistant to 4 µM Tcin and associated with the mitochondria displayed the wild type phenotype when grown on the YPDG media. When the Tcin-resistant *petite* mutants were grouped and analyzed using FUNSpec (http://funspec.med.utoronto.ca/), 32% encoded mitochondrial ribosomal proteins. In addition, 6 mitochondrial aminoacyl-tRNA-synthetases (*SLM5*, *AIM10*, *MSR1*, *MSK1*, *MSD1*, *MSF1*), one mitochondrial translation initiation (*IFM1*),

one elongation (*MEF2*), one termination (*RRF1*) factor and two translational control proteins (*CBP6, AEP1*) were included in the resistant group, providing evidence that mitochondrial translation may be a target of Tcin.

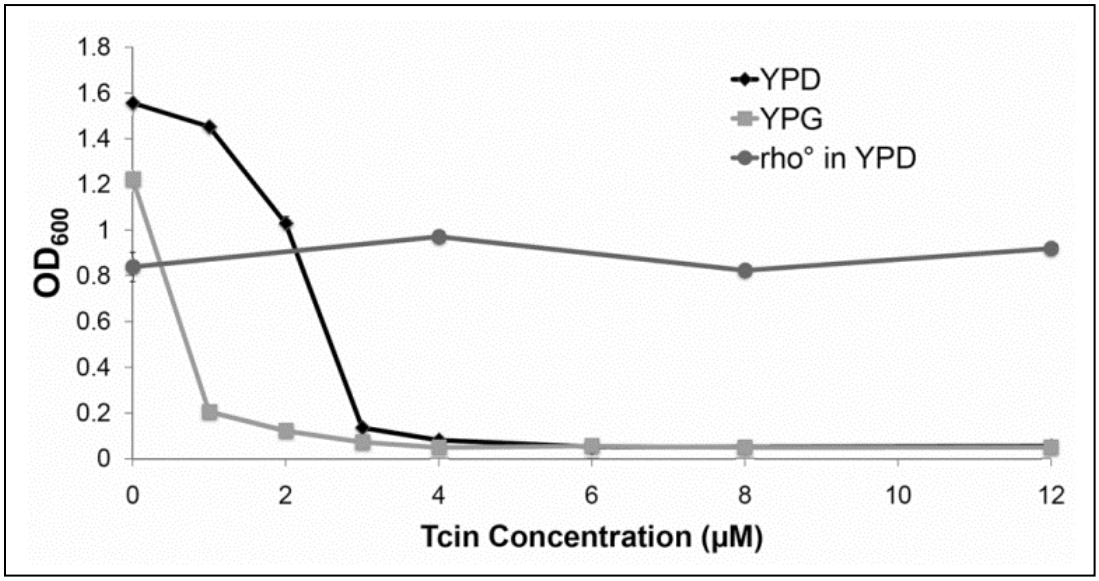

Fig. 2.1. Growth comparison of BY4743 in YPD or YPG media. The parental strain BY4743 was grown in liquid media supplemented with 2% dextrose (YPD) for 20 hours or with 3% glycerol (YPG) for 48 hours at 30°C in the presence of different concentrations of Tcin. The rho^0 version of BY4743 was grown for 48 hours at 30°C. The experiments were performed in triplicate and repeated twice. Growth is represented by mean OD_{600} values (±SE).

2.2.2 Tcin toxicity is significantly reduced in cells with reduced mitochondrial functions

The relatively large proportion of resistant strains that had defects associated with the mitochondria were surprising in light of the reported role of trichothecenes in inhibition of cytosolic, but not mitochondrial protein synthesis (Pestka, 2009; Rocha et al., 2005) and their lack of inhibition of bacterial growth and translation (Burmeister and Hesseltine, 1970; Ueno et al., 1973). To determine if mitochondria were critical for Tcin

sensitivity, the parental strain, BY4743, was grown in liquid media containing glycerol (YPG), thereby allowing the cells to depend on mitochondria for energy. The IC_{50} of BY4743 for Tcin was significantly reduced from 2.5 µM to 0.75 µM in YPG media (Fig. 2.1) reflecting a distinct mitochondrial role in the sensitivity to Tcin. To confirm this, we tested the sensitivity of a rho^0 strain derived from BY4743 by ethidium bromide treatment. Unlike the parental strain, the rho^0 strain was resistant to Tcin, confirming the role of mitochondria in Tcin sensitivity (Fig. 2.1). Furthermore, growth of BY4743 was inhibited by 2 µM Tcin on YPG media, but not YPD media, indicating that the wild type strain was more sensitive to Tcin when it depended on mitochondria for energy (Fig. 2.3). When the concentration of Tcin was doubled to 4 µM, growth of BY4743 was inhibited on both the YPG and the YPD media (Fig. 2.3). The most resistant strains grew well on YPG media, even at 12 µM Tcin (Fig. 2.4 A), suggesting that the resistance in these strains was due to the mitochondria.

2.2.3 The Tcin-resistant strains are cross-resistant to anisomycin and chloramphenicol, but not to other translation inhibitors

To test the specificity of the resistance, we screened the 15 most resistant deletion strains against other translation inhibitors. BY4743 and the resistant mutants failed to grow on 0.5 or 1 µg/ml cycloheximide (Fig. 2.5A) and were sensitive to hygromycin B (100 or 200 µg/ml) on YPD media, while 10 µg/ml hygromycin B inhibited their growth on YPG media (Fig. 2.5B). These results indicated that the observed resistance in the deletion strains did not extend to protein inhibitors in general.

The Tcin-resistant mutants were, however, resistant to 10 µg/ml anisomycin on YPD media (Fig. 2.4B). We examined growth on YPG media to determine if anisomycin resistance was due to a possible effect on mitochondrial translation. As shown in Fig. 2.6, 2.5 µg/ml anisomycin inhibited growth of BY4743 by 52% on YPG media relative to 12% inhibition on YPD, suggesting that anisomycin targets mitochondrial translation at low doses. The Tcin-resistant strains were resistant to 5 µg/ml anisomycin on YPG media when growth of BY4743 was inhibited by 94% (Fig. 2.6). Several Tcin-resistant strains (*ups1*Δ, *yap1802*Δ, *izh4*Δ, *cue3*Δ, *pba1*Δ, *flc3*Δ and *ydl173w*Δ) were more sensitive to 10 µg/ml anisomycin on YPG media (Fig. 2.4B), suggesting that anisomycin and Tcin have overlapping, but not identical effects on the mitochondria. Tcin-resistant strains were also cross-resistant to chloramphenicol, a known inhibitor of mitochondrial translation in eukaryotes, which binds to the A site and occupies the same position as the aminoacyl-tRNA (aa-tRNA), preventing peptide bond formation (Schlunzen et al., 2001). One mg/ml chloramphenicol reduced the growth of BY4743 and the top 15 resistant mutants by only 10% in YPD media (Fig. 2.4C), but was sufficient to inhibit BY4743 growth by 80% in YPG media, consistent with inhibition of mitochondrial translation. In contrast, growth of the top 15 mutants was either not inhibited at all or was markedly better than the parental strain (Fig. 2.4C). These results provided evidence that mitochondrial translation was critical for the toxicity of Tcin.

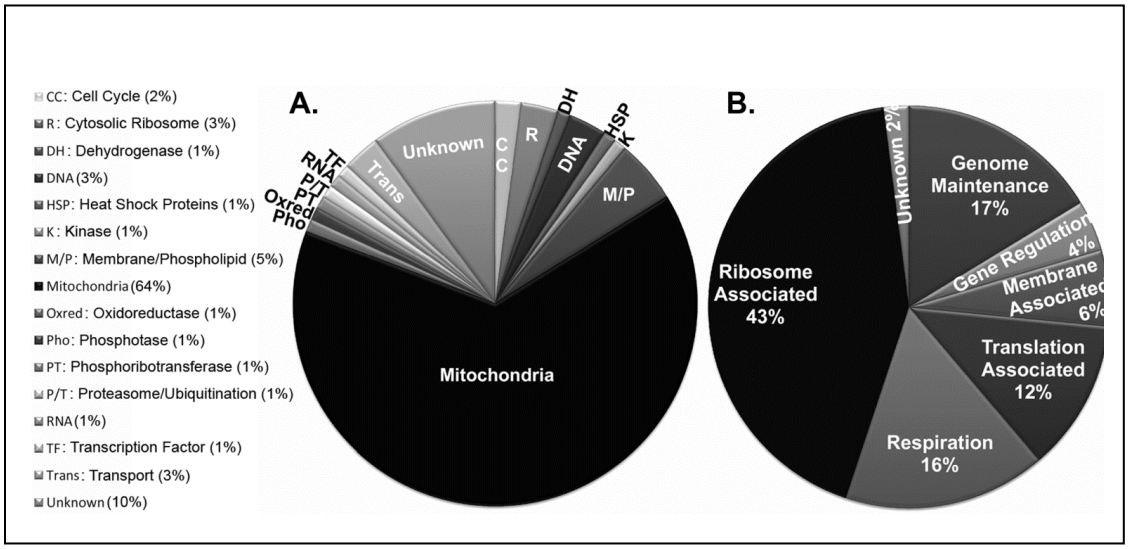

Fig. 2.2. Functional classification of yeast deletion mutants that conferred resistance to 4 µM Tcin. (A) Yeast deletion mutants exhibiting resistance to 4 µM Tcin were identified from the liquid growth assay. The figure legend shows the GO terms (www.yeastgenome.org) most associated with the 4µM Tcin-resistant mutants. Genes associated with heat shock protein, signal transduction, proteasome/ ubiquitination, transcription and RNA metabolism constitute the category "Other". The acronyms M/P and Ribo stand for Membrane/Phospholipid and Cytosolic ribosomes. (B) Further classification of the mitochondria-associated deletion mutants.

ORF#	Gene Name	Description
YGL119W	ABC1	Protein required for ubiquinone (coenzyme Q) biosynthesis and for respiratory growth; exhibits genetic interaction with COQ9, suggesting a common function; similar to prokaryotic proteins involved in early steps of ubiquinone biosynthesis
YMR064W	AEP1	Protein required for expression of the mitochondrial OLI1 gene encoding subunit 9 of F1-F0 ATP synthase
YPL005W	AEP3	Peripheral mitochondrial inner membrane protein, located on the matrix face of the membrane; stabilizes the bicistronic AAP1-ATP6 mRNA encoding subunits 6 and 8 of the ATP synthase complex
YER017C	AFG3	Component, with Yta12p, of the mitochondrial inner membrane m-AAA protease that mediates degradation of misfolded or unassembled proteins and is also required for

		correct assembly of mitochondrial enzyme complexes
YER087W	AIM10	Protein with similarity to tRNA synthetases; non-tagged protein is detected in purified mitochondria; null mutant is viable and displays elevated frequency of mitochondrial genome loss
YEL036C	ANP1	Subunit of the alpha-1,6 mannosyltransferase complex; type II membrane protein; has a role in retention of glycosyltransferases in the Golgi; involved in osmotic sensitivity and resistance to aminonitrophenyl propanediol
YDR421W	ARO80	Zinc finger transcriptional activator of the Zn2Cys6 family; activates transcription of aromatic amino acid catabolic genes in the presence of aromatic amino acids
YLR295C	ATP14	Subunit h of the F0 sector of mitochondrial F1F0 ATP synthase, which is a large, evolutionarily conserved enzyme complex required for ATP synthesis
YPL271W	ATP15	Epsilon subunit of the F1 sector of mitochondrial F1F0 ATP synthase, which is a large, evolutionarily conserved enzyme complex required for ATP synthesis; phosphorylated
YDR377W	ATP17	Subunit f of the F0 sector of mitochondrial F1F0 ATP synthase, which is a large, evolutionarily conserved enzyme complex required for ATP synthesis
YBR120C	CBP6	Mitochondrial translational activator of the COB mRNA; phosphorylated
YER061C	CEM1	Mitochondrial beta-keto-acyl synthase with possible role in fatty acid synthesis; required for mitochondrial respiration
YML110C	COQ5	2-hexaprenyl-6-methoxy-1,4-benzoquinone methyltransferase, involved in ubiquinone (Coenzyme Q) biosynthesis; localizes to the matrix face of the mitochondrial inner membrane in a large complex with other ubiquinone biosynthetic enzymes
YHR051W	COX6	Subunit VI of cytochrome c oxidase, which is the terminal member of the mitochondrial inner membrane electron transport chain; expression is regulated by oxygen levels
YDL067C	COX9	Subunit VIIa of cytochrome c oxidase, which is the terminal member of the mitochondrial inner membrane electron transport chain
YGL110C	CUE3	Protein of unknown function; has a CUE domain that binds ubiquitin, which may facilitate intramolecular monoubiquitination
YLR270W	DCS1	Non-essential hydrolase involved in mRNA decapping, may function in a feedback mechanism to regulate deadenylation, contains pyrophosphatase activity and a HIT (histidine triad) motif; interacts with neutral trehalase

		Nth1p
YBR163W	DEM1	Mitochondrial protein of unknown function; null mutant has defects in cell morphology and in response to air drying; may be regulated by the transcription factor Ace2
YMR287C	DSS1	3'-5' exoribonuclease, component of the mitochondrial degradosome along with the ATP-dependent RNA helicase Suv3p; the degradosome associates with the ribosome and mediates turnover of aberrant or unprocessed RNAs
YAL042W	ERV46	Protein localized to COPII-coated vesicles, forms a complex with Erv41p; involved in the membrane fusion stage of transport
YFR019W	FAB1	1-phosphatidylinositol-3-phosphate 5-kinase; vacuolar membrane kinase that generates phosphatidylinositol (3,5)P2, which is involved in vacuolar sorting and homeostasis
YBR101C	FES1	Hsp70 (Ssa1p) nucleotide exchange factor, cytosolic homolog of Sil1p, which is the nucleotide exchange factor for BiP (Kar2p) in the endoplasmic reticulum
YGL139W	FLC3	Putative FAD transporter, similar to Flc1p and Flc2p; localized to the ER
YDR519W	FPR2	Membrane-bound peptidyl-prolyl cis-trans isomerase (PPIase), binds to the drugs FK506 and rapamycin; expression pattern suggests possible involvement in ER protein trafficking
YBR179C	FZO1	Mitofusin, mitochondrial integral membrane protein involved in mitochondrial fusion and mitochondrial genome maintenance; contains N-terminal GTPase domain; targeted for destruction by cytosolic components of the ubiquitin-proteasome system
YER122C	GLO3	ADP-ribosylation factor GTPase activating protein (ARF GAP), involved in ER-Golgi transport; shares functional similarity with Gcs1p
YMR293C	HER2	Mitochondrial protein required for remodeling of ER caused by Hmg2p overexpression; null has decreased mitochondrial genome loss and decreased cardiolipin and phosphatidylethanolamine levels; like bacterial glutamyl-tRNA amidotransferases
YGL251C	HFM1	Meiosis specific DNA helicase involved in the conversion of double-stranded breaks to later recombination intermediates and in crossover control; catalyzes the unwinding of Holliday junctions; has ssDNA and dsDNA stimulated ATPase activity
YOL095C	HMI1	Mitochondrial inner membrane localized ATP-dependent DNA helicase, required for the maintenance of the

		mitochondrial genome; not required for mitochondrial transcription; has homology to E. coli helicase uvrD
YDR399W	HPT1	Dimeric hypoxanthine-guanine phosphoribosyltransferase, catalyzes the formation of both inosine monophosphate and guanosine monophosphate; mutations in the human homolog HPRT1 can cause Lesch-Nyhan syndrome and Kelley-Seegmiller syndrome
YDR291W	HRQ1	Putative RecQ helicase; belongs to the widely conserved RecQ family of proteins which are involved in maintaining genomic integrity; similar to the human RecQ4p implicated in Rothmund-Thomson syndrome(RTS)
YDR533C	HSP31	Possible chaperone and cysteine protease with similarity to E. coli Hsp31; member of the DJ-1/ThiJ/PfpI superfamily, which includes human DJ-1 involved in Parkinson's disease; exists as a dimer and contains a putative metal-binding site
YPR006C	ICL2	2-methylisocitrate lyase of the mitochondrial matrix, functions in the methylcitrate cycle to catalyze the conversion of 2-methylisocitrate to succinate and pyruvate; ICL2 transcription is repressed by glucose and induced by ethanol
YLR099C	ICT1	Lysophosphatidic acid acyltransferase, responsible for enhanced phospholipid synthesis during organic solvent stress; null displays increased sensitivity to Calcofluor white; highly expressed during organic solvent stress
YOL023W	IFM1	Mitochondrial translation initiation factor 2
YCR046C	IMG1	Mitochondrial ribosomal protein of the large subunit, required for respiration and for maintenance of the mitochondrial genome
YCR071C	IMG2	Mitochondrial ribosomal protein of the small subunit
YLL033W	IRC19	Putative protein of unknown function; YLL033W is not an essential gene but mutant is defective in spore formation; null mutant displays increased levels of spontaneous Rad52p foci
YOL101C	IZH4	Membrane protein involved in zinc metabolism, member of the four-protein IZH family, expression induced by fatty acids and altered zinc levels; deletion reduces sensitivity to excess zinc; possible role in sterol metabolism
YLR260W	LCB5	Minor sphingoid long-chain base kinase, paralog of Lcb4p responsible for few percent of the total activity, possibly involved in synthesis of long-chain base phosphates, which function as signaling molecules
YDL056W	MBP1	Transcription factor involved in regulation of cell cycle progression from G1 to S phase, forms a complex with

		Swi6p that binds to MluI cell cycle box regulatory element in promoters of DNA synthesis genes
YDL054C	MCH1	Protein with similarity to mammalian monocarboxylate permeases, which are involved in transport of monocarboxylic acids across the plasma membrane; mutant is not deficient in monocarboxylate transport
YAL010C	MDM10	Subunit of both the Mdm10-Mdm12-Mmm1 complex and the mitochondrial sorting and assembly machinery (SAM complex); functions in both the general and Tom40p-specific pathways for import and assembly of outer membrane beta-barrel proteins
YOL009C	MDM12	Mitochondrial outer membrane protein, required for transmission of mitochondria to daughter cells; component of the Mdm10-Mdm12-Mmm1 complex involved in import and assembly of outer membrane beta-barrel proteins
YJL102W	MEF2	Mitochondrial elongation factor involved in translational elongation
YOR241W	MET7	Folylpolyglutamate synthetase, catalyzes extension of the glutamate chains of the folate coenzymes, required for methionine synthesis and for maintenance of mitochondrial DNA
YJR144W	MGM101	Protein involved in mitochondrial genome maintenance; component of the mitochondrial nucleoid, required for the repair of oxidative mtDNA damage
YDR296W	MHR1	Protein involved in homologous recombination in mitochondria and in transcription regulation in nucleus; binds to activation domains of acidic activators; required for recombination-dependent mtDNA partitioning
YLL006W	MMM1	Mitochondrial outer membrane protein, component of the Mdm10-Mdm12-Mmm1 complex involved in import and assembly of outer membrane beta-barrel proteins
YGL064C	MRH4	Mitochondrial ATP-dependent RNA helicase of the DEAD-box family, plays an essential role in mitochondrial function
YOR201C	MRM1	Ribose methyltransferase that modifies a functionally critical, conserved nucleotide in mitochondrial 21S rRNA
YDL045W-A	MRP10	Mitochondrial ribosomal protein of the small subunit
YKL003C	MRP17	Mitochondrial ribosomal protein of the small subunit; MRP17 exhibits genetic interactions with PET122, encoding a COX3-specific translational activator
YPR166C	MRP2	Mitochondrial ribosomal protein of the small subunit
YBL090W	MRP21	Mitochondrial ribosomal protein of the small subunit; MRP21 exhibits genetic interactions with mutations in the

		COX2 and COX3 mRNA 5'-untranslated leader sequences
YPL118W	MRP51	Mitochondrial ribosomal protein of the small subunit; MRP51 exhibits genetic interactions with mutations in the COX2 and COX3 mRNA 5'-untranslated leader sequences
YNL005C	MRP7	Mitochondrial ribosomal protein of the large subunit
YNL284C	MRPL10	Mitochondrial ribosomal protein of the large subunit; appears as two protein spots (YmL10 and YmL18) on two-dimensional SDS gels
YKR006C	MRPL13	Mitochondrial ribosomal protein of the large subunit, not essential for mitochondrial translation
YLR312W-A	MRPL15	Mitochondrial ribosomal protein of the large subunit
YBR282W	MRPL27	Mitochondrial ribosomal protein of the large subunit
YDR462W	MRPL28	Mitochondrial ribosomal protein of the large subunit
YCR003W	MRPL32	Mitochondrial ribosomal protein of the large subunit
YBR122C	MRPL36	Mitochondrial ribosomal protein of the large subunit; overproduction suppresses mutations in the COX2 leader peptide-encoding region
YBR268W	MRPL37	Mitochondrial ribosomal protein of the large subunit
YLR439W	MRPL4	Mitochondrial ribosomal protein of the large subunit
YPL173W	MRPL40	Mitochondrial ribosomal protein of the large subunit
YPR100W	MRPL51	Mitochondrial ribosomal protein of the large subunit
YHR147C	MRPL6	Mitochondrial ribosomal protein of the large subunit
YGR220C	MRPL9	Mitochondrial ribosomal protein of the large subunit
YBR251W	MRPS5	Mitochondrial ribosomal protein of the small subunit
YPL104W	MSD1	Mitochondrial aspartyl-tRNA synthetase, required for acylation of aspartyl-tRNA; yeast and bacterial aspartyl-, asparaginyl-, and lysyl-tRNA synthetases contain regions with high sequence similarity, suggesting a common ancestral gene
YPR047W	MSF1	Mitochondrial phenylalanyl-tRNA synthetase, active as a monomer, unlike the cytoplasmic subunit which is active as a dimer complexed to a beta subunit dimer; similar to the alpha subunit of E. coli phenylalanyl-tRNA synthetase
YNL073W	MSK1	Mitochondrial lysine-tRNA synthetase, required for import of both aminoacylated and deacylated forms of tRNA(Lys) into mitochondria and for aminoacylation of mitochondrially encoded tRNA(Lys)
YHR091C	MSR1	Mitochondrial arginyl-tRNA synthetase
YDL044C	MTF2	Mitochondrial matrix protein that interacts with an N-terminal region of mitochondrial RNA polymerase (Rpo41p) and couples RNA processing and translation to

		transcription
YMR097C	MTG1	Peripheral GTPase of the mitochondrial inner membrane, essential for respiratory competence, likely functions in assembly of the large ribosomal subunit, has homologs in plants and animals
YML120C	NDI1	NADH:ubiquinone oxidoreductase, transfers electrons from NADH to ubiquinone in the respiratory chain but does not pump protons, in contrast to the higher eukaryotic multisubunit respiratory complex I; phosphorylated; homolog of human AMID
YJL208C	NUC1	Major mitochondrial nuclease, has RNAse and DNA endo- and exonucleolytic activities; has roles in mitochondrial recombination, apoptosis and maintenance of polyploidy
YPL052W	OAZ1	Regulator of ornithine decarboxylase (Spe1p), antizyme that binds to Spe1p to regulate ubiquitin-independent degradation; ribosomal frameshifting during synthesis of Oaz1p and its ubiquitin-mediated degradation are both polyamine-regulated
YKL134C	1-Oct	Mitochondrial intermediate peptidase, cleaves N-terminal residues of a subset of proteins upon import, after their cleavage by mitochondrial processing peptidase (Mas1p-Mas2p); may contribute to mitochondrial iron homeostasis
YPR044C	OPI11	Dubious open reading frame unlikely to encode a protein, based on available experimental and comparative sequence data; partially overlaps verified gene RPL43A/YPR043W; deletion confers sensitivity to GSAO
YLR199C	PBA1	Protein involved in 20S proteasome assembly; forms a heterodimer with Add66p that binds to proteasome precursors; similar to human PAC1 constituent of the PAC1-PAC2 complex involved in proteasome assembly
YPL219W	PCL8	Cyclin, interacts with Pho85p cyclin-dependent kinase (Cdk) to phosphorylate and regulate glycogen synthase, also activates Pho85p for Glc8p phosphorylation
YGR101W	PCP1	Mitochondrial serine protease required for the processing of various mitochondrial proteins and maintenance of mitochondrial DNA and morphology; belongs to the rhomboid-GlpG superfamily of intramembrane peptidases
YKR046C	PET10	Protein of unknown function that co-purifies with lipid particles; expression pattern suggests a role in respiratory growth; computational analysis of large-scale protein-protein interaction data suggests a role in ATP/ADP exchange
YER058W	PET117	Protein required for assembly of cytochrome c oxidase
YMR267W	PPA2	Mitochondrial inorganic pyrophosphatase, required for

		mitochondrial function and possibly involved in energy generation from inorganic pyrophosphate
YDR529C	QCR7	Subunit 7 of the ubiquinol cytochrome-c reductase complex, which is a component of the mitochondrial inner membrane electron transport chain; oriented facing the mitochondrial matrix; N-terminus appears to play a role in complex assembly
YDR004W	RAD57	Protein that stimulates strand exchange by stabilizing the binding of Rad51p to single-stranded DNA; involved in the recombinational repair of double-strand breaks in DNA during vegetative growth and meiosis; forms heterodimer with Rad55p
YGL246C	RAI1	Nuclear protein that binds to and stabilizes the exoribonuclease Rat1p, required for pre-rRNA processing
YCR028C-A	RIM1	Single-stranded DNA-binding protein essential for mitochondrial genome maintenance; involved in mitochondrial DNA replication
YPL089C	RLM1	MADS-box transcription factor, component of the protein kinase C-mediated MAP kinase pathway involved in the maintenance of cell integrity; phosphorylated and activated by the MAP-kinase Slt2p
YGL135W	RPL1B	N-terminally acetylated protein component of the large (60S) ribosomal subunit, nearly identical to Rpl1Ap and has similarity to E. coli L1 and rat L10a ribosomal proteins; rpl1a rpl1b double null mutation is lethal
YFR032C-A	RPL29	Protein component of the large (60S) ribosomal subunit, has similarity to rat L29 ribosomal protein; not essential for translation, but required for proper joining of the large and small ribosomal subunits and for normal translation rate
YJL189W	RPL39	Protein component of the large (60S) ribosomal subunit, has similarity to rat L39 ribosomal protein; required for ribosome biogenesis; loss of both Rpl31p and Rpl39p confers lethality; also exhibits genetic interactions with SIS1 and PAB1
YHR038W	RRF1	Mitochondrial ribosome recycling factor, essential for mitochondrial protein synthesis and for the maintenance of the respiratory function of mitochondria
YER050C	RSM18	Mitochondrial ribosomal protein of the small subunit, has similarity to E. coli S18 ribosomal protein
YJR101W	RSM26	Mitochondrial ribosomal protein of the small subunit
YGR215W	RSM27	Mitochondrial ribosomal protein of the small subunit
YPL047W	SGF11	Integral subunit of SAGA histone acetyltransferase complex, regulates transcription of a subset of SAGA-regulated genes, required for the Ubp8p association with

		SAGA and for H2B deubiquitylation
YPL026C	SKS1	Putative serine/threonine protein kinase; involved in the adaptation to low concentrations of glucose independent of the SNF3 regulated pathway
YCR024C	SLM5	Mitochondrial asparaginyl-tRNA synthetase
YLR139C	SLS1	Mitochondrial membrane protein that coordinates expression of mitochondrially-encoded genes; may facilitate delivery of mRNA to membrane-bound translation machinery
YHR014W	SPO13	Meiosis-specific protein, involved in maintaining sister chromatid cohesion during meiosis I as well as promoting proper attachment of kinetochores to the spindle during meiosis I and meiosis II
YPL057C	SUR1	Probable catalytic subunit of a mannosylinositol phosphorylceramide (MIPC) synthase, forms a complex with probable regulatory subunit Csg2p; function in sphingolipid biosynthesis is overlapping with that of Csh1p
YNL081C	SWS2	Putative mitochondrial ribosomal protein of the small subunit, has similarity to E. coli S13 ribosomal protein; participates in controlling sporulation efficiency
YLR262C-A	TMA7	Protein of unknown that associates with ribosomes; null mutant exhibits translation defects, altered polyribosome profiles, and resistance to the translation inhibitor anisomcyin
YKR010C	TOF2	Protein required for rDNA silencing and mitotic rDNA condensation; stimulates Cdc14p phosphatase activity and may function to coordinate the release of Cdc14p during anaphase; displays synthetic genetic interactions with TOP1, HPR1 and YCS4
YBR126C	TPS1	Synthase subunit of trehalose-6-phosphate synthase/phosphatase complex, which synthesizes the storage carbohydrate trehalose; also found in a monomeric form; expression is induced by the stress response and repressed by the Ras-cAMP pathway
YLR193C	UPS1	Mitochondrial intermembrane space protein that regulates alternative processing and sorting of Mgm1p and other proteins; required for normal mitochondrial morphology; ortholog of human PRELI
YOR359W	VTS1	Post-transcriptional gene regulator, RNA-binding protein containing a SAM domain; shows genetic interactions with Vti1p, which is a v-SNARE involved in cis-Golgi membrane traffic
YGR241C	YAP1802	Protein involved in clathrin cage assembly; binds Pan1p and clathrin; homologous to Yap1801p, member of the

		AP180 protein family
YPL087W	YDC1	Alkaline dihydroceramidase, involved in sphingolipid metabolism; preferentially hydrolyzes dihydroceramide to a free fatty acid and dihydrosphingosine; has a minor reverse activity
YBR104W	YMC2	Mitochondrial protein, putative inner membrane transporter with a role in oleate metabolism and glutamate biosynthesis; member of the mitochondrial carrier (MCF) family; has similarity with Ymc1p
YBR162W-A	YSY6	Protein whose expression suppresses a secretory pathway mutation in E. coli; has similarity to the mammalian RAMP4 protein involved in secretion
YBR144C		Dubious open reading frame unlikely to encode a protein, based on available experimental and comparative sequence data; YBR144C is not an essential gene
YDR509W		Dubious open reading frame unlikely to encode a functional protein, based on available experimental and comparative sequence data
YDL050C		Dubious ORF unlikely to encode a protein, based on available experimental and comparative sequence data
YDR157W		Dubious open reading frame unlikely to encode a functional protein, based on available experimental and comparative sequence data
YDR065W		Protein of unknown function, required for vacuolar acidification; the authentic, non-tagged protein is detected in highly purified mitochondria in high-throughput studies
YDL173W		Putative protein of unknown function; green fluorescent protein (GFP)-fusion protein localizes to the cytoplasm; YDL173W is not an essential gene
YGL218W		Dubious open reading frame, unlikely to encode a protein; not conserved in closely related Saccharomyces species; 93% of ORF overlaps the verified gene MDM34; deletion in cyr1 mutant results in loss of stress resistance
YGR219W		Dubious open reading frame unlikely to encode a protein, based on available experimental and comparative sequence data; partially overlaps the verified ORF MRPL9/YGR220C
YGR283C		Protein of unknown function; may interact with ribosomes, based on co-purification experiments; predicted to be involved in ribosome biogenesis; null mutant is resistant to fluconazole; GFP-fusion protein localizes to the nucleolus
YJL152W		Dubious ORF unlikely to encode a functional protein, based on available experimental and comparative sequence data
YJL132W		Putative protein of unknown function; localizes to the

		membrane fraction; possible Zap1p-regulated target gene induced by zinc deficiency; YJL132W is a non-essential gene
YJL119C		Dubious open reading frame unlikely to encode a functional protein, based on available experimental and comparative sequence data
YJL193W		Putative protein of unknown function, predicted to encode a triose phosphate transporter subfamily member based on phylogenetic analysis; similar to YOR307C/SLY41; deletion mutant has a respiratory growth defect
YKR012C		Dubious open reading frame unlikely to encode a protein, based on available experimental and comparative sequence data; partially overlaps the verified gene PRY2
YMR187C		Putative protein of unknown function; YMR187C is not an essential gene
YMR310C		Putative protein of unknown function; predicted to be involved in ribosome biogenesis; green fluorescent protein (GFP)-fusion protein localizes to the nucleus; YMR310C is not an essential gene
YNL011C		Putative protein of unknown function; YNL011C is not an essential gene
YOR356W		Mitochondrial protein with similarity to flavoprotein-type oxidoreductases; found in a large supramolecular complex with other mitochondrial dehydrogenases
YOR205C		Protein of unknown function; the authentic, non-tagged protein is detected in purified mitochondria in high-throughput studies
YPR116W		Putative protein of unknown function; null mutation results in a decrease in plasma membrane electron transport
YPL056C		Putative protein of unknown function; deletion mutant is fluconazole resistant
YPL080C		Dubious open reading frame unlikely to encode a protein, based on available experimental and comparative sequence data
YPL088W		Putative aryl alcohol dehydrogenase; transcription is activated by paralogous transcription factors Yrm1p and Yrr1p along with genes involved in multidrug resistance

Table 2. 1. List of Tcin-resistant mutants. Description of yeast diploid mutants resistant to 4µM Tcin based on *Saccharomyces* genome database (www.yeastgenome.org)

2.2.4 Tcin inhibited mitochondrial translation in wild-type yeast

The wild type cells were exposed to different concentrations of Tcin for one hour and the mitochondrial translation rate was determined by measuring [^{35}S]-Met incorporation into mitochondrial protein (Fox et al., 1991). At 6.4 µM Tcin, the mitochondrial translation efficiency was reduced by over 50% and at 13 µM Tcin, nearly complete inhibition of mitochondrial protein synthesis was observed (Fig. 2.7A). A general decrease in mitochondrial protein synthesis, which was not specific to any one particular protein, was observed by SDS-PAGE analysis followed by autoradiography (Fig. 2.7B). These results demonstrated that mitochondrial translation in the wild type strain is sensitive to Tcin.

Since the top 15 mutants were resistant to 8 µM or higher concentrations of Tcin in YPD media (Fig. 2.3), we examined the total and the mitochondrial translation efficiencies of the top 15 resistant strains in the presence of a final concentration of 8 µM Tcin/OD_{600} cells. To ensure accurate estimation of the translation rate, the [^{35}S]-Met incorporation was normalized against the protein concentrations. Tcin significantly inhibited total translation in the wild type (91%) and in all the resistant strains (55-93%) except *spo13*Δ, which showed minimal inhibition of total translation (32%) (Fig. 2.8A). The *ynl011c*Δ and *ict1*Δ, in which total translation was 93% and 85% affected, were resistant to the highest concentration of Tcin tested (24µM), indicating that Tcin resistance can be separated from the inhibition of total translation.

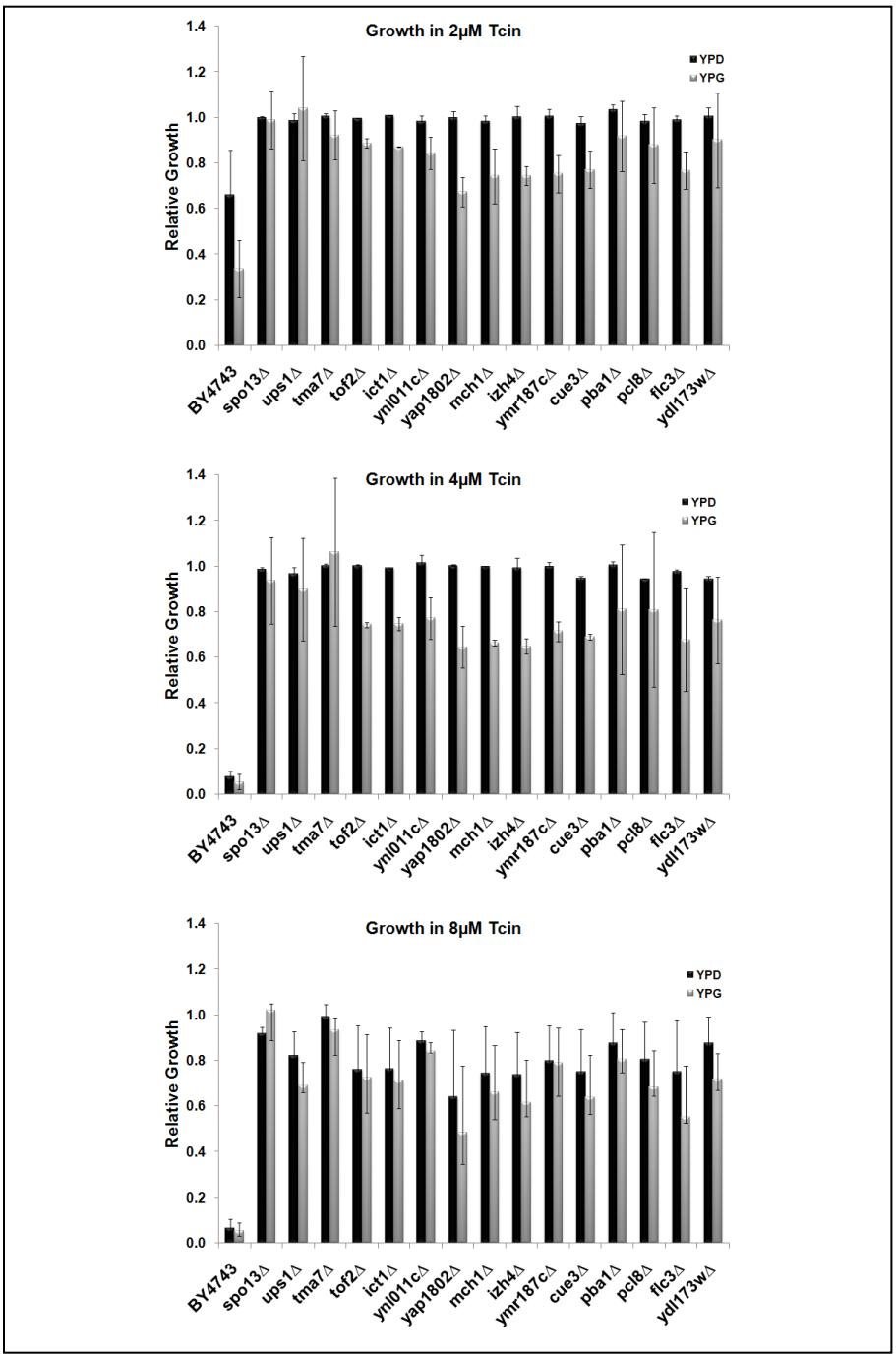

Fig. 2.3. Growth of the most resistant 15 strains in the presence of Tcin in YPD or YPG media. The most resistant 15 strains were grown on 2, 4 or 8 μM Tcin in liquid YPD or YPG media. Cells were incubated at 30°C for 20 hours in YPD media or for 48 hours at 30°C in YPG media. Relative growth was calculated as the ratio between the

growth of treated cells to that of untreated cells with a ratio of 1.0 indicating no effect on growth.

Analysis of mitochondrial translation by [^{35}S]-Met incorporation indicated that 8 µM Tcin/OD_{600} significantly inhibited mitochondrial translation (75%) in BY4743. In contrast, mitochondrial translation was inhibited only 15-51% in the most resistant 15 strains except in *ict1*Δ and *pcl8*Δ, which had 66-67% inhibition (Fig. 2.8B). Mitochondrial translation rates of mutants resistant to 24 µM Tcin (*spo13Δ, ups1Δ, tma7Δ, tof2Δ, ict1Δ*) were similar to the parental strain in the absence of Tcin (Fig. 2.8B). Mutants that had reduced mitochondrial translation efficiencies (*ymr187c*Δ*, cue3*Δ, and *flc3*Δ) were also not any more vulnerable to Tcin (Fig. 2.8B). Therefore, the resistance observed in these strains was not a result of a general defect in mitochondrial translation due to the individual gene deletion.

Translation percentages were calculated by comparing the translation rate of toxin-treated samples to their untreated controls and are presented as percentage of the untreated control in Fig. 2.7C. Comparison of the total and the mitochondrial translation in each mutant indicated that mitochondrial translation was inhibited less by Tcin than total translation in the 15 resistant strains (Fig. 2.7C). Total translation and mitochondrial translation were minimally affected in *spo13*Δ*, tma7*Δ and *tof2*Δ. Total translation was affected more than the mitochondrial translation in *ups1*Δ, *ict1*Δ, *ynl011c*Δ, *yap1802*Δ, *ymr187c*Δ, *cue3*Δ, *pba1*Δ*, flc3*Δ and *ydl173W*Δ, while in *mch1*Δ, *izh4*Δ and *pcl8*Δ, both cytosolic and mitochondrial translation were affected, although less than the wild type. These results indicated that inhibition of mitochondrial translation was critical for the

toxicity of Tcin. The reduction in inhibition of mitochondrial protein synthesis did not correlate with the level of resistance in several strains, suggesting that Tcin had additional effects. A general defect in drug uptake or metabolism was unlikely, since the mutants did not show any resistance to cycloheximide or hygromycin B.

2.2.5 Tcin promoted fragmentation of mitochondrial morphology in wild-type yeast

Five strains that showed resistance to Tcin (*pcp1*Δ, *mdm12*Δ, *mdm10*Δ, *fzo1*Δ, and *mmm1*Δ) displayed severe mitochondrial morphology defects as defined by the absence of cells with wild-type mitochondrial morphology, consistent with their classification in SGD. Several Tcin-resistant deletion strains were defective in mitochondrial fusion (*fzo1*Δ, *pcp1*Δ) or interfered with mitochondrial morphology leading to a fusion/fission imbalance and resulting in the development of fragmented mitochondria (*ups1*Δ) (Sesaki et al., 2006). Deletion of the proteins required for the maintenance of proper tubular morphology and fusion of the mitochondria led to resistance to 4 µM Tcin, implicating disruption of mitochondrial membranes in the toxicity of Tcin.

We investigated the effect of Tcin on mitochondrial morphology by transforming BY4743 with pVT100U-mtGFP encoding a constitutively expressed GFP targeted to the mitochondrial matrix (Westermann and Neupert, 2000). Mitochondria in BY4743-mtGPF cells showed the characteristic morphology of a uniformly tubular network and normal nuclear morphology (Fig. 2.9A). Exposure to 8 µM Tcin for 4 hours led to the fragmentation of the mitochondrial network (Fig. 2.9B). Tcin treated cells contained highly fragmented mitochondria that were very short tubules or spheres. Increasing the concentration of Tcin to 80 µM led to further mitochondrial fragmentation (Fig. 2.9C).

These cells had fragmented mitochondria similar to those observed in *fzo1*Δ mutant in the fusion pathway (Fig 2.9D). Treatment of *fzo1*Δ with 8 μM Tcin did not lead to further fragmentation (Fig. 2.9E). Similar results were also observed with *ups1*Δ. These results demonstrated that Tcin causes fragmentation of the tubular mitochondrial network. The mutants in the fusion machinery, but not the mutants in the fission machinery were resistant to Tcin (Table 2.1), suggesting that the observed fragmentation is mediated by the mitochondrial fission machinery.

2.3. Discussion

2.3.1 Mitochondria play a critical role in mediating trichothecin toxicity

In this study, we performed a genome-wide screen of the homozygous diploid yeast deletion library to gain insight into the mode of action of trichothecenes and identified genes involved in mitochondrial translation, membrane organization, respiration, cellular transport, cell cycle, signal transduction and RNA, DNA, and lipid metabolism (Table 2.1). Because *S. cerevisiae* is more sensitive to Tcin (IC_{50} ~2.5μM) than DON (IC_{50} is >2mM), we used Tcin as a representative type B trichothecene. The cytosolic ribosomes are reported to be the primary target of trichothecene action (Pestka, 2008; Rocha et al., 2005). However, our results indicated that *S. cerevisiae* was more sensitive to Tcin when grown in media with glycerol than glucose as the sole carbon source. Since utilization of a nonfermentable carbon source, such as glycerol requires mitochondrial function, this observation provided evidence for the involvement of

mitochondria in the cytotoxicity of Tcin. We confirmed this by demonstrating that the rho^0 strains derived from BY4743, unlike rho^+ were resistant up to 12 µM Tcin. Loss of mitochondrial genome (rho^0) is known to activate the pleiotropic drug resistance pathway via the overexpression of *PDR5*, the gene encoding the ATP-binding cassette transporter (Hallstrom and Moye-Rowley, 2000). Upregulation of *PDR5* in rho^o mutants is dependent on the presence of *PDR3* (Hallstrom and Moye-Rowley, 2000). In our screen, deletion of *PDR3* did not alter Tcin sensitivity of the parental rho^+ strain, nor did deletion of *PDR1* or *PDR5*. Both the rho^0 and rho^+ strains remained sensitive to 0.5-10 µg/ml cycloheximide. Taken together, these results imply that the acquired resistance due to loss of the mitochondrial genome is not simply a consequence of the activation of the pleiotropic drug resistance pathway, but rather it is specific to Tcin and its effect on the mitochondria.

2.3.2 Mitochondrial translation and membrane integrity are critical targets of Tcin toxicity

The largest group of the resistant strains associated with mitochondria encoded ribosomal proteins and translation factors, suggesting that Tcin affected mitochondrial translation. Although trichothecenes do not inhibit bacterial translation (Burmeister and Hesseltine, 1970; Ueno et al., 1973), Tcin inhibited mitochondrial translation in the wild type cells. Mitochondrial translation was only minimally affected by Tcin in majority of the most resistant 15 strains in comparison with the isogenic wild type strain (Fig. 2.7). The Tcin-resistant mutants were cross-resistant to anisomycin, but not to cycloheximide

or hygromycin B. Chloramphenicol, an inhibitor of mitochondrial translation, did not inhibit growth of the Tcin-resistant mutants at a concentration sufficient to inhibit growth of the wild type cells. Chloramphenicol and anisomycin bind at the active site crevice of the ribosome and block peptidyltransferase activity by preventing binding of aminoacyl tRNA (aa-tRNA) to the A site (Hansen et al., 2003), while hygromycin and cycloheximide inhibit translocation (Gonzalez et al., 1978; Rao and Grollman, 1967). The inhibitory effect of anisomycin on mitochondria has not been previously reported. At low doses, anisomycin inhibited growth of the wild type strain when glycerol was used as the carbon source, indicating that it inhibited mitochondrial translation. Taken together, these results suggest that Tcin and anisomycin target the peptidyltransferase center of mitochondrial ribosomes and inhibit an A site associated function. Consistent with this, deletion of *MRPL9*, encoding mitochondrial ribosomal protein L3 led to Tcin resistance (Table 2.1), suggesting that Tcin may inhibit mitochondrial peptidyltransferase activity by targeting the mitochondrial L3. The deletion mutant of the cytosolic ribosomal protein L3 was not included in the library, since it is an essential gene. The Tcin resistant mutants identified from this screen were either resistant to both Tcin and anisomycin or resistant solely to Tcin when glycerol was used as the carbon source, indicating that Tcin and anisomycin have common, as well as unique actions on the mitochondria.

Deletion of *TMA7*, associated with the 40S ribosomal subunit, conferred a high level of resistance to anisomycin, consistent with previous findings (Fleischer et al., 2006). The *tma7*Δ was highly resistant to Tcin. However, we did not observe a decrease

in the total protein synthesis in *tma7*Δ in the absence of Tcin (Fleischer et al., 2006). Total translation and mitochondrial translation were inhibited less by Tcin in *tma7*Δ than in the wild type strain. Similarly, *spo13*Δ and *tof2*Δ also showed a high level of resistance to Tcin and anisomycin and minimal inhibition of total and mitochondrial translation. The *spo13*Δ and *tof2*Δ were identified as highly resistant to the antimicrobial dermaseptins (Morton et al., 2007). Dermaseptin-induced nuclear DNA fragmentation, reactive oxygen species (ROS) production, and subsequent triggering of a caspase independent cell death were minimized in these strains (Morton et al., 2007). Tof2 is required for ribosomal DNA (rDNA) silencing and mitotic rDNA condensation, while Spo13 is a meiosis specific protein, involved in maintaining sister chromatid cohesion during meiosis. Both Tof2 and Spo13 are involved in cell cycle progression and their deletion increases levels of Rad52 foci, a marker for homologous recombination, which functions to maintain the integrity of genome through repair of DNA double-strand breaks (Alvaro et al., 2007). Additional genes involved in recombination and repair of double stranded DNA breaks (*RAD57*, *IRC19*, *MHR1*), and cell cycle progression (*MBP1*, *RAD57*, *HFM1*) were identified in our screen. These results suggest that DNA damage, a process known to trigger apoptosis, may be a consequence of the effects of Tcin and anisomycin on mitochondrial ribosomes. The absence of *SPO13* and *TOF2* might prevent the Tcin and anisomycin induced cell death by enhancing the DNA damage repair response. Like the dermaseptins (Morton et al., 2007), Tcin sensitivity of yeast was independent of the yeast metacaspase, Yca1, but in contrast to the dermaseptins, it was also independent of the apoptotic protein Aif1. Total

translation was inhibited more than the mitochondrial translation in the majority of the strains, which were resistant to both Tcin and anisomycin, (Fig. 2.7C). Inhibition of translation by cycloheximide has been shown to promote mitochondrial maintenance by alleviating age-related stress on the organelle (Wang et al., 2008). Since mutants in which total translation was reduced were further affected by the toxin, it is possible that the reduced cytosolic protein synthesis suppressed the mitochondrial degeneration mediated by Tcin.

Several mutants (*ups1*Δ, *yap1802*Δ, *izh4*Δ, *cue3*Δ, *pcl8*Δ, *flc3*Δ and *ydl173w*Δ) were uniquely resistant to Tcin, but not to anisomycin when mitochondria were used as the source of energy (Fig. 2.4B). These mutants were involved in maintaining the integrity of the mitochondrial membrane (*ups1*Δ), clathrin cage assembly (*yap1802*Δ), sterol metabolism (*izh4*Δ), monoubiquitination (*cue3*Δ), 20S proteasome assembly (*pba1*Δ) or FAD transport (*flc3*Δ).

2.3.3 Tcin-mediated toxicity also involves regulation of sphingolipid metabolism

A number of additional genes identified (*CEM1*, *FAB1*, *ICT1*, *UPS1*, *LCB5*, *SUR1*, *YDC1*) encoded proteins involved in phospholipid metabolism (Table 2.1). Early studies indicated that T-2 toxin interfered with the metabolism of membrane phospholipids and increased liver peroxides (Rocha et al., 2005). More recently, trichothecenes were shown to interfere with sphingolipid metabolism by inducing accumulation of glucosylceramide in neural cells (Kralj et al., 2007). *YDC1*, *LCB5* and *SUR1* encode proteins involved in the sphingolipid metabolism (Obeid et al., 2002).

Yeast mutants lacking *YDC1,* an alkaline dihydroceramidase had increased chronological life span, while overexpression of *YDC1* led to fragmentation of mitochondria and vacuoles, resulting in reduced life span and increased apoptotic cell death (Aerts et al., 2008). These results implicate sphingolipid metabolism in the toxicity of Tcin and suggest that membrane sphingolipids are either directly required for Tcin mediated growth inhibition and cell cycle arrest, or are indirectly affected.

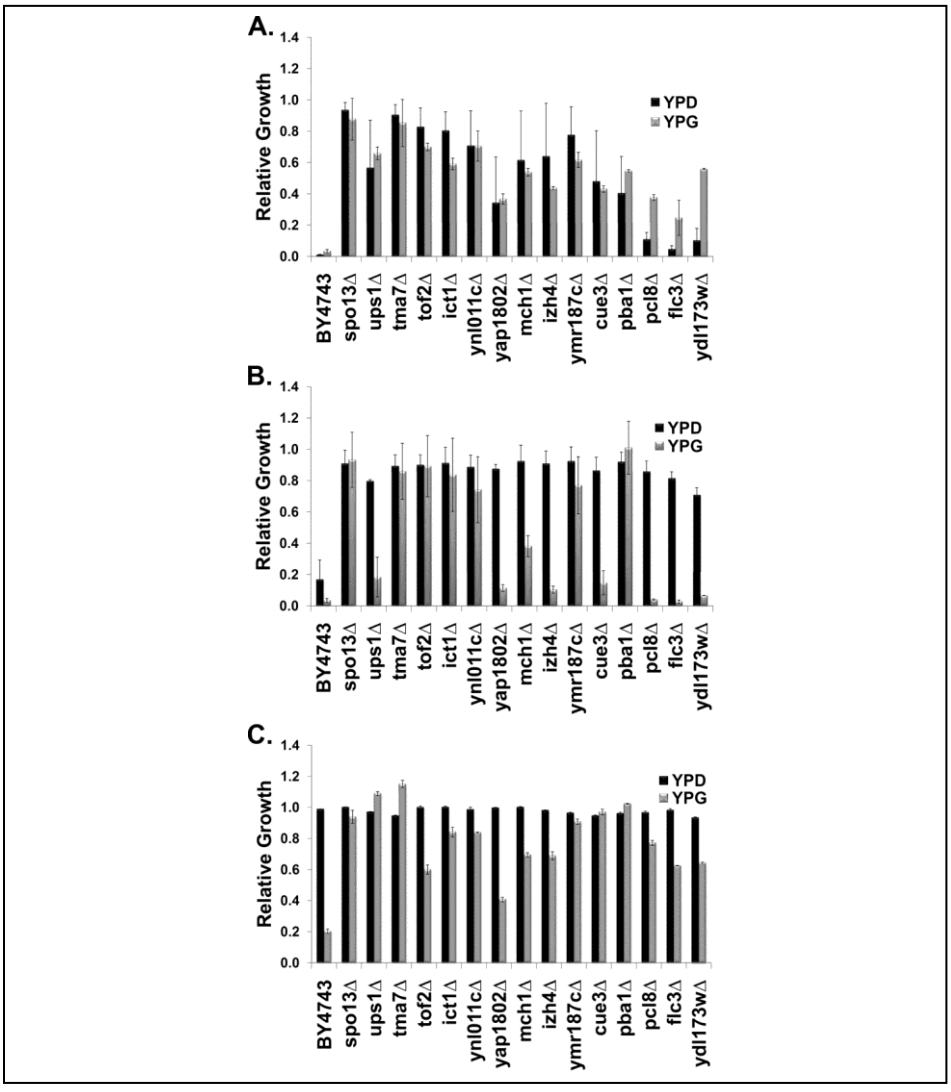

Fig. 2.4. Growth of the most resistant 15 deletion strains in the presence of different antibiotics in YPD or YPG media. The Tcin-resistant strains were grown in liquid YPD and YPG media containing (A) 12 µM Tcin, (B) 10 µg/ml anisomycin or (C) 1mg/ml chloramphenicol. Relative growth was calculated as the ratio between growth of treated cells to that of untreated cells with a ratio of 1.0 indicating no effect on growth. The experiments were performed in triplicate and repeated twice.

In contrast to the wild type cells, which contain tubular mitochondria, in Tcin treated cells the tubular structure of the mitochondria was largely broken. Deletion of genes involved in mitochondrial fusion (*FZO1*, *PCP1* and *AFG3*) and maintenance of the tubular morphology of mitochondria (*MMM1*, *MDM10* and *MDM12*) conferred resistance to Tcin, suggesting a possible effect on the mitochondrial membrane dynamics. Fzo1 is an outer mitochondrial membrane GTPase essential for mitochondrial fusion. In *fzo1*Δ yeast cells, mitochondria are highly fragmented due to a deficiency in mitochondrial fusion, a defect that in turn leads to loss of mitochondrial DNA and therefore respiratory activity (Hermann et al., 1998; Rapaport et al., 1998). Pcp1 and Ups1 are associated with the inner membrane and their deletion results in loss of fusion activity (McQuibban et al., 2003; Sesaki et al., 2006). Ups1 regulates cardiolipin metabolism, a mitochondria specific phospholipid required for the integrity of several protein complexes in the inner membrane and is essential for respiration (Tamura et al., 2009).

The Mmm1-Mdm10-Mdm12-Mdm34 complex has recently been shown to connect the endoplasmic reticulum (ER) and mitochondria (Kornmann et al., 2009). Mutations in this complex reduce cardiolipin levels and impair phospholipid biosynthesis (Kornmann et al., 2009). These observations imply a possible inhibitory effect of Tcin

on the membranes that connect the ER and mitochondria, leading to impairment of the interorgannellar phospholipid exchange.

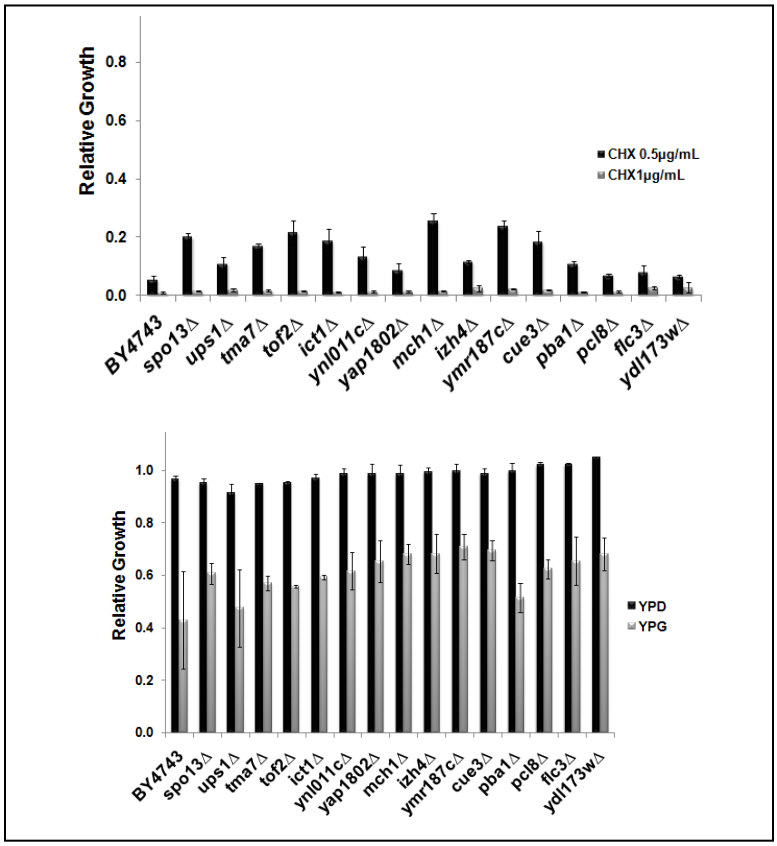

Fig. 2.5. Relative growth of BY4743 and the top 15 Tcin-resistant mutants in the presence of cycloheximide or hygromycin. Cells were grown in 0.5 µg/mL (Top Panel) or 1 µg/mL cycloheximide. (Bottom Panel) Cells were grown in 10 µg/mL hygromycin B in either liquid YPD or YPG media. Relative growth was calculated as the ratio between growth of treated cells to that of untreated cells with a ratio of 1.0 indicating no effect on growth. Error Bars represent standard error of two independent experiments with each experiment done in triplicate.

The mechanistic details by which trichothecene mycotoxins kill target cells are not yet fully delineated. Here, we identified genes in a number of cellular pathways previously unknown to play a role in trichothecene toxicity and demonstrated for the first

time that mitochondrial membrane maintenance and translation are critical for sensitivity to a trichothecene mycotoxin. Identification of a set of genes whose deletion leads to enhanced Tcin resistance suggests that orthologs of these genes may provide novel targets for developing resistance to trichothecene mycotoxinss in plants. This work also draws attention to the similarities between the toxic effects of trichothecenes on mammalian cells and toxin-induced cell death in *Saccharomyces cerevisiae*.

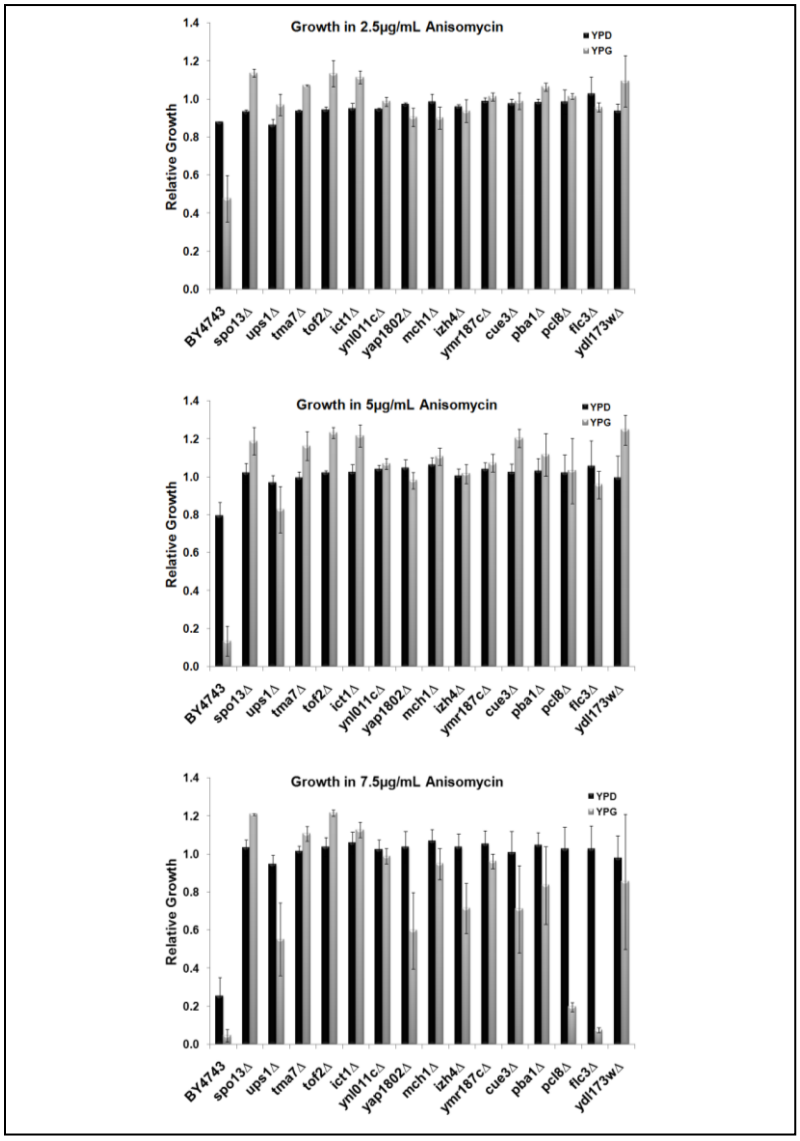

Fig. 2.6. Growth of the Tcin resistant 15 strains in the presence of anisomycin in YPD or YPG media. The Tcin resistant 15 strains were grown in YPD or YPG liquid media containing 2.5, 5 or 7.5 µg/ml anisomycin. Cells in YPD media were incubated at 30°C for 20 hours, while cells in YPG media were grown for 48 hours at 30°C. Relative growth was calculated as the ratio between growth of treated cells to that of untreated cells with a ratio of 1.0 indicating no effect on growth.

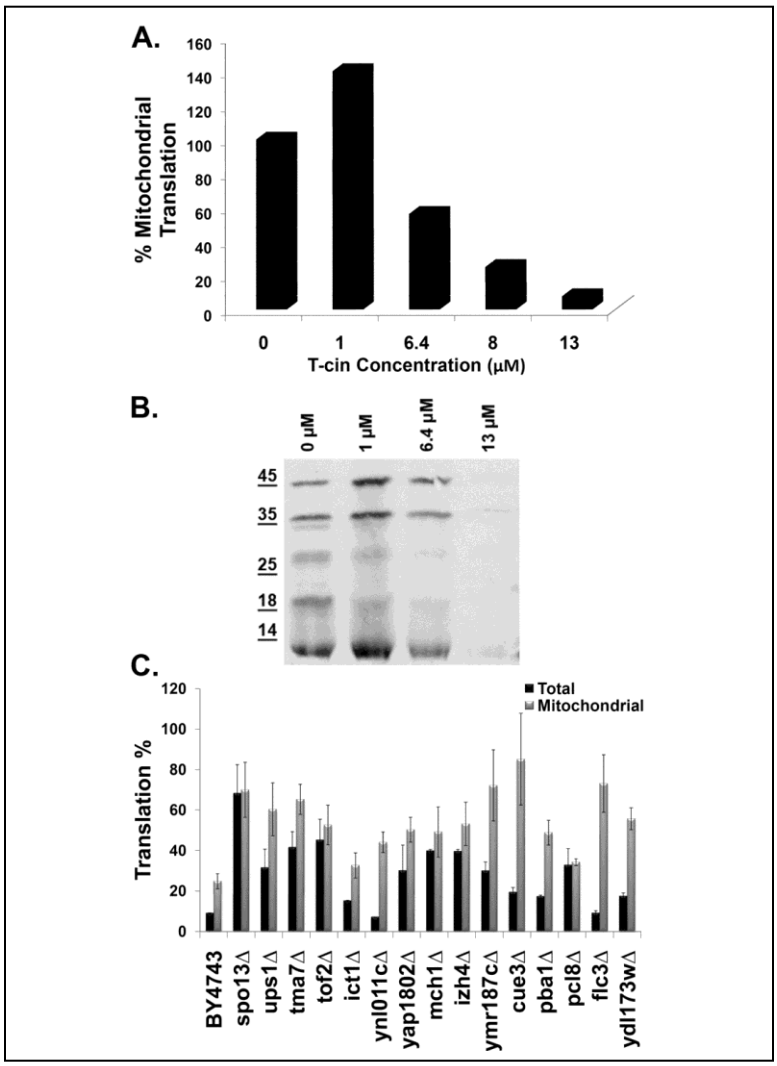

Fig. 2.7. Effect of Tcin on mitochondrial translation. (A) Mitochondrial translation rate of the BY4743 cells was determined by measuring the rate of [^{35}S]-methionine incorporation *in vivo* at increasing concentrations of Tcin. All treatments were performed for 1hr and the rate of translation in the absence of Tcin was normalized to 100%. (B) Autoradiogram of labeled mitochondrial translation products separated on a 15 % SDS-polyacrylamide gel. (C**)** Samples were treated with 8 µM Tcin/OD_{600} of cells for 1 hour as described in the Materials and Methods. The ratio of translation between Tcin-treated

and untreated samples for both total and mitochondrial translation is represented as percent of the untreated control. Each graph represents the mean of four independent experiments with error bars representing the standard deviation.

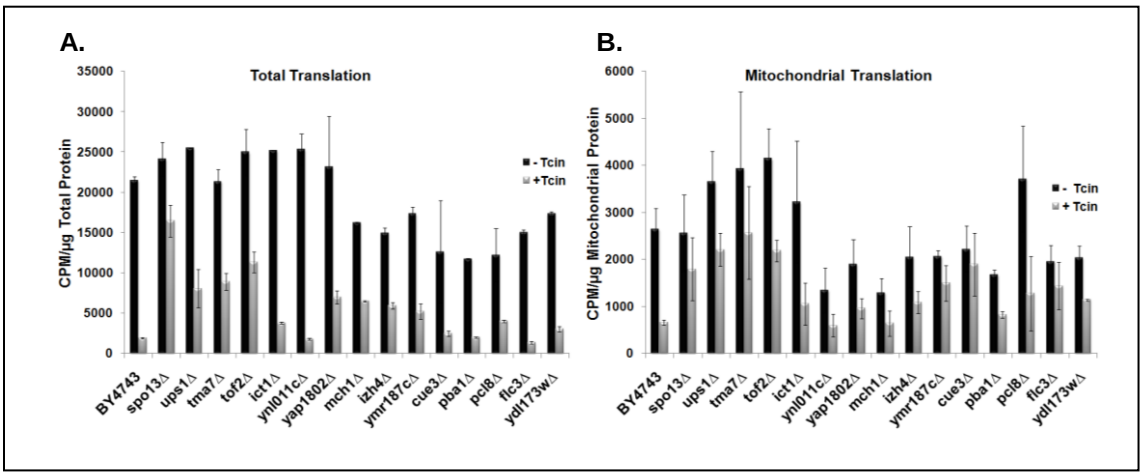

Fig. 2.8. Effects of Tcin on total and mitochondrial translation in the most resistant 15 deletion strains. Total translation (A) and mitochondrial translation (B) for the wild type and the most resistant 15 deletion mutants is shown. Samples were treated with 8 µM Tcin/OD_{600} of cells for 1 hour. Each graph represents the mean of four independent experiments with error bars representing the standard deviation.

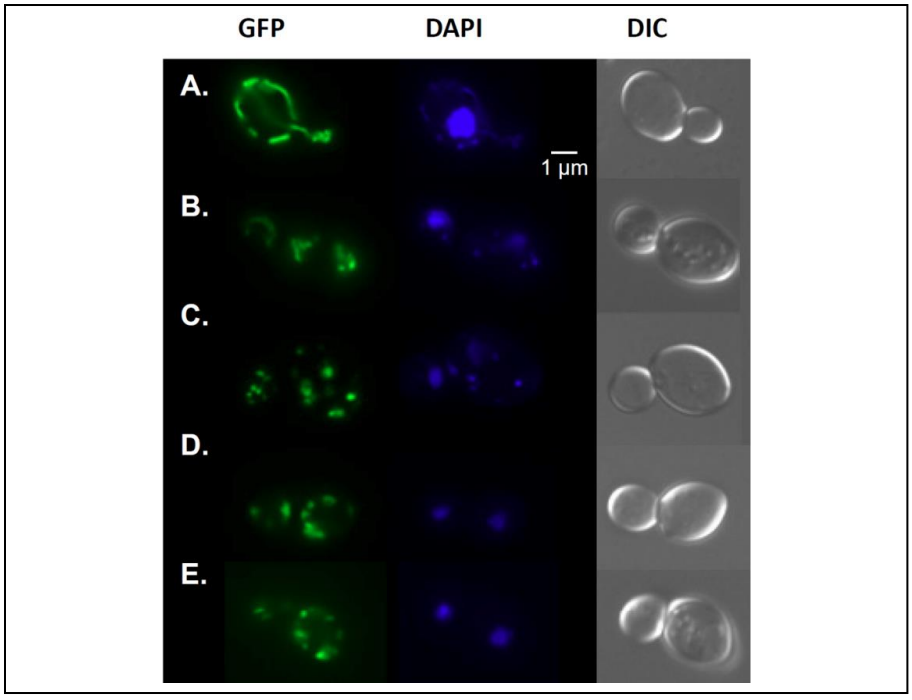

Fig. 2.9. Effect of Tcin on mitochondrial morphology. Mitochondrial morphology of (A) BY4743 control (B) BY4743 treated with 8 µM Tcin for 4 hours, (C) BY4743 treated with 80 µM Tcin for 4 hours, (D) *fzo1*Δ control, (E) *fzo1*Δ treated with 8 µM Tcin for 4 hours was analyzed using epifluorescence microscopy. Cells were transformed with pVT100U-mtGFP, containing GFP targeted to the mitochondrial matrix. Nuclear and mitochondrial DNA was stained with DAPI. Differential interference contrast (DIC) images of each cell are presented.

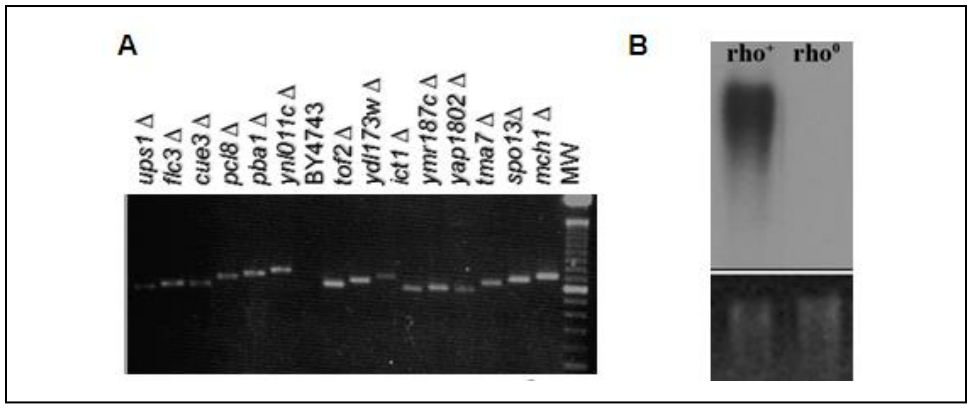

Fig 2.10. Verification of the top 15 Tcin-resistant deletion strains and the BY4743 rho^0 strain. (A) Each strain was verified using PCR amplification using specific cassette primers unique to each strain as described in the Materials and Methods. The amplification products were separated on a 1% agarose gel. MW denotes the molecular marker. The parental strain, BY4743, is included as the negative control. (B) Southern blot analysis of rho$^+$ BY4743 strain and a rho^0 strain derived from the parental BY4743 strain using a *COX1* probe. The lower panel shows the ethidium bromide stained DNA separated on a on a 1% agarose gel, indicating equal loading of the samples.

2.4 Materials and Methods

Tcin isolation. Trichothecin (Tcin) was isolated from liquid shake cultures of *Trichothecium roseum* (no. A27955 or NRRL3704). One liter cultures in yeast extract-peptone-dextrose (YEPD) were harvested after 7-14 days and extracted twice with equal

volumes of ethyl acetate. The combined extracts were concentrated under reduced pressure. The resulting syrup was initially separated on a silica gel (70-230 mesh, Sigma) column eluted with 5% methanol-dichloromethane. Column fractions were monitored with GCMS and fractions containing Tcin were combined and concentrated. Tcin was purified on a silica gel column eluted with hexane:ethyl acetate (3:1). Fractions were checked for purity with GCMS. Tcin was crystallized from hexane:ethyl acetate and petroleum ether. Tcin was a generous gift from Dr. Susan McCormick (Bacterial Foodborne Pathogens and Mycology Unit, USDA-ARS-NCAUR, Peoria, IL).

Yeast deletion library screen. The yeast genome homozygous diploid gene deletion set (Open Biosystems) was screened for resistance to 4 µM Tcin. The strains from the deletion library were replica plated into 96 deep-well plates containing YPD (2% glucose) liquid media with or without Tcin Experiments were performed in triplicate. Cells were grown for 20 hours in the HiGro shaker (GeneMachines) at 250 rpm at 30°C. The OD_{600} for treated and untreated samples was obtained and the relative growth determined as the growth ratio of toxin treatment to the control. A ratio of 1 indicated that the treatment had no effect on the strain. The resistance level of a particular strain was based jointly on the mean ratio score and the coefficient of variation (CV). The threshold for 4 µM Tcin resistance was defined as strains which had a ratio of 0.25 or higher and a CV of less than 0.5.

Antibiotic Assays. Overnight cultures were transferred using a 96-pin pronger into 96-well plates containing Tcin or the different antibiotics in liquid YPG (3% glycerol) or YPD. Antibiotics were used at the following concentrations: Tcin (1, 2, 4,

8, 12, 16, and 24 µM), cycloheximide (0.5, 1, and 10 µg/ml), chloramphenicol at 1 mg/ml, anisomycin (2.5, 5, 7.5 and 10 µg/ml) and hygromycin B (10, 50, 100 and 200 µg/ml). Cells were grown for 20 h in YPD and for 48 h in YPG media by shaking at 250 rpm and 30°C. The relative growth was measured as described above. All experiments were performed in triplicates and repeated twice.

Strain verification. Yeast strain verification was carried out by PCR using knockout cassette specific primers for each of the 15 Tcin-resistant deletion mutants (yeastdeletion.stanford.edu) (Fig. 2.10A).

rho^0 strains. rho^0 versions of BY4743 were generated as described previously (Rasmussen et al., 2003). The respiratory deficiency of the rho^0 strains was confirmed by the complete lack of growth on YPG (3% glycerol). The absence of mitochondrial DNA was confirmed by staining paraformaldehyde-fixed cells with DAPI and by Southern blot analysis (Fig. 2.10B) using a mitochondrial *COX1* probe (Cheng et al., 2009).

Total translation assay. Cultures of BY4743 and the top 15 resistant mutants were grown in SD-Met containing MSG as the nitrogen source and 2% glucose. Each culture, grown to an OD_{600} of 0.5-0.6 (4.5-5.4 X 10^7 cells/ml), was then split into two halves. One half was treated with 8 µM Tcin/OD_{600} cells and the other half with an equivalent amount of ethanol (0.03%) for 1h, shaking at 30°C. Cold methionine (50 µM) and 1 µl [^{35}S]-Met (PerkinElmer, NEG-009A, >1000 Ci/mmol) was added. The reaction was stopped after 60 min and [^{35}S]-Met incorporation was measured as previously described (Parikh et al., 2002). The rate of incorporation of [^{35}S]-Met was linear up to 60 min.

Mitochondrial translation assay. Mitochondrial translation was measured using a modified assay developed by Fox et al. (Fox et al., 1991). Fresh YPR (2% raffinose) media was added to an overnight yeast culture, grown in YPR, and incubated for 2-3 h. An equivalent of 10 OD_{600} cells were pelleted, washed twice and resuspended in SD-Met media supplemented with 2% raffinose and treated with 8 µM Tcin/OD_{600} or an equivalent amount of ethanol (control) for 1 h at 30°C. Cycloheximide was immediately added to each sample to stop cytosolic translation followed by addition of 25µCi [^{35}S]-Met. Mitochondria were isolated and [^{35}S]-Met incorporation was determined as described (Fox et al., 1991).

Microscopy. Mitochondrial morphology was examined by epifluorescence microscopy (Olympus BX41) using cells transformed with pVT100U-mtGFP. pVT100U-mtGPF is a 2µ plasmid with a *URA3* marker, which contains green fluorescent protein (GFP) targeted to the mitochondria using the presequence from the subunit 9 of the F0-ATPase of *Neurospora crassa* under the control of the constitutive ADH promoter (Westermann and Neupert, 2000).

CHAPTER 3

Mitochondrial functions are directly inhibited by type A and type B trichothecenes.

Acknowledgement: Experiments in this chapter was performed with some assistance from Debaleena Basu, a graduate student, who helped with isolation of mitochondria from yeast as well as the microscopic analysis of the yeast samples. Results and partial sections of this chapter have been published in the article (cited below) written by the thesis author. This chapter has modified and expanded this publication to include later findings and modifications to some of the figures that were present in the original publication.

Publication Citation: Bin-Umer, M.A., McLaughlin, J.E., Basu, D., McCormick, S., and Tumer, N.E. (2011). Trichothecene mycotoxins inhibit mitochondrial translation—Implication for the mechanism of toxicity. Toxins *3*, 1484-1501.

Abstract

Fusarium head blight (FHB) reduces crop yield and results in contamination of grains with trichothecene mycotoxins. We previously showed that mitochondria plays a critical role in the toxicity of a type B trichothecene. Here, we investigated the direct effects of type A and type B trichothecenes on mitochondrial translation and membrane integrity in *Saccharomyces cerevisiae*. Sensitivity to trichothecenes increased when functional mitochondria were required for growth, and they inhibited mitochondrial translation at concentrations, which did not inhibit total translation. *In organello* translation in isolated mitochondria was inhibited by type A and B trichothecenes, demonstrating that they have a direct effect on mitochondrial translation. In intact yeast cells trichothecenes showed dose-dependent inhibition of mitochondrial membrane potential and reactive oxygen species, but only at doses higher than those affecting mitochondrial translation. These results demonstrate that mitochondrial translation is a primary target of trichothecenes and is not a secondary effect of disruption of mitochondrial membranes.

3.1 Introduction

Mitochondrial translation, unlike cytosolic translation, has been poorly studied. The circular mitochondrial genome is roughly 85,000 base pair in size encoding eight proteins, essential for oxidative phosphorylation (OXPHOS). Mitochondrial transcripts are distinct from nuclear transcripts and hence they deviate from standard genetic code, lack the 5' mRNA cap and have short and non-polyadenylated untranslated regions (UTR) (Kuzmenko et al., 2013). Mitochondrial ribosomes which have lower sedimentation coefficient are assembled and anchored onto the inner mitochondrial membrane via anchoring proteins. Since mitochondrial translation machinery is membrane bound, changes in the lipid composition of the inner mitochondrial membrane (IMM) affects translation (Fox, 2012). Mitochondrial DNA (mtDNA) encoded proteins include the seven hydrophobic subunits of complexes III, IV, and V and the mitochondrial small ribosomal protein, Var1 (Kuzmenko et al., 2013).

Mitochondria encoded proteins that constitute the electron transport chain include cytochrome b (Cob) subunit of bc1 complex (III), Cox1, Cox2, and Cox3 subunits of cytochrome c oxidase (IV), Atp6, Atp8, and Atp9 subunits of ATP synthase (V) (Fox, 2012). Assembly of the different subunits into higher ordered complexes is tightly regulated because unassembled subunits especially Cox1 significantly promotes oxidative stress (Fox, 2012). Translation of mitochondrial mRNA transcripts in yeast is initiated by mRNA-specific translation activators which recognize their targets via 5'UTRs (Fontanesi, 2013; Fox, 2012).

Mitochondrial proteome, however, is largely encoded by nuclear genes. A large fraction (25%) of these nuclear encoded mitochondrial proteins is involved in mitochondrial genome maintenance and translation of mtDNA-encoded proteins while the rest are involved in energy metabolism (15%), protein translocation and folding (10%). Another 20% of these proteins remain to be characterized (Fox, 2012). Cytoplasmic synthesis of some mitochondrial proteins is localized to mitochondria. In some instances the 3'UTR of the mRNA transcript contains binding sites for proteins (eg. Puf3) located on the outer mitochondrial membrane (OMM). Some mRNA transcripts are selectively synthesized by mitochondria-bound polysomes because of the signal sequence in their 3'UTR while others are synthesized by free polysomes but then directed to the organelle by the mitochondria targeting sequence (MTS) (Fox, 2012).

Because mtDNA encodes an essential subset of the OXPHOS machinery responsible for ATP production, global reduction of mitochondrial translation leads to misassembly of the different complexes that constitute the electron transport chain and in turn adversely affects respiration (Bonawitz et al., 2006). In addition to its effect on oxidative phosphorylation, mitochondrial translation is also required for mitochondrial genome maintenance because defects in mitochondrial genome maintenance affect mitochondrial membrane dynamics. During metabolic or environmental stress the dynamic process of membrane fusion and fission maintains functional integrity of mitochondria. This is particularly important because perturbed fusion-fission machinery has been implicated in neurodegenerative diseases (Youle and van der Bliek, 2012). Fusion allows for mixing contents of partially damaged mitochondria via

complementation by sharing RNA and protein components (Knorre et al., 2013). Fusion also maximizes oxidative phosphorylation (OXPHOS) and oxidative capacity of the mitochondria to an extent during stress. On the other hand, fission creates new mitochondria as well as removes damaged segments of the mitochondrial network (Youle and van der Bliek, 2012). Fragmented mitochondrial membrane is generally characteristic of dying yeast. However, fission also occurs robustly in cells not undergoing cell death but the rate of fission is significantly higher in dying cells. Furthermore, mitochondrial matrix fragmentation has been suggested as a protective mechanism during cell death since it facilitates removal of damaged parts of mitochondria (Fannjiang et al., 2004).

Nuclear encoded genes involved in mitochondrial translation when knocked out also leads to loss of mitochondrial DNA and a petite phenotype (Contamine and Picard, 2000). This is particularly important because petite transformation can result in the upregulation of Pdr3 transcription factor which results in pleiotropic drug resistance (PDR) or multiple drug resistance (MDR) by activating efflux pumps and thus rendering the cells resistant to a plethora of growth inhibitors (Hallstrom and Moye-Rowley, 2000). Thus mitochondria has been a major focus in antifungal, antibacterial and cancer biology research.

Although not exhaustively investigated, mitochondria also plays a significant role in Fusarium pathogenesis and trichothecene toxicity. For instance, plant colonization by *F. oxysporum* requires a mitochondrial carrier protein because virulence was significantly reduced in mutants not expressing this protein (Inoue et al., 2002). Furthermore, the type B trichothecene, deoxynivalenol (DON) was found to localize to mitochondria in infected

wheat spikes and kernels (Kang and Buchenauer, 1999), transcription profile of genes associated with mitochondria were significantly altered in *Saccharomyces cerevisiae* treated with the type A trichothecene, T-2 (Iwahashi et al., 2008; Jossé et al., 2010), and mitochondria-dependent apoptotic pathways were activated in mammalian cells exposed to T-2 (Bouaziz et al., 2009). Moreover, in our genome-wide screening study we identified gene deletions affecting mitochondrial morphology and function to be the largest set of genes conferring resistance to Tcin, a type B trichothecene, in yeast (McLaughlin et al., 2009). Furthermore, we showed that mitochondrial translation in these yeast deletion mutants was not inhibited upon treatment with Tcin, unlike the parental strain (McLaughlin et al., 2009). However, in almost all instances inhibition of mitochondrial translation correlated with total translation (McLaughlin et al., 2009), suggesting that inhibition of mitochondrial translation could possibly be a secondary effect of trichothecenes' action on cytosolic translation. The objective of this study was, therefore, to investigate the direct effects of trichothecenes on mitochondrial translation separate from cytosolic translation.

In this study, to determine if trichothecenes have a direct effect on mitochondrial translation, we examined *in organello* translation in mitochondria in the presence of different trichothecenes. Our results demonstrate that type A and type B trichothecenes inhibit translation in isolated mitochondria. We further show that trichothecenes have a time and dose-dependent effect on mitochondrial membrane potential and generation of reactive oxygen species (ROS), but only at higher doses than those inhibiting mitochondrial translation, suggesting that organellar translation is a primary target of

both type A and type B trichothecenes and is not inhibited secondary to membrane damage.

3.2 Results

3.2.1 Mitochondria are important for sensitivity to type A and B trichothecenes

To determine if mitochondria were critical for sensitivity to different trichothecenes, yeast were grown in media containing a non-fermentable sugar, glycerol (YPG), which requires functional mitochondria for growth. As shown in Fig. 3.1, the sensitivity of wild type yeast (rho+) to trichothecenes increased when yeast was grown in YPG media. The rho^0 strains, devoid of functional mitochondria can only grow in media containing a fermentable sugar, such as glucose (YPD). A rho^0 strain derived from the wild type strain by ethidium bromide treatment was less sensitive to each trichothecene tested (Fig. 3.1). As shown in Table 3.1, a decrease in the IC_{50} values for each trichothecene was observed when rho+ cells were grown on YPG media compared to YPD media, indicating that wild type yeast were more sensitive to trichothecenes when functional mitochondria were required for survival. Conversely, rho^0 cells showed tolerance to significantly higher concentrations of trichothecenes, as indicated by the higher IC_{50} values (Table 3.1). Similar shifts in sensitivity were also observed in yeast cells treated with DON. These results were in agreement with our previous findings with Tcin (McLaughlin et al., 2009). Among the trichothecenes, T-2 was more toxic than DAS, while DON had the lowest toxicity. The type A trichothecenes are also more toxic than the type B trichothecenes to mammalian cells (Visconti et al., 1991), validating the

role of yeast as a model organism to study trichothecene mechanism of action. The increased sensitivity of actively respiring yeast cells to trichothecenes and their higher tolerance when devoid of functional mitochondria suggest a critical role for mitochondria in sensitivity to type A and type B trichothecenes.

	rho$^+$/Dex	**rho$^+$/Glyc**	**rho^0/Dex**
T-2	95 µM	37 µM	367 µM
DAS	300 µM	139 µM	2400 µM
Tcin [1]	2.5 µM	0.75 µM	17 µM

[1] IC_{50} values for Tcin were based on our earlier study (McLaughlin et al., 2009).

Table 3.1. IC_{50} values for trichothecenes in media containing dextrose (Dex) or glycerol (Glyc). The IC_{50} for each trichothecene was calculated using the growth curves generated from Figure 1.

3.2.2 Trichothecenes have a direct effect on mitochondrial translation

We previously showed that the Tcin (type B trichothecene) inhibited mitochondrial translation to a greater extent in the wild type yeast than in strains selected for growth resistance, implicating mitochondrial translation as a site of action (McLaughlin et al., 2009). We therefore investigated whether trichothecenes have dose-dependent effects on mitochondrial translation by varying trichothecene concentrations and treatment time period. At six hours post treatment with low concentrations of trichothecenes we found total translation to be largely unaffected when compared to the untreated control. In contrast, mitochondrial translation was inhibited 34% by 1 µM Tcin, 48% by 53.75 µM T-2, and 42% by 150 µM DAS (Fig. 3.2A). Total translation remained uninhibited even when the treatment time was increased to eighteen hours (Fig.

3.2B). However, in agreement with previous reports on translation inhibition of trichothecenes in mammalian cells (Cundliffe and Davies, 1977; McLaughlin et al., 1977), total translation was inhibited at high doses of trichothecenes. Six hours post treatment we observed a 44% and 33% inhibition of total translation in cells treated with 215 µM T-2 and 300 µM DAS respectively.

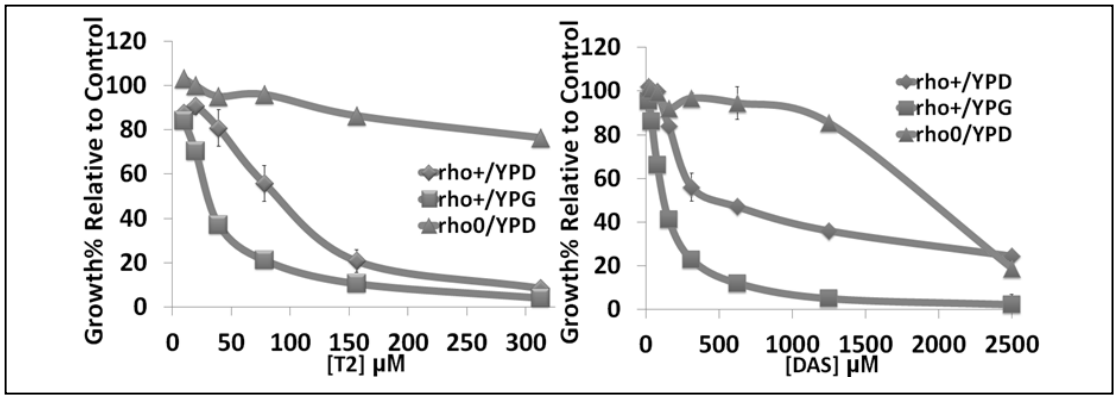

Figure 3.1. Growth of wild type BY4743 cells (rho^{+} & rho^{0}) in media containing dextrose *vs.* glycerol. Rho+ and rho0 cells were grown in liquid media supplemented with 2% dextrose (Dex) or with 3% glycerol (Glyc) in the presence or absence of varying concentrations of trichothecenes for 18 h. OD_{600} of cells treated with increasing concentrations of trichothecenes were compared to that of the untreated cells (control) to determine relative growth. The square plot indicates growth in dextrose-containing media and the diamond plot indicates growth in glycerol-containing media. The triangle plot indicates growth of rho0 in dextrose-containing media. Error bars indicate S.E. where *n* = 3 independent replicates.

To determine if trichothecenes directly inhibit mitochondrial translation, we used an *in organello* assay, in which mitochondria isolated from wild type yeast (Diekert et al., 2001) were treated with trichothecenes and translation was examined by [^{35}S]-methionine incorporation as described (Funes and Herrmann, 2007). As shown in Fig. 3.2C, mitochondrial protein synthesis decreased upon increasing the concentration of

trichothecenes. Thus 43% and 70% inhibition was seen with 4 µM and 8 µM Tcin, 49% and 67% inhibition with 430 µM and 860 µM T-2, and 30% and 55% inhibition with 900 µM and 1.8mM DAS respectively. The decreased sensitivity of *in organello* translation relative to mitochondrial translation in intact cells is likely due to the short (10 min) treatment of the isolated mitochondria relative to the 6 h treatment of intact cells.

The decrease in translation by the isolated yeast mitochondria upon treatment with increasing concentrations of type A and type B trichothecenes indicated that trichothecenes have a dose-dependent effect on mitochondrial protein synthesis. These results demonstrate that trichothecenes directly inhibit mitochondrial translation and provide evidence that inhibition of mitochondrial translation is not a secondary effect of the inhibition of cytosolic translation.

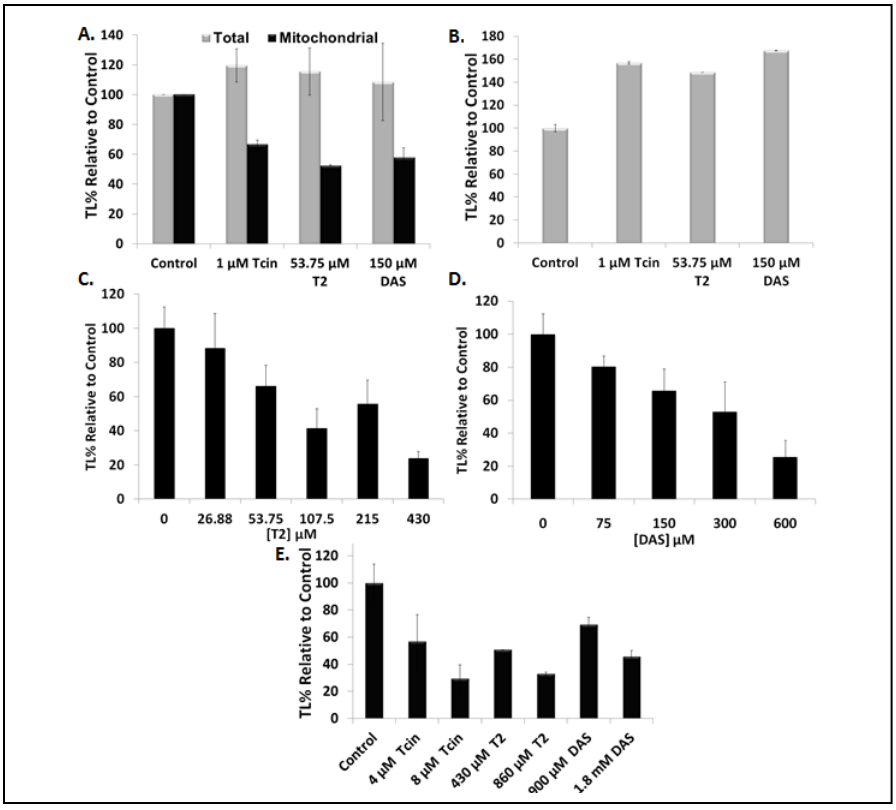

Figure 3.2. Effects of trichothecenes on total and mitochondrial protein synthesis. (A) Total and mitochondrial translation in wild type yeast cells treated with low doses of trichothecenes for 6 h prior to measuring [35S]-Met incorporation; (B) Total translation in wild type yeast cells treated with low doses of trichothecenes for 18 h prior to measuring [35S]-Met incorporation; (C) Mitochondrial translation in yeast cells treated with increasing concentrations of T-2 for 6 h prior to measuring [35S]-Met incorporation; (D) Mitochondrial translation in yeast cells treated with increasing concentrations of DAS for 6 h prior to measuring [35S]-Met incorporation; (E) *In organello* translation using equal amounts of mitochondria, isolated from wild type W303 yeast. 35[S]-methionine incorporation was measured after 10 min treatment with different oncentrations of trichothecenes. Final counts (CPM) for all experiments were normalized to the OD600 of each sample. Translation levels of trichothecene-treated samples were expressed as a percentage of the control samples set to 100%. Error bars indicate S.E. where $n = 3$ independent replicates.

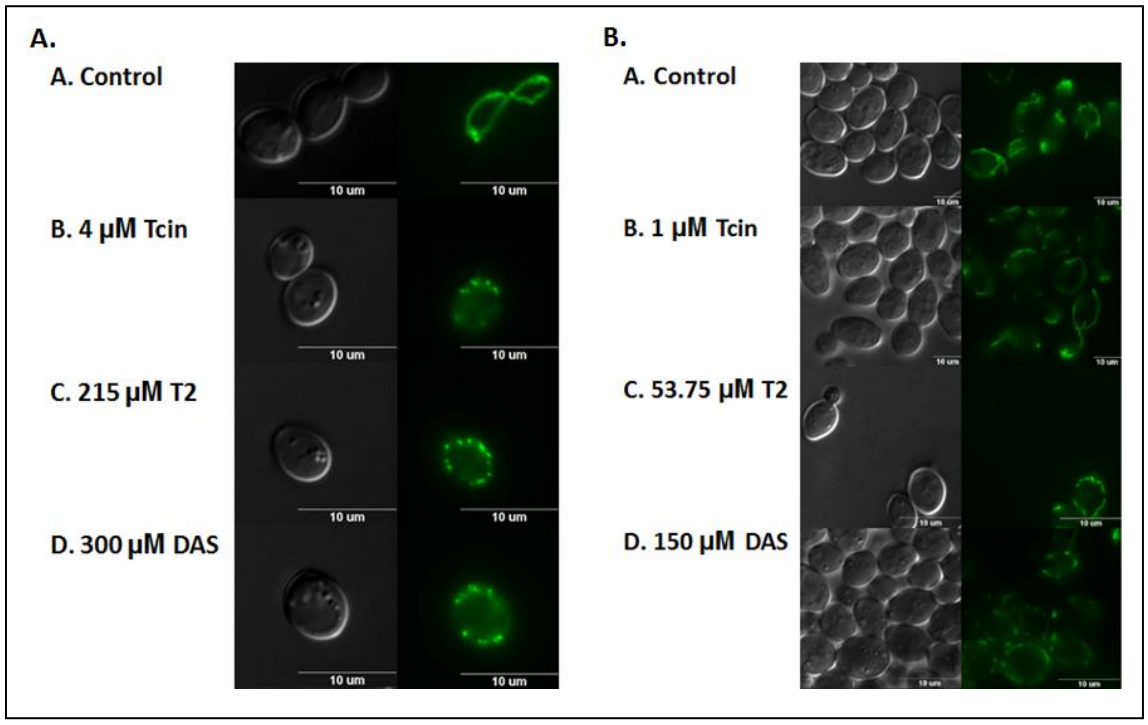

Figure 3.3. Effects of trichothecenes on mitochondrial morphology. Wild type yeast transformed with pVT100U-mtGFP, containing GFP targeted to the mitochondrial matrix was treated for 6 h with high (A) or low (B) doses of trichothecenes. Representative images are shown at 100X magnification using epifluorescence microscopy. Differential Interference Contrast (DIC) images of each cell are presented on the left (Scale bar, 10 µm).

3.2.3 Trichothecenes cause dose-dependent alteration of mitochondrial membrane morphology

We previously showed that Tcin treatment led to the fragmentation of the tubular mitochondrial network in yeast, and Tcin mediated cell death was partially rescued by mutants that regulate mitochondrial fusion and maintenance of the tubular network of mitochondria (McLaughlin et al., 2009). To determine if type A trichothecenes affect mitochondrial membrane morphology, we transformed wild type yeast with pVT100U-mtGFP, encoding a constitutively expressed GFP targeted to the mitochondrial matrix (Westermann and Neupert, 2000). As shown in Fig. 3.3A, wild type yeast showed characteristic morphology of uniformly tubular network (Fig. 3.3A). In contrast, yeast treated with 4 µM Tcin, 215 µM T-2, and 300 µM DAS, exhibited fragmented network of mitochondria. However, when the cells were treated with low doses of trichothecenes (1 µM Tcin, 53.75 µM T-2, and 150 µM DAS), the mitochondrial network remained largely unaffected (Fig. 3.3B). Although obvious changes to the mitochondrial morphology were not observed at these low doses, mitochondrial translation was inhibited (Fig. 3.2A). These results suggest that the inhibition of mitochondrial translation is not due to disruption of the mitochondrial membrane morphology and suggest that translation is inhibited upstream of mitochondrial membrane fragmentation.

3.2.4 Trichothecenes disrupt mitochondrial membrane potential and generation of ROS in a dose and time dependent manner

We previously showed that Tcin-induced cell death was partially rescued by mutants that regulate mitochondrial fusion and maintenance of the mitochondrial network, suggesting that Tcin may affect mitochondrial fusion (McLaughlin et al., 2009). Inhibition of mitochondrial fusion leads to fragmentation of the mitochondria (Chen et al., 2003a) and fusion defective cells show loss of mitochondrial membrane potential (MMP) (Chen et al., 2005a). To determine if type A and type B trichothecenes affect MMP, we used flow cytometric analysis of yeast cells stained with MitoTracker Red (Chen et al., 2003a). Wild type cells stained with MitoTracker Red exhibited an active mitochondrial membrane potential (Fig. 3.4A). In contrast, H_2O_2-treated cells exhibited a significant drop in MMP (44%) relative to the control (Fig. 3.4A). Treatment of the wild type cells with the decoupling agent, carbonyl cyanide 3-chlorophenylhydrazone (*CCCP)* decreased the MMP (22%) due to depolarization of the mitochondria (Gong et al., 1997) (Fig. 3.4A). As expected, the rho^0 cells showed little to no uptake of the MitoTracker Red stain (15%) due to the absence of functional mitochondria (Fig. 3.4A). A significant drop in the MMP was observed when yeast cells were treated with high doses of trichothecenes for 6h (Fig. 3.4C). Thus a 50%, 79%, and 83% drop in MMP was seen with 4 µM Tcin, 215 µM T-2, and 300 µM DAS respectively. This drop in MMP corresponded to the mitochondrial membrane fragmentation observed six hours after treatment with the same doses of trichothecenes, indicating that the loss of MMP correlated with the fragmented morphology of the mitochondria (Fig. 3.3A).

Reactive oxygen species production was quantified by flow cytometry using 2', 7'-dichlorfluorescein-diacetate (*DCFH*-DA) (Machida et al., 1998). Wild type cells

stained for ROS using DCFH-DA showed very low levels of ROS (Fig. 3.4B). In contrast, H_2O_2-treated cells exhibited a significant increase in ROS production relative to the control (Fig. 3.4B). ROS levels decreased by 21%, 70%, and 77% in cells treated with 4 µM Tcin, 215 µM T-2, and 300 µM DAS, respectively (Fig. 3.4D). Although Jossé *et al.* had shown an increase in ROS generation in yeast cells treated with 200 µM T-2 for 4h (Jossé et al., 2010), we observed a decrease at 6h (Fig. 3.4D), which is in agreement with the fragmented mitochondrial morphology (Fig. 3.3A) and the reduced MMP (Fig. 3.4A). These results indicate that at high doses, trichothecenes promote depolarization of the mitochondrial membranes and inhibit ROS production.

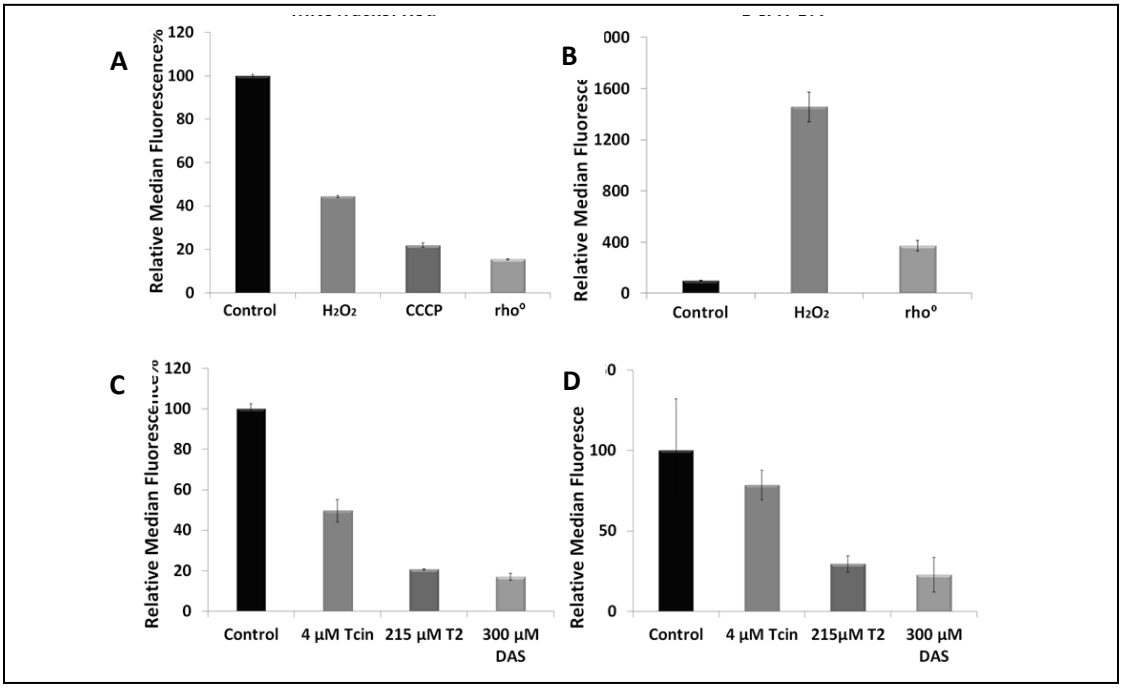

Figure 3.4. Mitochondrial membrane potential and ROS production in cells treated with trichothecenes for 6 h. Petite (rho^0) cells and wild type (rho^+) cells treated with 3 mM H_2O_2, 50 µM CCCP and stained with MitoTracker Red for changes in mitochondrial membrane potential (A) and DCFH-DA for ROS generation (B) Wild type (rho^+) cells treated with high doses of trichothecenes and stained with MitoTracker Red for changes in mitochondrial membrane potential (C) and DCFH-DA for ROS generation (D).

Median fluorescence unit for each treatment was normalized to that of the untreated control and represented as relative fluorescent unit. 25–50,000 cells from each sample were analyzed using an Accuri C6 flow cytometer. Error bars indicate S.E. where $n = 3$ independent replicates.

The effects of trichothecenes on ROS production and MMP were time-dependent when cells were treated with low doses of trichothecenes. At 6h post-treatment an increase in MMP was observed after treatment with 1 µM Tcin (53%) but not with 53.75 µM T-2 (4%) and 150 µM DAS (1%) (Fig. 3.5 A). Moderate increases in ROS production were also observed in 1 µM Tcin (20%) , 53.75 µM T-2 (12%) and 150 µM DAS (18%) treated yeast cells at 6h (Fig. 3.5B). The T-2-induced ROS generation is consistent with previous reports (Jossé et al., 2010). However, when the duration of the treatment was increased from six to eighteen hours, a decrease in MMP (Fig. 3.5C) and ROS levels (Fig. 3.5D) was observed. At 18h post treatment, a 63%, 75%, and 76% drop in MMP and a 37%, 50%, and 65% drop in ROS generation was observed in cells treated with 1 µM Tcin, 53.75 µM T-2, and 150 µM DAS, respectively. This was confirmed by fluorescence microscopy, which showed a decrease in the uptake of the MitoTracker Red in yeast treated with the different trichothecenes for 18h. These results indicate that the effects of trichothecenes on MMP and ROS generation are dose and time-dependent. Although mitochondrial membrane integrity was not compromised at six hours post treatment with the low doses of trichothecenes, mitochondrial translation was significantly inhibited, suggesting that the inhibition of mitochondrial translation is not a consequence of the damage to mitochondrial membrane integrity. Total translation was also not inhibited after treatment of yeast with trichothecenes for 18 h (Fig. 3.2B), but

MMP and ROS production were inhibited, suggesting that the effect of trichothecenes on mitochondrial membrane integrity is not a secondary effect of inhibition of total translation.

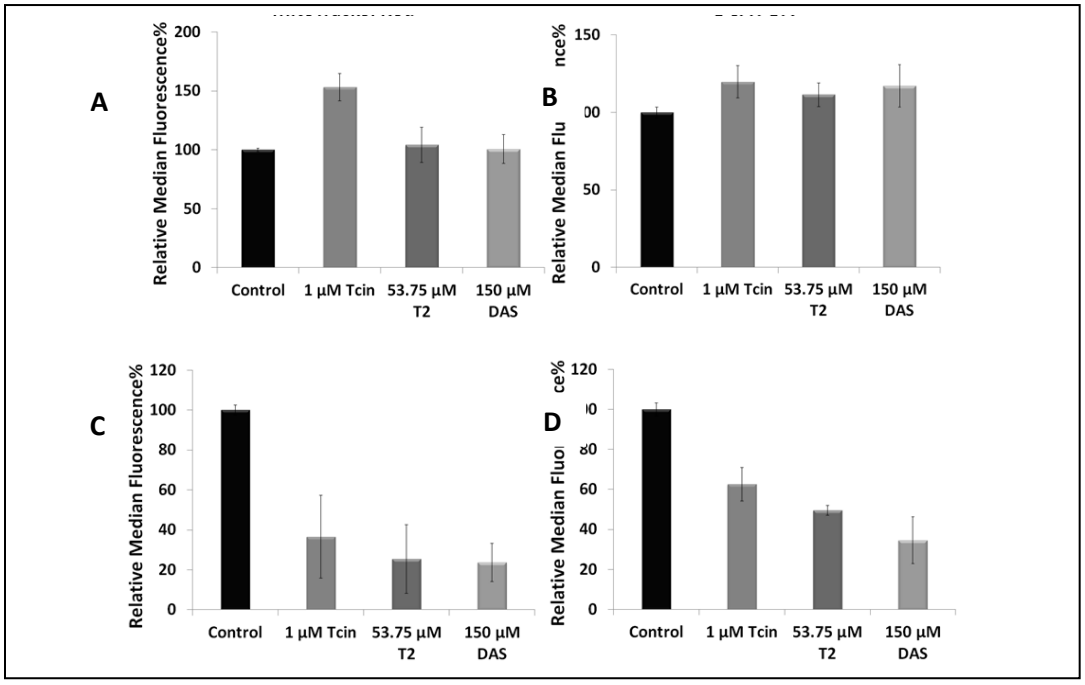

Figure 3.5. Mitochondrial membrane potential and ROS production and in cells treated with trichothecenes for 6 h and 18 h at low doses, which inhibit mitochondrial, but not total translation. Wild type yeast, treated with trichothecenes for 6 h and stained with MitoTracker Red for changes in mitochondrial membrane potential (A) and DCFH-DA for ROS generation (B). At 18 h post treatment with trichothecenes, wild type yeast cells were stained with MitoTracker Red for changes in mitochondrial membrane potential (C) and DCFH-DA for ROS generation (D). Median fluorescence unit for each treatment was normalized to that of the untreated control and represented as relative fluorescent unit. 25–50,000 cells from each sample were analyzed using an Accuri C6 flow cytometer. Error bars indicate S.E. where n = 3 independent replicates.

3.3. Discussion

3.3.1 Trichothecenes inhibit mitochondrial translation directly and prior to cytosolic translation

Trichothecenes have become a substantial health concern in the past decade due to the recurrence of *Fusarium graminearum* and related species in crop fields across the world (CAST, 2003). The changing global climate and the different farming practices have resulted in increased prevalence of trichothecene contamination in cereal grains (McMullen et al., 1997b; Paterson and Lima, 2010). Understanding the mechanisms of trichothecene toxicity at the cellular and biochemical level is critical for inhibiting the toxins' effects on plant productivity and animal and human health.

Trichothecenes induce many cellular and physiological changes and it is likely that they have multiple cellular targets. We previously showed that mitochondrial translation was inhibited less in the yeast knockout mutants that showed resistance to Tcin than the wild type (McLaughlin et al., 2009). In this study, we investigated the effect of type A (T-2 and DAS) and B (Tcin) trichothecenes on mitochondrial translation and membrane integrity. Wild type yeast treated with trichothecenes showed an increase in growth sensitivity when functional mitochondria were required for growth (Fig. 3.1). Yeast cells without a functional mitochondria remained largely resistant to otherwise lethal doses of trichothecenes (Fig. 3.1). Taken together these results provide evidence that mitochondria play a critical role in the sensitivity to type A and type B trichothecenes and suggest that trichothecenes may inhibit a mitochondrial function essential for growth that depends on respiratory activity.

To determine if trichothecenes affect mitochondrial translation, we examined inhibition of total and mitochondrial translation after exposure to increasing doses of trichothecenes. When yeast cells were treated with low doses of trichothecenes, total translation was not inhibited. In contrast, mitochondrial translation was significantly inhibited after treatment with the low doses for 6 h (Fig. 3.2A), suggesting that inhibition of mitochondrial translation was not a secondary effect of the inhibition of total translation. To determine if trichothecenes have a direct effect on mitochondrial translation, we examined *in organello* translation in isolated mitochondria. Translation was inhibited in isolated yeast mitochondria after treatment with increasing concentrations of trichothecenes (Fig. 3.2C). These results indicate that trichothecenes have a direct effect on mitochondrial translation independent of their effects on cytosolic translation.

3.3.2 Mitochondrial translation inhibition by trichothecenes is not a secondary effect of disrupted mitochondrial membrane dynamics

The inhibition of mitochondrial translation could be due to the damage to the mitochondrial membrane, which might render mitochondria nonfunctional. To address this possibility, we investigated the effects of type A and B trichothecenes on mitochondrial morphology. The tubular mitochondrial network, characteristic of actively respiring cells, was severely fragmented after treatment with the high doses of trichothecenes (Fig. 3.3A), but not after treatment with the low doses of trichothecenes (Fig. 3.3B), even though mitochondrial translation was inhibited. These results suggest

that inhibition of mitochondrial translation was not due to the effects of trichothecenes on the mitochondrial membrane morphology.

To further assess the effects of trichothecenes on mitochondrial membrane integrity, we measured MMP and ROS levels, two biomarkers for mitochondrial integrity. T-2 toxin was previously reported to promote severe damage to the DNA via generation of ROS in both yeast and mammals (Chaudhari et al., 2009; Iwahashi et al., 2008; Jossé et al., 2010). Mitochondrial ROS generation is believed to be dependent on mitochondrial membrane potential. Studies involving cell death induced by chemicals such as hydrogen peroxide (H_2O_2) and acetic acid (CH_3COOH) (Dumont et al., 1999; Ludovico et al., 2002; Ludovico et al., 2001; Whittemore et al., 1995) have shown that prior to ROS generation the mitochondrial membrane becomes hyperpolarized leading to excess ROS production followed by depolarization of the mitochondrial membrane (Eisenberg et al., 2007; Pozniakovsky et al., 2005). A depolarized mitochondrial membrane can also lead to the fragmentation of the mitochondrial tubular network (Chen et al., 2005b; Ishihara et al., 2003; Legros et al., 2002).

Unlike actively respiring cells which exhibited an active MMP (Fig. 3.4A) and low ROS production (Fig. 3.4B), cells treated with high doses of trichothecenes showed depolarization of mitochondrial membranes (Fig. 3.4C). A corresponding decrease in ROS levels was observed in yeast treated with the high doses of trichothecenes (Fig. 3.4D). The fragmented mitochondrial network observed after treatment with the high doses of trichothecenes (Fig. 3.3A) could therefore be due to the depolarization of the mitochondrial membranes. Mitochondrial membranes may be affected due to inhibition

of cytosolic translation. To address this possibility, we examined MMP and ROS levels in cells treated with the low levels of trichothecenes, which did not inhibit total translation.

MMP increased in cells treated with low doses of trichothecenes at 6h after treatment (Fig. 3.5A). Moderate increases in ROS levels (Fig. 3.5B) were observed in yeast treated with Tcin, T-2 and DAS at the 6h time point. However, when the duration of the treatment was increased from 6 to 18h, MMP (Fig. 3.5C) and ROS levels (Fig. 3.5D) decreased. The drop in MMP observed at 18 h could be due to an increase in ROS that occurred earlier. ROS levels may begin to drop as the mitochondrial membrane becomes depolarized by the trichothecenes. In a previous study, Chaudhari *et al.* (Chaudhari et al., 2009) showed significant increases in ROS levels in human cervical cancer cells within thirty minutes of treatment with T-2. ROS levels decreased 4h after treatment with T-2 (Chaudhari et al., 2009). These results indicate that trichothecenes have dose- and time-dependent effects on mitochondria.

Mitochondrial translation was inhibited when yeast were treated with low doses of trichothecenes for 6h (Fig. 3.2A), while the cells maintained the tubular mitochondrial morphology (Fig. 3.3B) and an active MMP (Fig. 3.5A). These results suggested that mitochondrial translation inhibition is independent of damage to the mitochondrial membranes and may occur upstream of the membrane damage. Treatment with low doses of trichothecenes after 18h caused significant depolarization of the mitochondrial membranes (Fig. 3.5C) and a decrease in ROS levels. Since total translation was not inhibited after 18h treatment (Fig. 3.2B), the time-dependent damage to mitochondrial

membranes was not a consequence of the inhibition of total translation. The mitochondrial membrane damage may occur downstream of inhibition of mitochondrial translation. Alternatively, trichothecenes may have an independent effect on mitochondrial membranes, which leads to the loss of MMP.

Recent studies have implicated mitochondria as a target of other toxins. A type I ribosome inactivating protein (RIP) Saporin-6 induces mitochondrial-dependent apoptosis independent of cytosolic translation inhibition (Sikriwal et al., 2008) and was recently shown to specifically cleave the human mitochondrial DNA D-loop (Gasperi-Campani et al., 2005). Mitochondrial dysfunction was implicated in the toxicity of several mycotoxins including zearalenone (Ayed-Boussema et al., 2008), enniatins (Tonshin et al., 2010), and acremonium (Kruglov et al., 2009). In almost all these instances respiration and apoptotic signaling have been the main focus of investigation. In light of our findings, it will be interesting to determine whether alterations in mitochondrial translation play a role in cell death induced by these toxins. It will be of significant importance to include the mitochondrial translation machinery as a potential target for drug discovery and for engineering crop plants resistant to FHB. It will also be important to investigate the effects of trichothecenes on mitochondria from higher eukaryotes and determine how the pathogen itself protects its own mitochondria from the deleterious effects of these toxins.

3.4 Materials and Methods

Yeast Strain. Yeast strain BY4743 (*MATa/α, his3Δ1/his3Δ1, leu2Δ0/leu2Δ0, LYS2/lys2Δ0, met15Δ0/MET15, ura3Δ0/ura3Δ0*) was used for all experiments except the *in organello* translation assay. Mitochondria, for the *in organello* translation assay, was isolated from W303 (*MATa/α, leu2-3, 112 trp1-1, can1-100, ura3-1, ade2-1, his3-11, 15*).

Trichothecene Isolation. Tcin was isolated from *Trichothecium roseum* and prepared as described previously (McLaughlin et al., 2009). 4,15- Diacetoxyscirpenol was isolated from YEPD cultures of *F. sporotrichioides* strain 1716 cos 9-1#1 (a mutant of *F. sporotrichioides* NRRL3299) (Hohn et al., 1993), and purified on a silica gel column eluted with 5% methanol in dichloromethane. T-2 toxin was isolated from YEPD cultures of *F. sporotrichioides* strain 5493 cos9-1 #11 (a mutant of *F. sporotrichioides* NRRL3299) (Hohn et al., 1993), and purified on silica gel columns eluted with 5% methanol in dichloromethane and hexane/ethyl acetate/methanol (12:12:1). All trichothecenes were provided as a generous gift from Dr. Susan McCormick (Bacterial Foodborne Pathogens and Mycology Unit, USDA-ARS-NCAUR, Peoria, IL).

Growth Assay. Wild type BY4743 cells were grown in yeast peptone (YP) media supplemented with either 2% dextrose (YPD) or 3% glycerol (YPG) at 200 rpm at 30°C. Growth at OD_{600} was measured using the SpectraMax® Plus384 (Molecular Devices, Sunnyvale CA).

Total In vivo Translation Assay. Cells were grown in synthetic methionine dropout (SD-Met) media containing MSG as the nitrogen source and 2% raffinose.

Cultures grown to an OD_{600} of 0.2–0.3 were then split into two: One-half treated with the specified amount of trichothecenes and the other half with an equivalent amount of ethanol. Treatments were carried out for the specified amount of time, shaking at 30°C. At the end of trichothecene treatment, OD_{600} was measured and 3 OD_{600} cells washed with minimal media and resuspended in 500 µL SD-Met (+ 2% raffinose). To each sample, 1 µL [^{35}S]-Met (Perkin-Elmer, NEG-009A, >1,000 Ci/mmol) was added. The reaction was stopped after 20 min (linear range) by washing and resupending cells in 500 µL (20 mM) cold methionine and 75 µL Rodel Mix (560 µL 5 M NaOH, 0.11 mL β-mercaptoethanol, 0.76 mL H_2O, 0.075 mL 1 mM PMSF). An equal volume of 50% TCA (trichloroacetic acid) was added to the mix and filtered through 2.4 cm glass fiber filters (grade 691, VWR). Filters were then washed, once each, with 5% TCA and 95% ethanol and scintillation counts per minute (CPM) measured. CPM readings were finally normalized to OD_{600} to indicate total translation.

Mitochondrial In vivo Translation Assay. Mitochondrial translation assay was done as outlined in section 2.4 (Total *In vivo* Translation Assay) with some modifications as described previously (Barrientos et al., 2002). Prior to the addition of [^{35}S]-Met, 20 µL (7.5 mg/mL) freshly prepared cycloheximide was added to each sample and incubated for 5 min. Following cycloheximide treatment, [^{35}S]-Met was added as described in section 2.4 and incorporation measured and normalized to OD_{600}.

Mitochondrial Isolation from Yeast. Mitochondria were isolated from yeast as described previously (Diekert et al., 2001). Briefly 10 g (wet weight) yeast cells were collected from an overnight culture grown, in YP media supplemented with 2% lactate, to

1-2 OD_{600}. All spins, unless otherwise noted, were done for 5 min at 2500g. The pellet was washed with H_2O and incubated in freshly prepared TD buffer (100 mM Tris–SO4, pH 9.4, 10 mM DTT) for 5 min with gentle shaking. The pellet was then resuspended in SP buffer (1.2 M sorbitol, 20 mM potassium phosphate, pH 7.4) to which zymolyase was added for spheroplast formation. The spheroplasts were carefully collected and resuspended in 2X SHP buffer (1.2 M sorbitol, 40 mM HEPES–KOH, pH 7.4, 1 mM PMSF) to which equal volumes of ice-cold H_2O containing 1 mM PMSF was added. The resulting suspension was then carefully homogenized with a glass homogenizer. The homogenate was then centrifuged twice at 4°C and the supernatant collected from each spin was combined and centrifuged for a further 10 min at 12000g at 4°C. The resulting pellet was resuspended in 1X SH buffer (0.6 M sorbitol, 20 mM HEPES–KOH, pH 7.4) for the *in organello* translation assay after protein quantification by Bradford assay (Kruger, 2002).

Mitochondrial in organello Translation Assay. In organello translation, using isolated yeast mitochondria, was done as described previously (Diekert et al., 2001) with some modifications. All incubations were done at 30°C. Briefly, following a ten minute treatment with trichothecenes, 1 µL [^{35}S]-Met was added to 20 µg of freshly isolated mitochondria, resuspended in the 1X SH buffer, as outlined in section 2.4 and incubated for 20 min. Labeling was stopped by adding 10 µL (200 mM) cold methionine and incubating for 5 min. Mitochondria were collected by centrifugation for 10 min at 20,000g at 4°C. The pellet was washed with 1X SH buffer and then filtered through 2.4cm glass fiber filters. Filters were washed once each with 5% TCA and 95% ethanol

and scintillation counts per minute (CPM) measured. Readings were expressed as CPM/µg mitochondrial protein.

Staining, Microscopy & Image Analysis. Mitochondrial morphology was examined using an epifluorescence microscope (Olympus BX41). BY4743 cells were transformed with pVT100U-mtGFP, which contains the green fluorescent protein (GFP) targeted to the mitochondria, with the presequence from the subunit 9 of the F0-ATPase of *Neurospora crassa*, as described previously (Westermann and Neupert, 2000). Trichothecene-treated and untreated cells were stained with 2', 7'-dichlorfluorescein-diacetate (DCFH-DA) for ROS generation and *MitoTracker Red* CMXRos for mitochondrial membrane potential according to manufacturer's protocol. Stained cells were then examined with the Olympus BX41 microscope. All images were captured and analyzed using the *MetaMorph*® Microscopy Automation & Image Analysis software (Molecular Devices, Sunnyvale CA).

Flow Cytometry. Trichothecene-treated and untreated cells, following staining with the appropriate dyes, were analyzed using the Accuri C6 Flow Cytometer® (Accuri Cytometers Inc., Ann Arbor MI). For each sample 25-50,000 events were recorded. Channel gating and histogram plots were made using the CFlow Plus Analysis software (Accuri Cytometers Inc., Ann Arbor MI). Changes in MitoTracker Red and DCFH-DA fluorescence were detected using the FL1 and FL3 channel respectively.

Data Analysis & Graphing. Data from the growth and translation assays were analyzed and the graphs were plotted using Microsoft Excel.

CHAPTER 4

Mitophagy plays a prosurvival role in alleviating mitochondrial ROS-mediated trichothecene cytotoxicity.

Acknowledgement: Experiments in this chapter was performed with some assistance from Matthew Butterly, an undergraduate student, who helped with growth assays and flow cytometric analysis of yeast samples. The author is currently preparing a manuscript with results and conclusions from this chapter which will be submitted for publication in the near future.

Abstract

Trichothecene mycotoxins are food-borne toxins that poison humans and animals by inhibiting multiple cellular processes, including mitochondrial functions. To understand the molecular mechanism of trichothecene cytotoxicity we have screened the *Saccharomyces cerevisiae* knockout library for increased sensitivity to nonlethal concentrations of trichothecin (Tcin) and identified 121 deletion mutants exhibiting higher sensitivity than wild type. A dose-dependent increase in reactive oxygen species (ROS) levels were observed in wild type yeast treated with trichothecenes, but not when respiratory functions were affected, suggesting that ROS generation requires actively respiring mitochondria. The most sensitive strains exhibited higher levels of Tcin-induced ROS relative to wild-type. Tcin-induced mitochondrial ROS (mtROS) levels and cytotoxicity were alleviated after treatment of wild type cells with antioxidants, but not the sensitive mutants. Mitophagy was blocked during trichothecene treatment while rapamycin treatment reduced ROS levels and cytotoxicity by inducing mitophagy in wild type cells. These results suggest that mitophagy plays a prosurvival role in protecting cells against mitochondrial ROS generated by trichothecenes by preventing the accumulation of damaged mitochondria. Our findings suggest mitophagy as a novel cellular mechanism to reduce mtROS-mediated trichothecene cytotoxicity and thus a possible etiological link between neurodegenerative diseases and trichothecenes.

4.1 Introduction

Mitochondria houses the electron transport chain (ETC) which is responsible for oxidative phosphorylation and ATP production. However, one of the byproducts of cellular respiration is generation of reactive oxygen species (ROS) which include super oxide anion (O_2^-), hydrogen peroxide (H_2O_2) and hydroxyl ions (OH^-) (Orrenius et al., 2007). When oxygen is partially reduced it is converted to O_2^- and H_2O_2 and is in turn reduced to OH^-, which is the most reactive and toxic (Grant et al., 1997). The ROS thus generated pose a serious threat to the integrity of the cell because they can oxidize different cellular macromolecules such as DNA, proteins, and lipids and compromise their function and form toxic aggregates. As a major source of ROS production mitochondrial components are prime targets causing, among others, mitochondrial DNA (mtDNA) damage leading to ETC disruption, peroxidation of mitochondrial membrane lipids, and mitochondrial protein oxidation. These ROS-mediated damages lead to mitochondrial dysfunction and eventual cell death (Grant et al., 1997; Orrenius et al., 2007). Hence the cell contains several enzymatic and non-enzymatic ROS scavengers to minimize oxidative damage by ROS. Enzyme-mediated ROS conversion includes O_2^- converted into H_2O_2 by superoxide dismutase (SOD) which is further detoxified into H_2O and O_2 by catalases or peroxidases (Lin and Beal, 2006). The main redox buffer of the cell, however, is glutathione which is primarily localized in the cytosol (Scherz-Shouval and Elazar, 2011).

ROS, despite their high reactivity and short life, can act as signaling molecules by modulating activity of their oxidized targets (Scherz-Shouval and Elazar, 2011). ROS, particularly H_2O_2, has been suggested to be a likely messenger for autophagy. Studies have shown exogenously added H_2O_2 to trigger ROS, mitochondrial damage leading to loss of mitochondrial membrane potential (MMP) and cytochrome c release, and activation of autophagy (Chen and Gibson, 2008; Scherz-Shouval and Elazar, 2011). Autophagy is a degradation process targeting proteins or organelles and involving double membrane compartments called autophagosomes which in turn fuses with lysosomes or vacuoles for degradation (Kurihara et al., 2012). By selectively removing damaged mitochondria, which is the major source of ROS, autophagy serves the role of an antioxidant. The increased generation of ROS leading to significant depolarization of MMP triggers recruitment of the fission machinery leading to fission of the damaged mitochondria from the tubular network (Chen and Gibson, 2008). The fragmented mitochondrion is then targeted for degradation via cellular processes such as mitophagy (Scherz-Shouval and Elazar, 2011).

During mitophagy, which is a selective type of autophagy, the outer mitochondrial membrane (OMM) protein Atg32 is recognized and bound by the cytosolic adaptor protein Atg11 (Bhatia-Kiššová and Camougrand, 2012). The mitochondria-bound Atg11 then recruits the fission complex via interaction with the fission protein Fis1 (Mao et al., 2013; Scherz-Shouval and Elazar, 2011). Atg11, which is bound to the fragmented mitochondrion then interacts with the autophagosome-anchored docking protein Atg8 and delivers it to the phagophore assembly site (PAS) where the organelle is taken in and

degraded. Mitophagy is an important cellular process that ensures mitochondrial quality control and prevent accumulation of dysfunctional mitochondria (Bhatia-Kiššová and Camougrand, 2012; Kurihara et al., 2012; Lemasters, 2005; Mendl et al., 2011). Furthermore, mitophagy-defective yeast mutants exhibited higher rates of mtDNA deletion (Kurihara et al., 2012). Hence disrupted mitophagy has been implicated in neurodegenerative diseases like Parkinson's and Huntington's disease (Chen and Chan, 2009).

In this chapter we investigate mitochondria as a source of trichothecene-induced ROS and the possible role of mitophagy as a means to clear ROS-producing damaged mitochondria and thereby alleviating trichothecene cytotoxicity. We previously screened the yeast knockout (YKO) library and found several gene deletions affecting mitochondrial functions rendered the cells resistant to Tcin cytotoxicity (McLaughlin et al., 2009). These included mutations that regulate mitochondrial genome maintenance and fusion machinery suggesting a critical role for mitochondria. We also identified that trichothecenes inhibited mitochondrial translation directly prior to depolarization and fragmentation of the mitochondrial membrane and independent of cytosolic translation inhibition (Bin-Umer et al., 2011; McLaughlin et al., 2009). These time and concentration-dependent inhibitory effects of trichothecenes on mitochondria are of significance (Bin-Umer et al., 2011). Impaired mitochondrial translation leads to faulty oxidative phosphorylation resulting in toxic levels of reactive oxygen species (ROS), overwhelming the cell's antioxidant capacity, and causing oxidative stress (Bandy and Davison, 1990; Bonawitz et al., 2006; Chen et al., 2003b; Davidson and Schiestl, 2001).

Furthermore, mitochondrial dysfunction and the ensuing oxidative stress has been implicated in several neurodegenerative diseases (Lin and Beal, 2006). Thus having a quality control mechanism like mitophagy (Bhatia-Kiššová and Camougrand, 2012; Kurihara et al., 2012; Lemasters, 2005) to prevent accumulation of dysfunctional mitochondria is critical for cell survival during trichothecene cytotoxicity and neurodegenerative diseases.

Here, to further explore the molecular mechanism of trichothecene toxicity we have screened the YKO library to identify gene deletions exhibiting increased sensitivity to Tcin which revealed a likely relationship between cytotoxicity and oxidative stress. Antioxidant treatment and defective mitochondrial respiration inhibited ROS generation by trichothecenes suggesting that cytotoxicity requires fully functional mitochondria with a direct role for mitochondrial ROS (mtROS). Interestingly, rapamycin-induced mitophagy also alleviated ROS levels and cytotoxicity in wild-type yeast in which mitophagy was inhibited by trichothecenes. The ability to cause mitochondrial dysfunction and disrupt mitophagy makes trichothecenes highly neurotoxic since these two inhibitory effects have also been implicated in many neurodegenerative diseases. Our results provide insights into the complex interplay between mitochondrial damage, ROS, and mitophagy during trichothecene-induced cell death.

4.2 Results

4.2.1 Genome-wide analysis of yeast knockout mutants suggests oxidative stress mediate trichothecene toxicity

Tcin inhibits yeast growth in a dose-dependent manner. We had previously identified concentrations which were lethal (> 4μM), sublethal (2 μM) and nonlethal (≤ 1μM) (Bin-Umer et al., 2011; McLaughlin et al., 2009). Hence, to identify genes that were essential for conferring resistance to trichothecenes, we systematically screened the yeast deletion library of 4720 nonessential gene knockout mutants against 1μM Tcin (as described in Materials and Methods), at which growth of the parental strain BY4743 was not significantly inhibited (≤ 15% inhibition) (Fig.1). Four independent screens identified and confirmed 121 deletion strains to be sensitive to Tcin as their growth were severely inhibited (≥ 75% inhibition) at 1μM Tcin (Table 4.1). These mutants were further analyzed for function, localization and phenotype using the MIPS FunCat database (Fig. 4.1A). Several of these mutants were disrupted in functions pertaining to DNA repair and damage response (DNA metabolism, 15.7%), RNA degradation and stability (RNA metabolism, 14.9%), and ribosome biogenesis and protein degradation (Protein, 12.4%). This functional clustering of the sensitive mutants points to the genotoxic effects of Tcin and the destabilizing effects it has on protein synthesis. Interestingly, a large group of the sensitive mutants (42%) were o reported to exhibit very high sensitivity to oxidative stress (www.yeastgenome.org).

We therefore measured Tcin-induced ROS levels in these mutants. BY4743 and the 27 most sensitive mutants were selected (Fig. 4.1B) and treated with 1μM Tcin for 1h prior to staining with the ROS sensitive dye DCFH-DA, which only fluoresces upon ROS

contact. The ratio of ROS-positive cells (detected as staining above background for DCF by flow cytometer) for treated and untreated samples for each mutant was determined and normalized to that of BY4743. Relative to the parental strain, all 27 strains exhibited increased ROS generation upon Tcin treatment with dep1Δ, snf6Δ, rei1Δ, sap30Δ, atg32Δ, and yor152CΔ showing a 2-fold or higher increase in ROS levels (Fig. 4.1C). To further confirm that oxidative stress and particularly ROS may play a role in mediating Tcin toxicity we determined ROS levels in the 15 YKO mutants that exhibited the highest resistance to Tcin from our earlier screening (McLaughlin et al., 2009). At 4μM Tcin, which did not inhibit growth of the Tcin-resistant mutants, no increase was observed (Fig. 4.2A) but BY4743 showed a 2.24-fold increase in Tcin-induced ROS levels. Thus the level of ROS generated in these YKO mutants by Tcin affected their growth which rendered them as either resistant or sensitive to the toxin.

YKO#	Gene Name	Description
YHR030C	SLT2	Serine/threonine MAP kinase involved in regulating the maintenance of cell wall integrity and progression through the cell cycle; regulated by the PKC1-mediated signaling pathway
YGR104C	SRB5	Subunit of the RNA polymerase II mediator complex; associates with core polymerase subunits to form the RNA polymerase II holoenzyme; essential for transcriptional regulation; involved in telomere maintenance
YKL213C	DOA1	WD repeat protein required for ubiquitin-mediated protein degradation, forms complex with Cdc48p, plays a role in controlling cellular ubiquitin concentration; also promotes efficient NHEJ in postdiauxic/stationary phase
YKR093W	PTR2	Integral membrane peptide transporter, mediates transport of di- and tri-peptides; conserved protein that contains 12 transmembrane domains; PTR2 expression is regulated by the N-end rule pathway via repression by Cup9p
YNR051C	BRE5	Ubiquitin protease cofactor, forms deubiquitination

		complex with Ubp3p that coregulates anterograde and retrograde transport between the endoplasmic reticulum and Golgi compartments; null is sensitive to brefeldin A
YJR102C	VPS25	Component of the ESCRT-II complex, which is involved in ubiquitin-dependent sorting of proteins into the endosome
YIL146C	ATG32	Mitochondrial outer membrane protein required to initiate mitophagy; recruits the autophagy adaptor protein Atg11p and the ubiquitin-like protein Atg8p to the mitochondrial surface to initiate mitophagy, the selective vacuolar degradation of mitochondria in response to starvation; can promote pexophagy when placed ectopically in the peroxisomal membrane
YKR082W	NUP133	Subunit of the Nup84p subcomplex of the nuclear pore complex (NPC), localizes to both sides of the NPC, required to establish a normal nucleocytoplasmic concentration gradient of the GTPase Gsp1p
YMR077C	VPS20	Myristoylated subunit of ESCRTIII, the endosomal sorting complex required for transport of transmembrane proteins into the multivesicular body pathway to the lysosomal/vacuolar lumen; cytoplasmic protein recruited to endosomal membranes
YHL025W	SNF6	Subunit of the SWI/SNF chromatin remodeling complex involved in transcriptional regulation; functions interdependently in transcriptional activation with Snf2p and Snf5p
YAL013W	DEP1	Transcriptional modulator involved in regulation of structural phospholipid biosynthesis genes and metabolically unrelated genes, as well as maintenance of telomeres, mating efficiency, and sporulation
YAL002W	VPS8	Membrane-associated protein that interacts with Vps21p to facilitate soluble vacuolar protein localization; component of the CORVET complex; required for localization and trafficking of the CPY sorting receptor; contains RING finger motif
YJL095W	BCK1	Mitogen-activated protein (MAP) kinase kinase kinase acting in the protein kinase C signaling pathway, which controls cell integrity; upon activation by Pkc1p phosphorylates downstream kinases Mkk1p and Mkk2p
YLR025W	SNF7	One of four subunits of the endosomal sorting complex required for transport III (ESCRT-III); involved in the sorting of transmembrane proteins into the multivesicular body (MVB) pathway; recruited from the cytoplasm to endosomal membranes
YLR027C	AAT2	Cytosolic aspartate aminotransferase, involved in nitrogen

		metabolism; localizes to peroxisomes in oleate-grown cells
YLR234W	TOP3	DNA Topoisomerase III, conserved protein that functions in a complex with Sgs1p and Rmi1p to relax single-stranded negatively-supercoiled DNA preferentially, involved in telomere stability and regulation of mitotic recombination
YLR322W	VPS65	Dubious open reading frame, unlikely to encode a protein; not conserved in closely related Saccharomyces species; 75% of ORF overlaps the verified gene SFH1; deletion causes a vacuolar protein sorting defect
YLR330W	CHS5	Component of the exomer complex, which also contains Csh6p, Bch1p, Bch2p, and Bud7p and is involved in export of selected proteins, such as chitin synthase Chs3p, from the Golgi to the plasma membrane
YLR417W	VPS36	Component of the ESCRT-II complex; contains the GLUE (GRAM Like Ubiquitin binding in EAP45) domain which is involved in interactions with ESCRT-I and ubiquitin-dependent sorting of proteins into the endosome
YML062C	MFT1	Subunit of the THO complex, which is a nuclear complex comprised of Hpr1p, Mft1p, Rlr1p, and Thp2p, that is involved in transcription elongation and mitotic recombination; involved in telomere maintenance
YML013C-A		Dubious open reading frame unlikely to encode a protein, based on available experimental and comparative sequence data; partially overlaps the verified gene SEL1
YML008C	ERG6	Delta(24)-sterol C-methyltransferase, converts zymosterol to fecosterol in the ergosterol biosynthetic pathway by methylating position C-24; localized to both lipid particles and mitochondrial outer membrane
YMR032W	HOF1	Bud neck-localized, SH3 domain-containing protein required for cytokinesis; regulates actomyosin ring dynamics and septin localization; interacts with the formins, Bni1p and Bnr1p, and with Cyk3p, Vrp1p, and Bni5p
YMR263W	SAP30	Subunit of a histone deacetylase complex, along with Rpd3p and Sin3p, that is involved in silencing at telomeres, rDNA, and silent mating-type loci; involved in telomere maintenance
YNL236W	SIN4	Subunit of the RNA polymerase II mediator complex; associates with core polymerase subunits to form the RNA polymerase II holoenzyme; contributes to both postive and negative transcriptional regulation; dispensible for basal transcription
YNL229C	URE2	Nitrogen catabolite repression transcriptional regulator that acts by inhibition of GLN3 transcription in good nitrogen

		source; altered form of Ure2p creates [URE3] prion
YOR026W	BUB3	Kinetochore checkpoint WD40 repeat protein that localizes to kinetochores during prophase and metaphase, delays anaphase in the presence of unattached kinetochores; forms complexes with Mad1p-Bub1p and with Cdc20p, binds Mad2p and Mad3p
YOR035C	SHE4	Protein containing a UCS (UNC-45/CRO1/SHE4) domain, binds to myosin motor domains to regulate myosin function; involved in endocytosis, polarization of the actin cytoskeleton, and asymmetric mRNA localization
YOR036W	PEP12	Target membrane receptor (t-SNARE) for vesicular intermediates traveling between the Golgi apparatus and the vacuole; controls entry of biosynthetic, endocytic, and retrograde traffic into the prevacuolar compartment; syntaxin
YOR124C	UBP2	Ubiquitin-specific protease that removes ubiquitin from ubiquitinated proteins, cleaves at the C terminus of ubiquitin fusions; capable of cleaving polyubiquitin and possesses isopeptidase activity
YOR152C		Putative protein of unknown function; has no similarity to any known protein; YOR152C is not an essential gene
YOR290C	SNF2	Catalytic subunit of the SWI/SNF chromatin remodeling complex involved in transcriptional regulation; contains DNA-stimulated ATPase activity; functions interdependently in transcriptional activation with Snf5p and Snf6p
YOL004W	SIN3	Component of the Sin3p-Rpd3p histone deacetylase complex, involved in transcriptional repression and activation of diverse processes, including mating-type switching and meiosis; involved in the maintenance of chromosomal integrity
YOL068C	HST1	NAD(+)-dependent histone deacetylase; essential subunit of the Sum1p/Rfm1p/Hst1p complex required for ORC-dependent silencing and mitotic repression; non-essential subunit of the Set3C deacetylase complex; involved in telomere maintenance
YPL084W	BRO1	Cytoplasmic class E vacuolar protein sorting (VPS) factor that coordinates deubiquitination in the multivesicular body (MVB) pathway by recruiting Doa4p to endosomes
YPR173C	VPS4	AAA-type ATPase that is regulated by Vta1p; required for late endosome to vacuole transport; catalyzes the release of an endosomal membrane-associated class E VPS protein complex; regulates cellular sterol metabolism

YDR049W		Zinc finger protein; putative transcription factor that may interact with proteins involved in histone acetylation or deacetylation; may be involved in altering acetylation on histone lysines
YDR264C	AKR1	Palmitoyl transferase involved in protein palmitoylation; acts as a negative regulator of pheromone response pathway; required for endocytosis of pheromone receptors; involved in cell shape control; contains ankyrin repeats
YDR266C		Protein of unknown function that may interact with ribosomes, based on co-purification experiments;green fluorescent protein (GFP)-fusion protein localizes to the cytoplasm; contains a RING finger domain
YEL044W	IES6	Protein that associates with the INO80 chromatin remodeling complex under low-salt conditions
YER070W	RNR1	Ribonucleotide-diphosphate reductase (RNR), large subunit; the RNR complex catalyzes the rate-limiting step in dNTP synthesis and is regulated by DNA replication and DNA damage checkpoint pathways via localization of the small subunits
YER087W	AIM10	Protein with similarity to tRNA synthetases; non-tagged protein is detected in purified mitochondria; null mutant displays decreased frequency of mitochondrial genome loss (petite formation), severe growth defect in minimal glycerol media
YFR010W	UBP6	Ubiquitin-specific protease situated in the base subcomplex of the 26S proteasome, releases free ubiquitin from branched polyubiquitin chains; deletion causes hypersensitivity to cycloheximide and other toxic compounds
YGL012W	ERG4	C-24(28) sterol reductase, catalyzes the final step in ergosterol biosynthesis; mutants are viable, but lack ergosterol
YGR006W	PRP18	Splicing factor involved in the positioning of the 3' splice site during the second catalytic step of splicing, part of snRNP U5, interacts with Slu7p
YGR196C	FYV8	Protein of unknown function, required for survival upon exposure to K1 killer toxin
YCR077C	PAT1	Topoisomerase II-associated deadenylation-dependent mRNA-decapping factor; also required for faithful chromosome transmission, maintenance of rDNA locus stability, and protection of mRNA 3'-UTRs from trimming; functionally linked to Pab1p
YDL107W	MSS2	Peripherally bound inner membrane protein of the mitochondrial matrix involved in membrane insertion of C-

		terminus of Cox2p, interacts genetically and physically with Cox18p
YDL136W	RPL35B	Protein component of the large (60S) ribosomal subunit, identical to Rpl35Ap and has similarity to rat L35 ribosomal protein
YNL084C	END3	EH domain-containing protein involved in endocytosis, actin cytoskeletal organization and cell wall morphogenesis; forms a complex with Sla1p and Pan1p
YNL054W	VAC7	Integral vacuolar membrane protein involved in vacuole inheritance and morphology; activates Fab1p kinase activity under basal conditions and also after hyperosmotic shock
YBR023C	CHS3	Chitin synthase III, catalyzes the transfer of N-acetylglucosamine (GlcNAc) to chitin; required for synthesis of the majority of cell wall chitin, the chitin ring during bud emergence, and spore wall chitosan
YLR370C	ARC18	Subunit of the ARP2/3 complex, which is required for the motility and integrity of cortical actin patches
YGR063C	SPT4	Protein that forms a complex with Spt5p and mediates both activation and inhibition of transcription elongation, and plays a role in pre-mRNA processing; in addition, Spt4p is involved in kinetochore function and gene silencing
YGR092W	DBF2	Ser/Thr kinase involved in transcription and stress response; functions as part of a network of genes in exit from mitosis; localization is cell cycle regulated; activated by Cdc15p during the exit from mitosis
YJL129C	TRK1	Component of the Trk1p-Trk2p potassium transport system; 180 kDa high affinity potassium transporter; phosphorylated in vivo and interacts physically with the phosphatase Ppz1p, suggesting Trk1p acitivy is regulated by phosphorylation
YJL175W		Dubious open reading frame unlikely to encode a functional protein; deletion confers resistance to cisplatin, hypersensitivity to 5-fluorouracil, and growth defect at high pH with high calcium; overlaps gene for SWI3 transcription factor
YJL184W	GON7	Protein proposed to be involved in the modification of N-linked oligosaccharides, osmotic stress response, telomere uncapping and elongation, transcription; component of the EKC/KEOPS protein complex with Kae1p, Cgi121p, Pcc1p, and Bud32p
YKR023W		Putative protein of unknown function; the authentic, non-tagged protein is detected in highly purified mitochondria in high-throughput studies

YBR112C	CYC8	General transcriptional co-repressor, acts together with Tup1p; also acts as part of a transcriptional co-activator complex that recruits the SWI/SNF and SAGA complexes to promoters
YNL070W	TOM7	Component of the TOM (translocase of outer membrane) complex responsible for recognition and initial import steps for all mitochondrially directed proteins; promotes assembly and stability of the TOM complex
YNL097C	PHO23	Probable component of the Rpd3 histone deacetylase complex, involved in transcriptional regulation of PHO5; C-terminus has similarity to human candidate tumor suppressor p33(ING1)
YKL053C-A	MDM35	Mitochondrial intermembrane space cysteine motif protein; mutation affects mitochondrial distribution and morphology
YOR269W	PAC1	Protein involved in nuclear migration, part of the dynein/dynactin pathway; targets dynein to microtubule tips, which is necessary for sliding of microtubules along bud cortex; synthetic lethal with bni1; homolog of human LIS1
YOR302W		CPA1 uORF , Arginine attenuator peptide, regulates translation of the CPA1 mRNA
YNR052C	POP2	RNase of the DEDD superfamily, subunit of the Ccr4-Not complex that mediates 3' to 5' mRNA deadenylation
YPL268W	PLC1	Phosphoinositide-specific phospholipase C, hydrolyzes phosphatidylinositol 4,5-biphosphate (PIP2) to generate inositol 1,4,5-triphosphate (IP3) and 1,2-diacylglycerol (DAG); involved in kinetochore function and pseudohyphal differentiation
YPR043W	RPL43A	Protein component of the large (60S) ribosomal subunit, identical to Rpl43Bp and has similarity to rat L37a ribosomal protein; null mutation confers a dominant lethal phenotype
YER151C	UBP3	Ubiquitin-specific protease that interacts with Bre5p to co-regulate anterograde and retrograde transport between endoplasmic reticulum and Golgi compartments; inhibitor of gene silencing; cleaves ubiquitin fusions but not polyubiquitin
YBR081C	SPT7	Subunit of the SAGA transcriptional regulatory complex, involved in proper assembly of the complex; also present as a C-terminally truncated form in the SLIK/SALSA transcriptional regulatory complex
YGR271W	SLH1	Putative RNA helicase related to Ski2p, involved in translation inhibition of non-poly(A) mRNAs; required for repressing propagation of dsRNA viruses

YOL148C	SPT20	Subunit of the SAGA transcriptional regulatory complex, involved in maintaining the integrity of the complex
YGL038C	OCH1	Mannosyltransferase of the cis-Golgi apparatus, initiates the polymannose outer chain elongation of N-linked oligosaccharides of glycoproteins
YDL013W	SLX5	Subunit of the Slx5-Slx8 substrate-specific ubiquitin ligase complex; stimulated by prior attachment of SUMO to the substrate
YDL023C		Dubious open reading frame, unlikely to encode a protein; not conserved in other Saccharomyces species; overlaps the verified gene GPD1; deletion confers sensitivity to GSAO; deletion in cyr1 mutant results in loss of stress resistance
YDL075W	RPL31A	Protein component of the large (60S) ribosomal subunit, nearly identical to Rpl31Bp and has similarity to rat L31 ribosomal protein; associates with the karyopherin Sxm1p
YDR495C	VPS3	Component of CORVET tethering complex; cytoplasmic protein required for the sorting and processing of soluble vacuolar proteins, acidification of the vacuolar lumen, and assembly of the vacuolar H+-ATPase
YHR013C	ARD1	Subunit of the N-terminal acetyltransferase NatA (Nat1p, Ard1p, Nat5p); N-terminally acetylates many proteins, which influences multiple processes such as the cell cycle, heat-shock resistance, mating, sporulation, and telomeric silencing
YCR094W	CDC50	Endosomal protein that regulates cell polarity, controls polarized growth; similar to Ynr048wp and Lem3p
YGR262C	BUD32	Protein kinase proposed to be involved in bud-site selection, telomere uncapping and elongation, and transcription; component of the EKC/KEOPS protein complex with Kae1p, Cgi121p, Pcc1p, and Gon7p
YOL086C	ADH1	Alcohol dehydrogenase, fermentative isozyme active as homo- or heterotetramers; required for the reduction of acetaldehyde to ethanol, the last step in the glycolytic pathway
YML094W	GIM5	Subunit of the heterohexameric cochaperone prefoldin complex which binds specifically to cytosolic chaperonin and transfers target proteins to it
YML112W	CTK3	Gamma subunit of C-terminal domain kinase I (CTDK-I), which phosphorylates the C-terminal repeated domain of the RNA polymerase II large subunit (Rpo21p) to affect both transcription and pre-mRNA 3' end processing
YKL002W	DID4	Class E Vps protein of the ESCRT-III complex, required for sorting of integral membrane proteins into lumenal vesicles of multivesicular bodies, and for delivery of newly

		synthesized vacuolar enzymes to the vacuole, involved in endocytosis
YLR226W	BUR2	Cyclin for the Sgv1p (Bur1p) protein kinase; Sgv1p and Bur2p comprise a CDK-cyclin complex involved in transcriptional regulation through its phosphorylation of the carboxy-terminal domain of the largest subunit of RNA polymerase II
YLR240W	VPS34	Phosphatidylinositol 3-kinase responsible for the synthesis of phosphatidylinositol 3-phosphate; forms membrane-associated signal transduction complex with Vps15p to regulate protein sorting; activated by the GTP-bound form of Gpa1p
YLR337C	VRP1	Proline-rich actin-associated protein involved in cytoskeletal organization and cytokinesis; related to mammalian Wiskott-Aldrich syndrome protein (WASP)-interacting protein (WIP)
YLR338W	OPI9	Dubious open reading frame unlikely to encode a protein, based on available experimental and comparative sequence data; partially overlaps the verified ORF VRP1/YLR337C
YOL051W	GAL11	Subunit of the RNA polymerase II mediator complex; associates with core polymerase subunits to form the RNA polymerase II holoenzyme; affects transcription by acting as target of activators and repressors
YPL254W	HFI1	Adaptor protein required for structural integrity of the SAGA complex, a histone acetyltransferase-coactivator complex that is involved in global regulation of gene expression through acetylation and transcription functions
YPL129W	TAF14	Subunit of TFIID, TFIIF, INO80, SWI/SNF, and NuA3 complexes, involved in RNA polymerase II transcription initiation and in chromatin modification; contains a YEATS domain
YPL050C	MNN9	Subunit of Golgi mannosyltransferase complex also containing Anp1p, Mnn10p, Mnn11p, and Hoc1p that mediates elongation of the polysaccharide mannan backbone; forms a separate complex with Van1p that is also involved in backbone elongation
YPL045W	VPS16	Subunit of the vacuole fusion and protein sorting HOPS complex and the CORVET tethering complex; part of the Class C Vps complex essential for membrane docking and fusion at Golgi-to-endosome and endosome-to-vacuole protein transport stages
YPL042C	SSN3	Cyclin-dependent protein kinase, component of RNA polymerase II holoenzyme; involved in phosphorylation of the RNA polymerase II C-terminal domain; involved in

		glucose repression
YPR072W	NOT5	Subunit of the CCR4-NOT complex, which is a global transcriptional regulator with roles in transcription initiation and elongation and in mRNA degradation
YBL058W	SHP1	UBX (ubiquitin regulatory X) domain-containing protein that regulates Glc7p phosphatase activity and interacts with Cdc48p; interacts with ubiquitylated proteins in vivo and is required for degradation of a ubiquitylated model substrate
YBL093C	ROX3	Subunit of the RNA polymerase II mediator complex; associates with core polymerase subunits to form the RNA polymerase II holoenzyme
YBR267W	REI1	Cytoplasmic pre-60S factor; required for the correct recycling of shuttling factors Alb1, Arx1 and Tif6 at the end of the ribosomal large subunit biogenesis; involved in bud growth in the mitotic signaling network
YGL058W	RAD6	Ubiquitin-conjugating enzyme (E2), involved in postreplication repair (with Rad18p), sporulation, telomere silencing, and ubiquitin-mediated N-end rule protein degradation (with Ubr1p)
YGL070C	RPB9	RNA polymerase II subunit B12.6; contacts DNA; mutations affect transcription start site; involved in telomere maintenance
YBR279W	PAF1	RNAP II-associated protein; defines large complex biochemically and functionally distinct from the Srb-Mediator form of Pol II holoenzyme; required for full expression of a subset of cell cycle-regulated genes; homolog of human PD2/hPAF1
YCR020W-B	HTL1	Component of the RSC chromatin remodeling complex; RSC functions in transcriptional regulation and elongation, chromosome stability, and establishing sister chromatid cohesion; involved in telomere maintenance
YCR044C	PER1	Protein of the endoplasmic reticulum, required for GPI-phospholipase A2 activity that remodels the GPI anchor as a prerequisite for association of GPI-anchored proteins with lipid rafts; functionally complemented by human ortholog PERLD1
YAL047C	SPC72	Component of the cytoplasmic Tub4p (gamma-tubulin) complex, binds spindle pole bodies and links them to microtubules; has roles in astral microtubule formation and stabilization
YJR090C	GRR1	F-box protein component of the SCF ubiquitin-ligase complex; involved in carbon catabolite repression, glucose-dependent divalent cation transport, high-affinity glucose

		transport, morphogenesis, and sulfite detoxification
YDL106C	PHO2	Homeobox transcription factor; regulatory targets include genes involved in phosphate metabolism; binds cooperatively with Pho4p to the PHO5 promoter; phosphorylation of Pho2p facilitates interaction with Pho4p
YJL028W		Protein of unknown function; may interact with ribosomes, based on co-purification experiments
YNL133C	FYV6	Protein of unknown function, required for survival upon exposure to K1 killer toxin; proposed to regulate double-strand break repair via non-homologous end-joining
YNL064C	YDJ1	Protein chaperone involved in regulation of the HSP90 and HSP70 functions; involved in protein translocation across membranes; member of the DnaJ family
YKL139W	CTK1	Catalytic (alpha) subunit of C-terminal domain kinase I (CTDK-I), which phosphorylates the C-terminal repeated domain of the RNA polymerase II large subunit (Rpo21p) to affect both transcription and pre-mRNA 3' end processing
YBR289W	SNF5	Subunit of the SWI/SNF chromatin remodeling complex involved in transcriptional regulation; functions interdependently in transcriptional activation with Snf2p and Snf6p
YNL140C		Dubious open reading frame unlikely to encode a protein, based on available experimental and comparative sequence data; partially overlaps the verified gene RLR1/YNL139C
YDR442W		Dubious open reading frame unlikely to encode a functional protein, based on available experimental and comparative sequence data
YDR532C		Protein of unknown function that localizes to the nuclear side of the spindle pole body and along short spindles; deletion mutants have short telomeres; forms a complex with Spc105p
YBL071W-A	KTI11	Zn-ribbon protein that co-purifies with Dph1, Dph2, Eft2 and Elongator subunits Iki3p, Elp2p, and Elp3p as a complex required for synthesis of diphthamide, a modified histidine residue, and for modification of wobble nucleosides in tRNA
YAL021C	CCR4	Component of the CCR4-NOT transcriptional complex, which is involved in regulation of gene expression; component of the major cytoplasmic deadenylase, which is involved in mRNA poly(A) tail shortening
YKR004C-A	ECM9	Non-essential protein of unknown function

YMR202W	ERG2	C-8 sterol isomerase, catalyzes the isomerization of the delta-8 double bond to the delta-7 position at an intermediate step in ergosterol biosynthesis
YNL147W	LSM7	Lsm (Like Sm) protein; part of heteroheptameric complexes (Lsm2p-7p and either Lsm1p or 8p): cytoplasmic Lsm1p complex involved in mRNA decay; nuclear Lsm8p complex part of U6 snRNP and possibly involved in processing tRNA, snoRNA, and rRNA
YOR298C-A	MBF1	Transcriptional coactivator that bridges the DNA-binding region of Gcn4p and TATA-binding protein Spt15p; suppressor of frameshift mutations
YDR433W		Dubious open reading frame unlikely to encode a functional protein, based on available experimental and comparative sequence data

Table 4. 1. List of Tcin-sensitive mutants. Yeast diploid knockout mutants sensitive to 1µM Tcin and their description is listed based on the Saccharomyces genome database (SGD) (www.yeastgenome.org).

4.2.2 ROS-mediated mitochondrial membrane damage plays a direct role in trichothecene cytotoxicity

We determined whether ROS levels and cytotoxicity was also linked in cells treated with other trichothecenes. As seen previously (Bin-Umer et al., 2011) we observed a dose-dependent inhibition of wild-type yeast growth upon treatment with type A (T-2 and DAS) and type B (Tcin and DON) trichothecenes (Fig. 4.3A). When stained for ROS, treated cells exhibited significantly higher levels (2-4 fold) than the untreated cells (Fig. 4.3B) in a dose-dependent manner. This increase in trichothecene-induced ROS levels was further confirmed with the Amplex Red/peroxidase system which also showed a dose-dependent increase in endogenous H_2O_2 production. (Fig. 4.2A). Hence a strong correlation can be observed between toxigenic capacity and ROS generation. The

more cytotoxic T-2 and Tcin therefore induced higher ROS generation than their congeners DAS and DON respectively (Fig. 4.3). Thus ROS is likely playing a critical role in mediating trichothecene cytotoxicity.

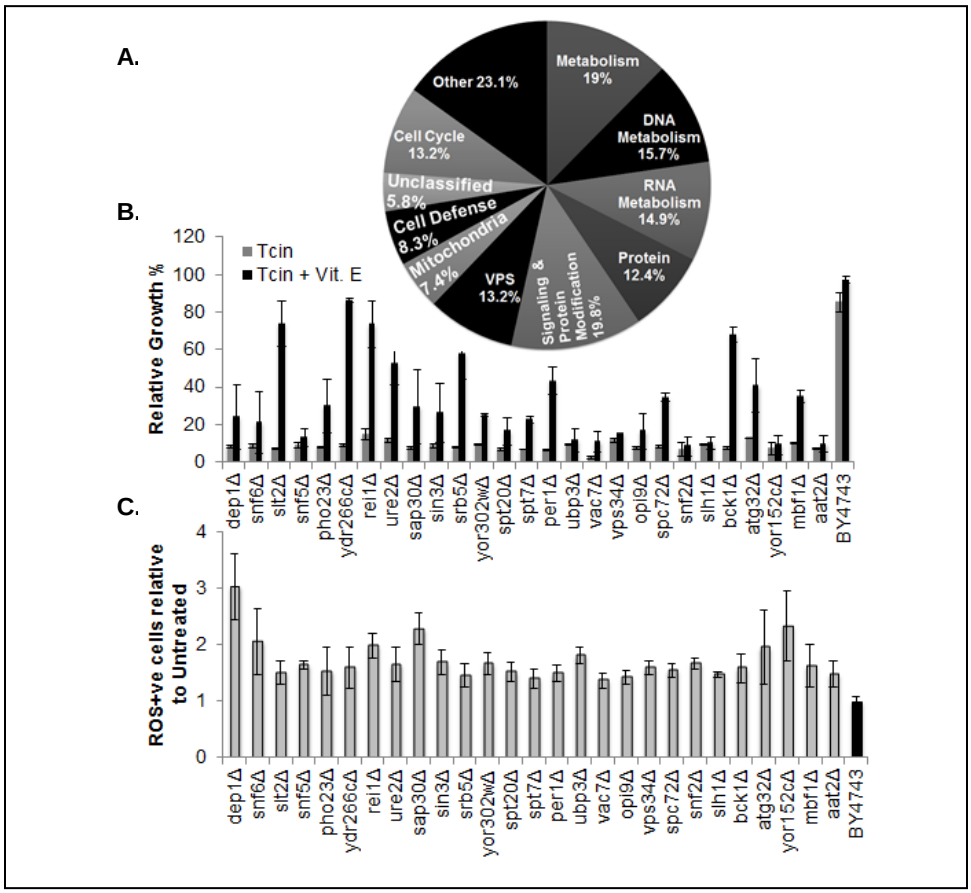

Figure 4.1. Growth, ROS and classification of yeast mutants exhibiting increased sensitivity to Tcin. (A) Yeast deletion mutants exhibiting increased sensitivity to nonlethal doses of Tcin (≤ 1µM Tcin) were identified and classified based on MIPS FunCatDB terms. (B) The top 27 YKO mutants exhibiting the highest sensitivity to Tcin and BY4743 were grown in liquid YPD media with or without 1µM Tcin and in the presence or absence of 4.5mM vitamin E. At 18hpt, growth at OD_{600} was measured to determine relative growth. Relative growth was calculated as the ratio of growth of treated cells to that of untreated with a ratio of 1 indicating no effect on growth. (C) Following 1hpt of the Tcin-sensitive YKOs and BY4743 with 1µM Tcin, Equal OD_{600} cells were stained with DCFH-DA prior to detecting fluorescence from ROS-producing

cells using flow cytometer. The ratio of ROS positive cells for each treatment relative to the untreated control was used to calculate the fold increase.

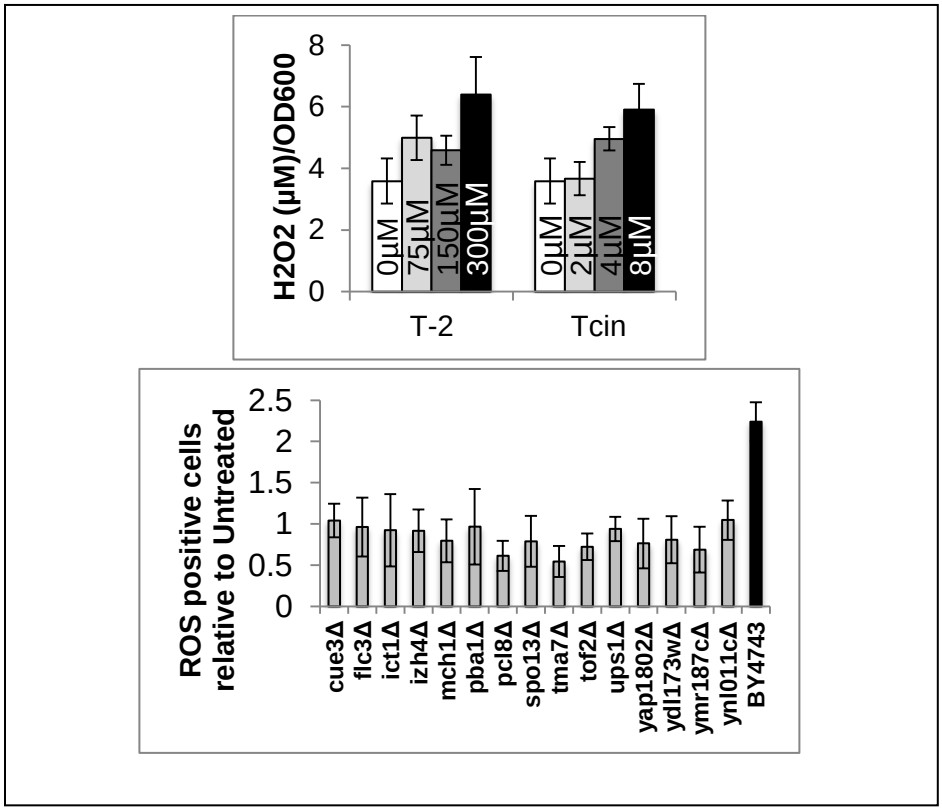

Figure 4.2. Effect of trichothecenes on ROS generation in wild type yeast and Tcin-resistant mutants. (Top panel**)** Wild type yeast cells were treated with two to four fold increasing concentrations of T-2 (0-300µM) or Tcin (0-8µM). Intracellular H2O2 was measured fluorometrically by staining treated and untreated treated cells with the Amplex Red/peroxidase mix for 30min . Readings were then normalized to OD_{600} for each treatment. (Bottom panel) Yeast diploid knockout mutants conferring highest resistance to Tcin toxicity were treated with 4µM Tcin for 1h. Equal OD_{600} cells were stained with DCFH-DA prior to detecting fluorescence using flow cytometer. The ratio of ROS positive cells for each treatment relative to the untreated control was used to calculate the fold increase.

Trichothecenes inhibit multiple cellular processes particularly cytosolic translation (Bin-Umer et al., 2011; McLaughlin et al., 2009; Rocha et al., 2005). To rule out ROS generation is a secondary effect of translation inhibition we determined ROS levels in cells treated, for 1h, with increasing concentrations of cycloheximide and

anisomycin (Fig. 4.4A). Unlike T-2 and Tcin, which showed a 3-4 fold increase in ROS levels with increasing concentrations, inhibiting total translation with cycloheximide and anisomycin, showed no such increase (Fig. 4.4A). We also assayed ROS levels in cells cotreated with 2.5mM H_2O_2 and either trichothecenes or cycloheximide (Fig. 4.4B). Within 1hpt, significant increase in ROS levels was seen with H_2O_2-treated cells (41.53% ROS-positive cells) relative to untreated (2.76%). This H_2O_2-induced ROS generation was further increased when cotreated with T-2 (58.19%) or Tcin (51.64%). However with cycloheximide (22.36%) no such increase was observed (Fig. 4.4B) which further confirms that trichothecene-triggered ROS generation is not due to their inhibitory effects on protein synthesis.

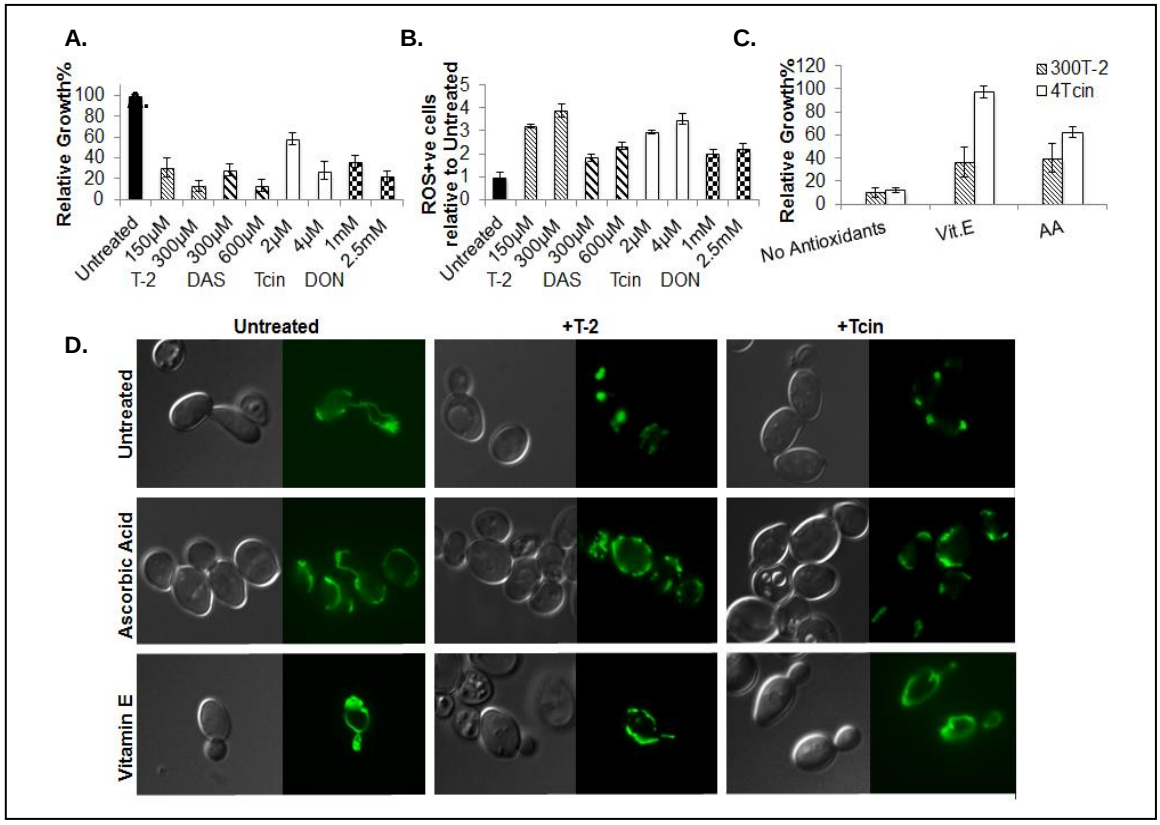

Figure 4.3. Effect of trichothecenes on ROS generation in wild type yeast and Tcin-resistant mutants. (A) Wild type yeast cells were treated with increasing concentrations of trichothecenes overnight. At 18hpt OD_{600} readings were taken. Relative growth is the ratio of OD_{600} for treated cells to untreated. (B) Equal OD_{600} cells were stained with DCFH-DA prior to detect fluorescence using flow cytometer. Following gating of live/dead cells, those fluorescing above the background were detected as staining positive for DCHF and identified as ROS positive. The ratio of ROS positive cells for each treatment relative to the untreated control was used to calculate the fold increase. (C) Wild type yeast cells were cotreated with either ascorbic acid (AA) or vitamin E (Vit.E) and trichothecenes overnight prior to calculaing OD_{600}. Relative growth is the ratio of OD_{600} of treated cells to the untreated control. (D) Wild type yeast cells constitutively expressing mtGFP were cotreated with either ascorbic acid (AA) or vitamin E (Vit.E) and trichothecenes for 6h. Cells were photographged using an epifluorescence microscopy at 100X magnification.

If ROS played a direct role in mediating trichothecene toxicity we reasoned that scavenging trichothecene-induced ROS should alleviate cytotoxicity. Yeast cells were cotreated, overnight, with trichothecenes and either the water soluble antioxidant ascorbic acid or the lipophilic antioxidant vitamin E (Fig. 4.3C). Cell survival increased from 10% (no antioxidant) to 36.6% (4.5mM vitamin E) and 40% (80mM ascorbic acid) during T-2 treatment while a more significant effect was observed in Tcin-treated cells with 97.3% and 62.5% cell survival respectively (vs. 12%). To determine whether antioxidants also reduced cytotoxicity in the Tcin-sensitive mutants we treated the most sensitive strains with 1μM in the presence or absence of vitamin E. Similar to the wild-type, in the 27 strains tested, 19 showed a 2-fold or higher increase in cell survival in the presence of vitamin E (Fig. 4.1B), suggesting a direct role for ROS in mediating trichothecene cytotoxicity.

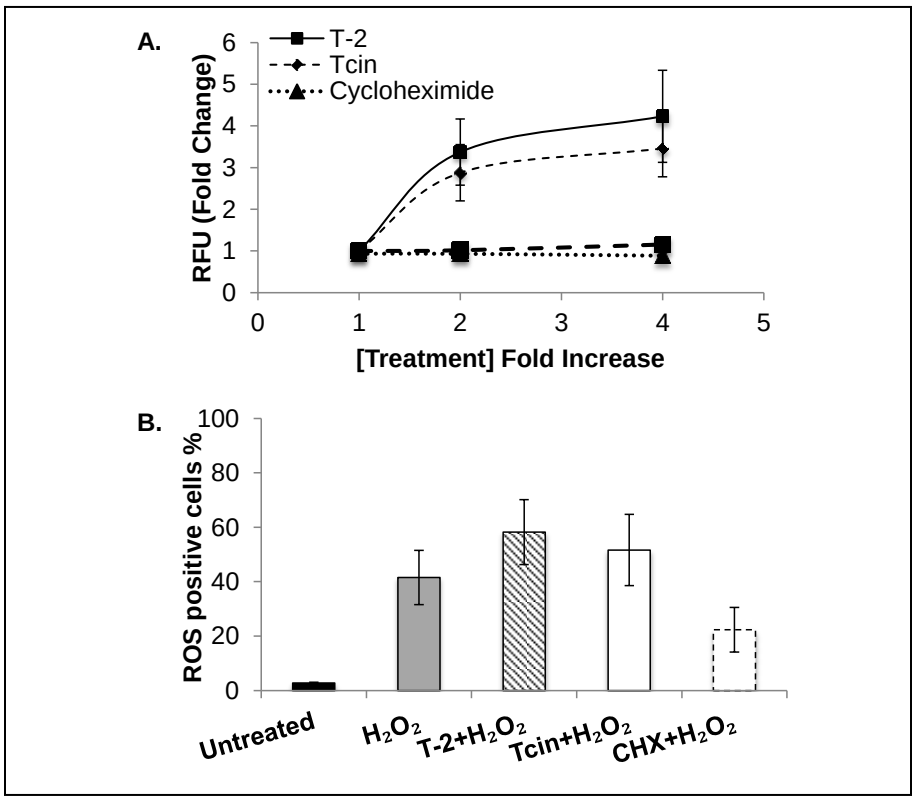

Figure 4.4. ROS generation in response to translation inhibition. (A) Wild type yeast cells were treated with two to four fold increasing concentrations of T-2 (0-300µM), Tcin (0-4µM) cycloheximide (0-1µg/mL) or anisomycin (0-50µg/mL) overnight. Equal OD_{600} cells were stained with DCFH-DA prior to live/dead cell gating and detecting fluorescence using flow cytometer. Relative fluorescence unit (RFU) is the ratio of median fluorescence of treated cells to that of untreated control. (B) Wild type yeast cells were cotreated with 2.5mM H2O2 and either 300µM T-2, 4µM Tcin or 1µg/L cycloheximide (CHX) for 1h prior to DCHF-DA staining and flowcytometric analysis. Following gating of live/dead cells, those fluorescing above the background were detected as staining positive for DCHF and identified as ROS positive.

Although both antioxidants scavenge ROS, vitamin E is particularly known for its inhibitory effects on lipid peroxidation which can lead to significant damage to membrane lipids including mitochondrial membrane (Fryer, 1992). We therefore investigated mitochondrial membrane morphology of trichothecene-treated cells in the

presence of the two antioxidants (vitamin E and ascorbic acid). Wild type yeast cells transformed with a constitutively expressing GFP targeted to the mitochondrial matrix (mtGFP) were treated with 300µM T-2 or 4µM Tcin in the presence of either ascorbic acid or vitamin E. Significant fragmentation of the tubular network of mitochondria was observed in trichothecene-treated cells in the absence of the antioxidants (Fig. 4.3D). However this fragmentation was only moderately visible when cotreated with ascorbic acid (Fig. 4B). When cotreated with vitamin E, the cell's tubular network remained largely intact with little to no fragmentation (Fig. 4.3D), despite trichothecene treatment, suggesting that antioxidants rescued cells by significantly reducing mitochondrial membrane damage by trichothecene-induced ROS.

4.2.3 Trichothecenes require actively respiring mitochondria for ROS-mediated cytotoxicity

Since mitochondria is a major source of ROS (Chen et al., 2003b) we investigated the role of functional mitochondria in ROS generation during trichothecene cytotoxicity (Fig. 4.5). When treated with trichothecenes for 1h and stained for ROS (Fig. 4.5A), grande (ρ^+)cells exhibited a significant increase in the number of ROS-positive cells with 300µM T-2 (6.3%) and 4µM Tcin (6.1%) treatment, relative to non-treatment (2.4%). However trichothecenes failed to generate similar levels in petite cells (ρ^0) (Fig. 4.5A), which lack mitochondrial DNA (mtDNA) and therefore contain nonfunctional mitochondria with defunct electron transport chain (ETC). ROS-positive cells did not increase in T-2 (1.68%) or Tcin (1.97%) treated cells relative to the untreated petite cells (2.1%). We further confirmed our findings by treating ρ^+ cells with carbonyl-cyanide p-

trifluoromethoxyphenylhydrazone (FCCP), an uncoupler which significantly depolarizes mitochondria (Bin-Umer et al., 2011). The number of ROS-positive cells dropped from 6.3% to 3.28% for T-2 and from 6.1% to 3% for Tcin, upon FCCP pretreatment (Fig. 4.5A). Thus trichothecene-induced ROS generation is dependent on actively respiring mitochondria. Strikingly, FCCP pretreatment also alleviated cytotoxicity (Fig. 4.5B) of T-2 (only 29-61% cell death with FCCP pretreatment vs. 60-76.7% without pretreatment) and Tcin (20-36.2% cell death vs. 61-75.7%). This suggests that ROS generation and cytotoxicity in trichothecene-treated cells are dependent on actively respiring mitochondria.

4.2.4 Mitophagy is disrupted during trichothecene treatment leading to accumulation of damaged mitochondria, increased ROS generation and cell death

Since mitochondrial functions are significantly impaired during trichothecene treatment (Bin-Umer et al., 2011; McLaughlin et al., 2009) we reasoned that limiting the damage from trichothecene-induced defective mitochondria would alleviate ROS-mediated trichothecene cytotoxicity. Moreover several Tcin-sensitive strains (atg32Δ, slt2Δ, vps34Δ) were identified to be components of the vacuolar protein sorting (VPS) pathway which is critical for different autophagic processes. Hence we investigated whether pharmacologically enhancing the efficiency with which cells cleared out ROS-producing damaged mitochondria (mitophagy) would decrease ROS levels during trichothecene treatment (Fig. 4.6). Hence, yeast cells were cotreated with the mitophagy enhancer rapamycin (Mendl et al., 2011) and either 300μM T-2 or 4μM Tcin, for 1h, and

stained for ROS (Fig. 4.6A). As expected, trichothecene-treatment increased the number of ROS-positive cells (14.59% with T-2 and 8.91% with Tcin) relative to untreated (2.76%). Although 5nM rapamycin treatment alone moderately increased the number of ROS-positive cells (4.69% vs. 2.76%), rapamycin cotreatment reduced trichothecene-induced ROS levels (Fig. 4.6A). ROS-positive cells dropped from 14.59% to 9.40% with 300µM T-2 while in 4µM Tcin-treated cells it dropped from 8.91% to 5.63%. A similar inhibition was also observed with H_2O_2-induced ROS generation upon rapamycin cotreatment (41.53% to 18.62%) (Fig. 4.6A). Thus trichothecene and H_2O_2-induced ROS levels are significantly lowered upon cotreatment with rapamycin.

Interestingly, rapamycin cotreatment also increased cell survival in trichothecene-treated cells from 17.2% to 41.1% (T-2) (Fig. 4.6B), from 14.5% to 23.2% (Tcin) (Fig. 4.6C) and from 56.5% to 73.7% (H_2O_2) (data not shown). To verify alleviation of trichothecene cytotoxicity by rapamycin is due to enhanced mitophagy, we investigated whether rapamycin cotreatment also rescued cells defective for mitophagy. Several mutants knocked out for genes (slt2Δ, whi2Δ, uth1Δ, atg32Δ, and hog1Δ) implicated in mitophagy (Bhatia-Kiššová and Camougrand, 2012) were screened. Rapamycin failed to rescue mitophagy-defective mutants from T-2 (Fig. 4B) and Tcin (Fig. 4.6C) toxicity since no increase in cell survival was observed (Fig. 4.6B) unlike the wild-type. However, rapamycin alleviated toxicity moderately in some (pho23Δ, ubp3Δ, vac7Δ, mbf1Δ) but not all of the Tcin-sensitive mutants that are not defective for mitophagy (Fig. 4.7). Thus, while 5nM rapamycin treatment alone did not affect the growth of the mutants (data not shown), it rescued wild-type but not the mitophagy-defective mutants

from the cytotoxic effects of trichothecenes suggesting that trichothecene induced ROS primarily originate from damaged mitochondria and their selective removal via mitophagy increases cell survival.

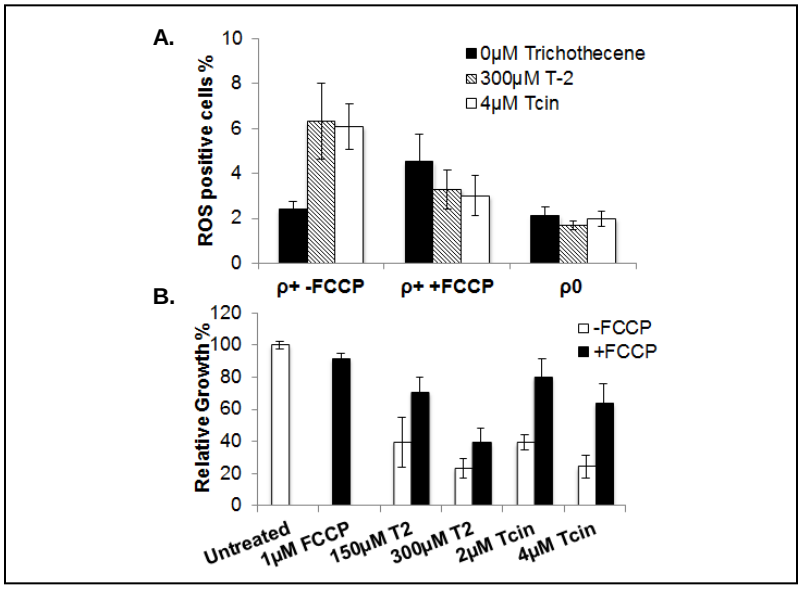

Figure 4.5. Effect of membrane depolarization on trichothecene-induced ROS generation and growth inhibition. (A) Wild type yeast cells that are either grande (ρ^+), petite (ρ^0) or grande (ρ^+) pretreated with 0.4μM FCCP for 1h were treated with trichotheceens for 1h prior to DCHF-DA staining and flowcytometric analysis. Following gating of live/dead cells, those fluorescing above the background were detectected as staining positive for DCHF and identified as ROS positive. (B) Wild type yeast cells were pretreated with 1μM FCCP prior to treating with increasing concentrations of trichothecenes overnight prior to calculaing OD_{600}. Relative growth is the ratio of OD_{600} of treated cells to the untreated control.

We also monitored mitophagy in trichothecene-treated cells by assaying for the level of processing of a GFP-tagged mitochondrial protein (Kanki et al., 2009). During mitophagy, vacuolar degradation of mitochondria should release the intact GFP from the mitochondrial protein which is then detected by immunostaining. BY4743 and mitophagy-defective atg32Δ cells transformed with mtGFP were initially grown in lactate

media to significantly promote mitochondrial mass and number and later switched to glucose which represses mitochondrial functions (Kanki et al., 2009; Kurihara et al., 2012). The switch then triggers the mitophagy pathway to clear out excess mitochondria which otherwise would promote ROS-mediated damage (Kanki et al., 2009; Kurihara et al., 2012; Lemasters, 2005; Mendl et al., 2011). Following the media switch cells were treated with 300µM T-2, 4µM Tcin or 1µM Rapamycin for 18hpt and equal number of cells collected for immunodetection of free vs. intact GFP. In untreated BY4743, multiple bands were detected including the high MW band of intact GFP-tagged mitochondrial protein and the low MW band of free GFP suggesting some level of mitophagy (Fig. 4.6D). This was also the case with BY4743 cells treated with rapamycin, which induces mitophagy (Mendl et al., 2011). However, such pattern of GFP processing was not observed in T-2 or Tcin-treated cells. In the mitophagy-defective atg32Δ cells, as anticipated, processing of GFP was almost non-existent in both treated and untreated samples (Fig. 4.6D). Thus mitophagy is disrupted in trichothecene-treated yeast leading to accumulation of damaged mitochondria and increased ROS generation.

4.3 Discussion

Our genome-wide screening of the yeast deletion library has identified 121 genes that encode functions critical for Tcin tolerance. The inhibitory effects of trichothecenes on DNA, RNA, proteins, and lipids have been identified previously (Rocha et al., 2005) and thus our screening identified, among others, several mutants (Table 4.1) defective for DNA maintenance and repair (rad6Δ, fyv6Δ), RNA processing and stability (slh1Δ,

lsm7Δ), ribosome biogenesis (rpl31AΔ, rpl35BΔ, rpl43AΔ), protein degradation (ubp3Δ, ubp6Δ) and phospholipid metabolism (vac7Δ, sin3Δ) (Fig. 4.1). Several mutants defective in the vacuolar protein sorting (VPS) pathway were also identified including mutants defective for autophagy (vps34Δ, vps36Δ, vps6Δ) and mitophagy (atg32Δ). These functions are critical during trichothecene toxicity because their disruption rendered cells highly sensitive to 1μM Tcin which is, however, not lethal to the parental BY4743 (Fig. 4.1). Genetic perturbations affecting molecular mechanisms involved in protecting the cell from damage due to different environmental stresses can render the deletion strains cross sensitive to xenotoxic agents like trichothecenes. However a significant number of these gene deletions (42%) particularly affected resistance to various oxidants including H_2O_2, acetic acid, and cumene hydroperoxide (Higgins et al., 2002). This indicates an overlap of mechanisms involved in cellular response to oxidative stress and trichothecene toxicity. Since oxidative stress occurs when ROS levels overwhelm the cell's antioxidant capacity (Bonawitz et al., 2006) and trichothecenes have been suggested to induce oxidative stress (Desmond et al., 2008) we investigated the likely role for ROS in rendering these mutants sensitive to Tcin.

4.3.1 Trichothecene-induced oxidative stress directly mediated cytotoxicity

Tcin-induced ROS levels were significantly higher in several of the Tcin-sensitive mutants (Fig. 4.1C) relative to the parental BY4743 while Tcin failed to generate ROS in mutants highly resistant to Tcin (Fig. 4.2A). Like Tcin, we also found T-2, DAS and DON to induce significant ROS generation in BY4743 in a dose dependent manner and correlating to their cytotoxicity (Fig. 4.3A and 2B), which, however, cannot be attributed

to translation inhibition (Sanchez et al., 1997) (Fig. 4.4B). Trichothecene-induced ROS generation is also time-dependent since ROS levels at 1hpt (Fig. 4.3B) have been shown to significantly drop at 6hpt (Bin-Umer et al., 2011) in trichothecene-treated cells likely due to significant depolarization of the mitochondrial membrane (Bin-Umer et al., 2011). Trichothecenes also elicited hydrogen peroxide production (Fig. 4.2B) similar to DON-treatment in plants (Desmond et al., 2008) further confirming our findings. While the role of oxidative stress during trichothecene toxicosis has been previously reported in mammalian studies, such extensive studies are, however, lacking in yeast and plants (Geddes et al., 2008; Iwahashi et al., 2008). By identifying the level of ROS generated and susceptibility to oxidative stress (Fig. 4.1) to be critical factors in determining the cell's tolerance to trichothecenes (Fig. 4.3), this study suggests a critical role for ROS in mediating cell death during trichothecene toxicity in yeast.

4.3.2 Antioxidants rescued cells from trichothecene-induced mitochondrial membrane damage

Since oxidative stress is associated with trichothecene toxicity (Desmond et al., 2008; Rizzo et al., 1994; Sanchez et al., 1997) and a critical role for ROS in trichothecene cytotoxicity is evident (Fig. 4.3) exogenous addition of antioxidants is an effective approach to alleviating cytotoxicity. Dietary usage of antioxidants has been previously reported to show some protection against trichothecene toxicosis in rats (Rizzo et al., 1994) although the mechanism remains unclear. The lipid soluble vitamin E stabilizes and maintains membrane integrity (Fryer, 1992) and has been reported to alleviate membrane damage due to lipid peroxidation induced by ROS (Niki et al., 1991). While

the water soluble ascorbic acid directly scavenges ROS by reducing H_2O_2 to water via the ascorbate-peroxidase reaction (Asada, 1992). As anticipated, addition of antioxidants particularly vitamin E significantly increased survival (Fig. 4.3C) in the wild-type and in several of the Tcin-sensitive mutants (Fig. 4.1B and 4.3C). Furthermore, in the trichothecene-treated cells rescued by antioxidants, mitochondrial membrane lipids were protected to varying degrees, as evident from the mitochondrial membrane morphology (Fig. 4.3D). The interconnected tubular mitochondrial network is disrupted leading to fragmented membrane morphology upon trichothecene treatment (Fig. 4.3B). However, addition of ascorbic acid or vitamin E protected mitochondrial membrane fragmentation with the latter providing the highest protection (Fig. 4.3B). The protection of membrane lipids from trichothecene-induced ROS generation correlates with alleviation of trichothecene-induced growth inhibition by the antioxidants (Fig. 4.3C) and confirms that mitochondrial membrane is a critical target for ROS (for lipid peroxidation) during trichothecene cytotoxicity. Moreover, the mitochondrial origin of trichothecene-induced ROS generation and its role in trichothecene cytotoxicity was suggested when ROS levels did not increase in trichothecene-treated petite (ρ^0) cells or in cells treated with FCCP (Fig. 4.5A), which also increased cell survival (Fig. 4.5B). Thus trichothecene cytotoxicity requires actively respiring mitochondria. This also explain why ρ^0 cells exhibited high tolerance to trichothecenes in previous reports and the largest group of Tcin-resistant strains from our previous screening were deletions affecting mitochondrial functions (Bin-Umer et al., 2011; McLaughlin et al., 2009). Interestingly H_2O_2 cytotoxicity was also alleviated by FCCP pretreatment (Fig. 4.4B) suggesting that like

H_2O_2, trichothecene-triggered cell death is also mediated by ROS via the mitochondrial dependent cell death pathway.

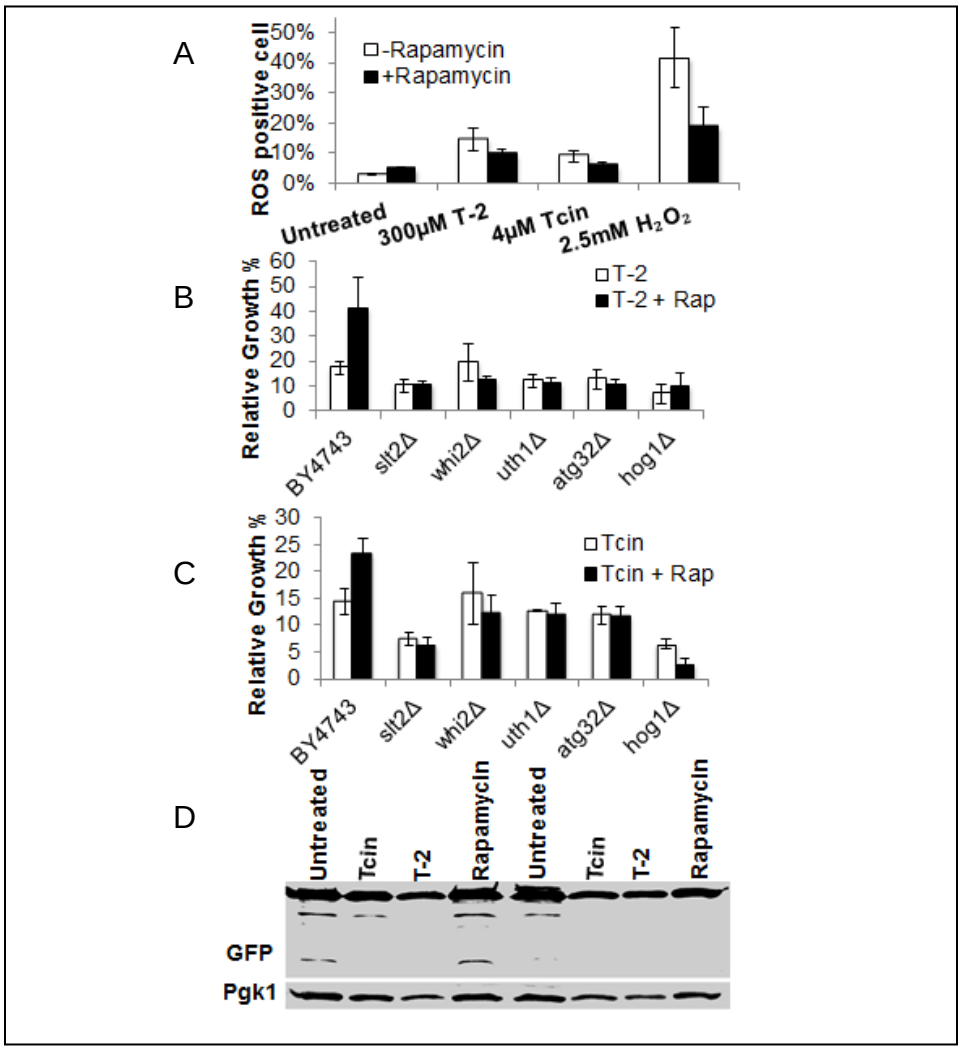

Figure 4.6. Effect of enhanced mitophagy on trichothecene cytotoxicity and ROS generation. (A) Wild type yeast cells cotreated with rapamycin and either 300μM T-2, 4μM Tcin or 2.5mM H_2O_2 for 1h prior to DCHF-DA staining and flow cytometric analysis. Following gating of live/dead cells, those fluorescing above the background were detected as staining positive for DCHF and identified as ROS positive. Wild type yeast and mutants were cotreated with rapamcyin and either (B) 300μM T-2 or (C) 4μM Tcin overnight prior to calculaing OD_{600}. Relative growth is the ratio of OD_{600} of treated cells to the untreated control. (D) Whole cell lysate from trichothecene or rapamycin-treated cells were separated on 12% SDS-PAGE gel following 18hpt and immunostained with anti-GFP antibody and later with anti-Pgk1 antibody for loading control.

Minimizing, if not inhibiting, trichothecene-induced ROS induction is significant (Ponts et al., 2007) because Ponts et al. in a recent study observed that oxidative stress, such as an oxidative burst of H_2O_2, can enhance DON production by *F. graminearum* via upregulation of various Tri genes involved in trichothecene biosynthesis (Ponts et al., 2007). Antioxidants like vitamin E and ascorbic acid therefore present a cheaper and more effective alternative approach, unlike resveratrol (Fanelli et al., 2003), to contain these oxidative bursts during Fusarium infection of crop plants and in turn inhibit the development of the pathogenic fungi as well as the production of trichothecenes, which serve as virulence factors. In light of this and previous findings (Bandy and Davison, 1990; Bjelland and Seeberg, 2003; Bonawitz et al., 2006) we suggest that mitochondrial translation inhibition by trichothecenes (Bin-Umer et al., 2011) increases ROS generation to a level overwhelming the cell's antioxidant (Bonawitz et al., 2006) resulting in oxidative damage to mitochondrial proteins, DNA and membranes (Bandy and Davison, 1990; Bonawitz et al., 2006). This adversely affects assembly of the respiratory complexes, resulting in a faulty ETC and further generation of ROS, leading to formation of toxic aggregates and further damage to mitochondrial and other cellular functions and eventual cell death (Bandy and Davison, 1990; Bjelland and Seeberg, 2003). Bonawitz et al. had also identified that genetic perturbations in cells, causing imbalanced and reduced mitochondrial translation, lead to increased sensitivity to H_2O_2-mediated oxidative stress and high levels of intracellular ROS (Bonawitz et al., 2006). This also explains why we found trichothecene-treated cells to be more sensitive to oxidative stress since ROS levels increased further in cells treated with H_2O_2 and trichothecenes (Fig. 4.4B). We have

therefore not only shown a direct role for mtROS in mediating trichothecene toxicity but also attempted to identify the molecular mechanism of trichothecene-induced oxidative stress.

4.3.3 Mitophagy is a novel cellular mechanism to alleviate trichothecene cytotoxicity

Endogenously or exogenously damaged mitochondria can trigger a cascade of events leading to cell death. Hence the timely and selective removal of dysfunctional mitochondria is very critical (Kurihara et al., 2012) for cell survival. This is likely the case during trichothecene treatment since accumulation of damaged mitochondria (Bin-Umer et al., 2011) leads to increased ROS generation (Fig. 4.3B and Fig. 4.2B) which in turn damage the mitochondrial membrane integrity (Fig. 4.3D) causing significantly depolarized membrane potential (Bin-Umer et al., 2011) and eventually resulting in cell death (Fig. 4.1A). Thus enhancing the selective removal of dysfunctional mitochondria via mitophagy, a selective type of autophagy, should likely reduce trichothecene cytotoxicity. This was first hinted when our screening identified mutants that were defective for autophagy/mitophagy (Fig. 4.1A and Table 4.1) which not only exhibited high sensitivity to Tcin (Fig. 4.1B) but also high levels of ROS (Fig. 4.1C). Later this was confirmed by the rapamycin study (Fig. 4.6). Rapamycin is an established enhancer of mitophagy (Mendl et al., 2011) which has been previously reported to alleviate rotenone-induced apoptosis by significantly reducing accumulation of damaged mitochondria (Pan et al., 2009). Rapamycin treatment also protected mammalian cells from Bax-induced apoptosis and *D. melanogaster* from paraquat-induced apoptosis which are mediated by ROS via the mitochondrial pathway (Ravikumar et al., 2006). We observed a similar

result when rapamycin alleviated growth inhibition by trichothecenes (Fig. 4.6B and 4.6C) and H_2O_2 (data not shown). The significant role of dysfunctional mitochondria in promoting ROS to lethal levels was further evident when rapamycin treatment reduced trichothecene and H_2O_2-induced ROS production (Fig. 4.6A). We attributed this drop in ROS levels to increased mitophagy since rapamycin is not a scavenger of ROS. A similar reduction in the cellular load of ROS by rapamycin has also been reported in the yeast frataxin knock-out mutant yfh1Δ (Marobbio et al., 2012). While yeast mutants defective for autophagy/mitophagy has been observed to exhibit high levels of ROS, this has been attributed to altered expression of ROS scavenging enzymes as a result of the genetic perturbations (Suzuki et al., 2011). However, we have shown for the first time in yeast, that rapamycin-triggered mitophagy reduces intracellular ROS generated by oxidants (H_2O_2) or mitochondrial toxins (trichothecenes) that affect mitochondrial translation and membrane integrity.

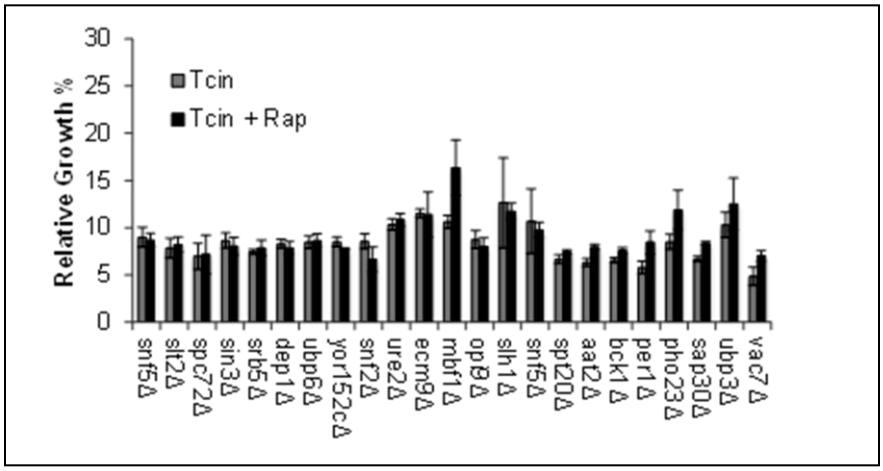

Figure 4.7. Effect of enhanced mitophagy on Tcin cytotoxicity in Tcin-sensitive mutants. Tcin-sensitive mutants were treated with 1µM Tcin alone or cotreated with

overnight prior to calculating OD_{600}. Relative growth is the ratio of OD_{600} of treated cells to the untreated control.

During mitophagy the MAPK signaling pathways Slt2 and Hog1 activates Atg32 which mediates recruitment of damaged mitochondria (Mendl et al., 2011). Deletion of any one of these genes inhibits mitophagy to varying degrees and in our study also rendered the cells more sensitive to T-2 (Fig. 4.6B) and Tcin (Fig. 4.6C) further suggesting an important role for mitophagy in alleviating trichothecene cytotoxicity. Moreover the inability of rapamycin to rescue these mitophagy-defective mutants from trichothecene cytotoxicity (Fig. 4.6B and 4.6C) confirms that rapamycin rescued trichothecene-treated cells by selectively removing damaged mitochondria via mitophagy. Interestingly trichothecenes blocked mitophagy in wild-type yeast (Fig. 4.6D) which were grown in conditions that promoted mitophagy (Kurihara et al., 2012; Lemasters, 2005; Mendl et al., 2011). Hence while untreated wild-type cells exhibited some level of mitophagy-induced GFP processing, trichothecene-treated wild-type yeast and the mitophagy-defective atg32Δ did not (Fig. 4.6D). These findings would therefore for the first type link mitochondrial dysfunction, ROS, mitophagy and cytotoxicity during trichothecene-mediated cell death: Trichothecene toxicity leads to mitochondrial dysfunction resulting in toxic levels of ROS. However since trichothecenes block mitophagy the damaged mitochondria is not cleared out and they accumulate leading to further production of ROS and finally resulting in cell death. This also confirms why enhancing the clearance of dysfunctional mitochondria by rapamycin should alleviate ROS to non-lethal levels and thereby alleviate cytotoxicity.

Our finding that mitophagy is disrupted during trichothecene toxicity is of particular significance since mitochondrial dysfunction and defective mitophagy has been implicated in several neurodegenerative diseases including Parkinson's, Alzheimer's and Huntington's disease (Chen and Chan, 2009). Moreover the dual potential to cause mitochondrial dysfunction and block mitophagy makes trichothecenes highly neurotoxic. Trichothecenes are unavoidable natural contaminants of cereal grains and epidemiological studies linking consumption of moldy grains to different human illness have been previously reported (Bryden, 2007). We have thus identified a novel target of trichothecenes and shown for the first time the importance of mitophagy for cell survival during ROS-mediated trichothecene toxicity, suggesting a possible etiological link between neurodegenerative diseases and the neurotoxic trichothecenes.

4.4 Materials and Methods

Yeast Knockout Library Screen. We used the homozygous diploid knockout collection from Thermo Scientific® (Waltham, MA)for the sensitivity screening as described previously (McLaughlin et al., 2009) with some modifications. Briefly, the strains from the collection were replicated using the Singer HTS Rotor onto 96-deep-well plates containing liquid YP+ 2% Dextrose (YPD). Cells were grown for 20h in a GeneMachines® HiGRo shaker at 250rpm and 30°C and then printed with the Rotor onto Nunc® OmniTrays containing solid YPD media with or without Tcin. Sensitivity was scored by identifying those strains that failed to grow after 2days at 30°C in a static incubator. The screening was repeated twice and the select strains were collected and

growth at OD_{600} measured in liquid YPD media at a range of concentrations (0-2µM Tcin). Liquid growth assay was repeated twice before characterizing the 121 deletion mutants as Tcin-sensitive.

Reagents. Antioxidants ascorbic acid and vitamin E were purchased from Sigma-Aldrich® (St. Louis, MO). A 460mM stock solution was made with vitamin E using absolute ethanol while ascorbic acid was dissolved in water for a stock concentration of 1M. FCCP was purchased from Enzo Lifesciences® (Farmingdale, NY) and dissolved in absolute ethanol to make a stock concentration of 20mM.

Liquid Growth Assay. Yeast cells were grown in YP media supplemented with 2% dextrose. Following treatment cells were grown for the specified time in a shaker at 30°C and growth at OD_{600} recorded at every 60 minutes for a period of 18-24 hours.

Flow Cytometry. Treated and untreated cells were stained with 2',7'-dichlorfluorescein-diacetate (DCFH-DA) for ROS generation and MitoTracker Red CMXRos for mitochondrial membrane potential according to manufacturer's protocol. In all instances cells were stained with DCFH-DA for 30 minutes at 30°C while for MitoTracker Red staining was performed for 30 minutes at 37°C. Following staining with the appropriate dyes, cells were analyzed using the Accuri C6 Flow Cytometer® (Accuri Cytometers Inc., Ann Arbor, MI). For each sample 15,000 events were recorded. Live/Dead cells were gated using the forward (FSC) and side (SSC) scatter prior to assessing for fluorescence. Channel gating and histogram plots were made using the CFlow Plus Analysis software (Accuri Cytometers Inc., Ann Arbor, MI). Changes in MitoTracker

Red and DCFH-DA fluorescence were detected using the FL1 and FL3 channel respectively.

mtGFP processing assay. BY4743 and atg32Δ cells transformed with mtGFP were grown in SD-Ura media supplemented with 2% lactate for several generations. Cells were then shifted to SD-Ura media supplemented with 2% dextrose and grown in the presence or absence of 300μM T-2, 4μM Tcin, or 1μM rapamycin for 18h. Equal number of cells was collected for each treatment and whole cell lysate was separated on a 12% SDS-PAGE gel, transferred to a nitrocellulose membrane and then immunostained for free and intact GFP.

Data Analysis & Graphing. Data from the growth and translation assays were plotted and IC_{50} values and translation inhibition calculated using Microsoft Excel.

CHAPTER 5

Two Arabidopsis nsLTPs with antioxidant activity protect yeast mitochondria from ROS-mediated damage during trichothecene cytotoxicity.

Acknowledgement: Experiments in this chapter was performed with some assistance from Dr. John McLaughlin, a Research Associate, who originally identified the two lipid transfer proteins from his Arabidopsis screening. Matthew Butterly, an undergraduate student, helped with growth assays and flow cytometric analysis of yeast samples. The author is currently preparing a manuscript with results and conclusions from this chapter which will be submitted for publication in the near future.

Abstract

Trichothecenes are highly toxic metabolites produced by several Fusarium species including the cereal-grain pathogen, *F. graminearum*, which is the causative agent of wheat and barley scab. Overexpression of two type IV Arabidopsis-derived nonspecific lipid transfer proteins (nsLTP), LTP4.4 and LTP4.5, enhanced resistance to trichothecene toxicity in yeast. Trichothecenes inhibited total protein synthesis and elicited ROS production leading to mitochondrial membrane damage and eventual cell death. However, when overexpressed, nsLTPs were found to be associated with mitochondria and selectively prevented significant inhibition of mitochondrial translation. LTP4.4 and LTP4.5 proteins exhibited antioxidant activity by alleviating basal ROS levels and attenuating ROS generation by trichothecenes as well as oxidants. ROS-mediated damage to mitochondrial membrane integrity during trichothecene toxicity was also minimized in the nsLTP overexpressing cells suggesting a likely role for mitochondria in nsLTP-mediated resistance to trichothecene toxicity and Fusarium pathogenesis.

5.1 Introduction

Recent changes in world climate and varying cultural practices in harvesting have promoted the growth of *F. graminearum* and a reemergence of FHB in several regions posing difficult challenges to the agriculture and cattle industries (McMullen et al., 1997a). Iin the absence of uniform global regulatory standards, the worldwide food supply risks introduction of contaminated food grains in the global food supply and the detrimental consequences associated with trichothecene toxicoses to human health (Cardwell et al., 2001). Hence, interest in understanding the underlying mechanisms of trichothecene toxicity to improve resistance to *F. graminearum* infection, FHB and trichothecene contamination have been on the rise.

Several approaches are currently being investigated and employed to manage and prevent FHB outbreaks including developing highly resistant transgenic plants (Collinge et al., 2010). Improved host resistance to FHB has been the primary objective of several breeding programs in the U.S. Although this might reduce yield loss, it does not necessarily deal with trichothecene contamination and thereby making it unsuitable for cattle and human consumption. Identifying and characterizing the mechanism of action of trichothecenes at the cellular level might prove an effective approach to developing varied strategies to minimize and eradicate trichothecene-associated diseases like FHB. Hence our studies have been largely focused on identifying genetic resistance not only to FHB but also to trichothecene toxicity. Recently we employed an activation tagging approach (Weigel et al., 2000) to identify plant genes that confer resistance to trichothecenes. Activation tagging is a mutation generating technique whereby plants are

transformed with T-DNAs, which are engineered to contain enhancer sequences to either knockout or overexpress neighboring genes resulting in both loss-of-function and gain-of-function mutants, respectively (Weigel et al., 2000). Nearly 250,000 activation tagged Arabidopsis seeds were screened for resistance to Tcin and a resistant line, overexpressing two non-specific lipid transfer protein (nsLTP) genes, designated as LTP4.4 and LTP4.5, were identified (Manuscript in prep/press).

Nonspecific lipid transfer proteins (nsLTPs) are a class of basic cysteine rich proteins characterized by an eight cysteine motif (8CM) backbone (C-Xn-C-Xn-CC-Xn-CXC-Xn-C-Xn-C) with four disulfide linkages to form a highly plastic and flexible hydrophobic tunnel, which can bind lipids of varying sizes (Boutrot et al., 2008). First identified in spinach (Kader et al., 2005), for their ability to shuttle phospholipids between membrane vesicles or organelles *in vitro*, not all nsLTPs share this function (Boutrot et al., 2008). Furthermore, their function *in vivo* is not yet fully characterized. These low molecular weight proteins are synthesized as precursors with an N-terminal signal sequence and are often associated with cell wall in plants (Blein et al., 2002). Several nsLTPs have been shown to have defense roles with antibacterial and antifungal activities (Blein et al., 2002; Isaac Kirubakaran et al., 2008; Molina and García-Olmedo, 2003). However, unlike other defense proteins, nsLTPs are not phytotoxic and hence found to accumulate at very high levels in seeds (Regente and De La Canal, 2001). In *A. thaliana*, nsLTPs belong to a multigene family with over 40 genes and have been classified into nine groups (types) based on sequence homology (Boutrot et al., 2008). LTP4.4 and LTP4.5 belong to the type IV nsLTP family along with LTP4.2, LTP4.3 and

DIR1 (formerly LTP4.1) which is involved in systemic acquired resistance (SAR) signaling pathway (Maldonado et al., 2002). Some nsLTPs are relevant to human health due to their likely role as food allergens and in triggering asthma (Blein et al., 2002).

In this study, we overexpressed the Arabidopsis derived nsLTPs in yeast and found both LTP4.4 and LTP4.5 to confer resistance to both type A (T-2 and DAS) and type B (Tcin and DON) trichothecenes. Not only was this response unique to these two nsLTPs, this was not seen against other inhibitors of yeast growth. Our results have identified mitochondrial ROS-mediated cell death as a novel hallmark of trichothecene toxicity in yeast, which plays a critical role in nsLTP-mediated resistance to trichothecenes: LTP4.4 and LTP4.5 serve as antioxidants selectively protecting mitochondrial translation and minimizing ROS generation and thereby protecting mitochondrial membrane integrity and subsequent cell death. Our study, therefore, provides valuable insight into novel mechanisms by which resistance to trichothecene toxicity can be increased in yeast and higher eukaryotes as well as the increasingly critical role for mitochondria during trichothecene triggered cell death.

5.2 Results

5.2.1 Yeast cells overexpressing nsLTPs are resistant to trichothecene toxicity

To determine whether nsLTP overexpression provided resistance to trichothecenes in yeast, cells overexpressing the nsLTPs were grown against increasing concentrations of type A (T-2 and DAS) and type B (Tcin and DON) trichothecenes (Fig. 5.1) and average IC_{50} values were estimated. As shown in table 5.1, IC_{50} values increased

for nsLTP overexpressing cells (LTP4.4 and LTP4.5) relative to cells carrying the empty vector (VC) when grown against T-2 (182µM and 154µM vs. 127 µM), DAS (353µM and 304µM vs. 256µM), Tcin (4.7µM and 3.7µM vs. 2.8µM) and DON (1.73mM and 1.56mM vs. 1.30mM). Thus nsLTP overexpressing cells exhibited enhanced tolerance to otherwise lethal doses of trichothecenes, albeit to varying degrees.

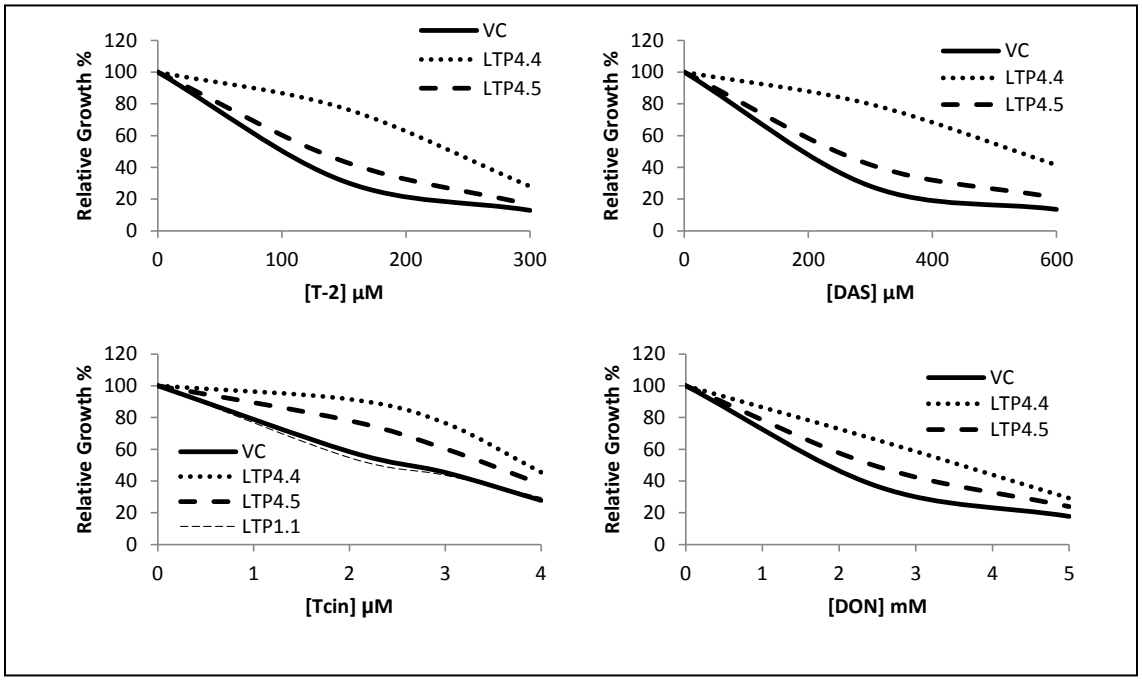

Figure 5.1. Growth of BY4743 overexpressing type IV AtLTPs against type A and type B trichothecenes. BY4743 cells overexpressing HA-tagged nsLTPs were treated with increasing concentrations of T-2, DAS, Tcin and DON for 36h. OD_{600} readings were recorded every 60min. with continuous shaking at 30°C in a BioTek (Synergy) plate reader.

Several nsLTPs from other groups within *A. thaliana* and from other organisms have been previously identified to have inhibitory effects against different phytopathogens including *F. graminearum* (Isaac Kirubakaran et al., 2008; Molina and

García-Olmedo, 2003; Regente and De La Canal, 2001; Wang et al., 2004). We therefore investigated the ability of two different nsLTPs in mediating resistance to trichothecene toxicity, namely LTP1.1, a type I Arabidopsis nsLTP (Boutrot et al., 2008) and *Ta*LTP3, a wheat LTP which was found to be overexpressed in FHB-resistant cultivars (Foroud et al., 2011). Cells overexpressing LTP1.1 did not show resistance when grown against Tcin and hence the lower IC_{50} value of 2.6µM. Interestingly, overexpressing LTP1.1 rendered the cells more sensitive to Tcin, when compared to the growth of cells carrying the vector alone (2.6µM vs. 2.8µM). However, cells overexpressing *Ta*LTP3, when treated with Tcin grew very similar to LTP4.4 overexpressing cells with an IC_{50} of 4.5µM. Thus not all nsLTPs mediate resistance to trichothecene toxicity.

In all instances, we found LTP4.4 overexpressing cells to be more resistant than LTP4.5 overexpressing cells while LTP1.1 overexpressing cells were not resistant to trichothecene toxicity. This led us to question whether these plant nsLTPs were expressed at similar levels in yeast. Since the nsLTPs were expressed as a fusion protein with an HA tag, following separation, we used anti-HA antibody to immunostain and determine the expression levels. All plant nsLTPs tested in this study were expressed optimally in yeast (Fig. 5.2A). Although expressed at similar levels, the nsLTPs appeared differently, with multiple bands seen in the case of LTP4.5 unlike LTP4.4 or LTP1.1 (Fig. 5.2A). Taken together this suggests that all nsLTPs in this study, including LTP4.4 and LTP4.5, are expressed optimally but exist differently *in vivo* in yeast. However, the varying degree of resistance observed between LTP4.4 and LTP4.5 overexpressing cells against trichothecenes, is not due to differences in their expression levels.

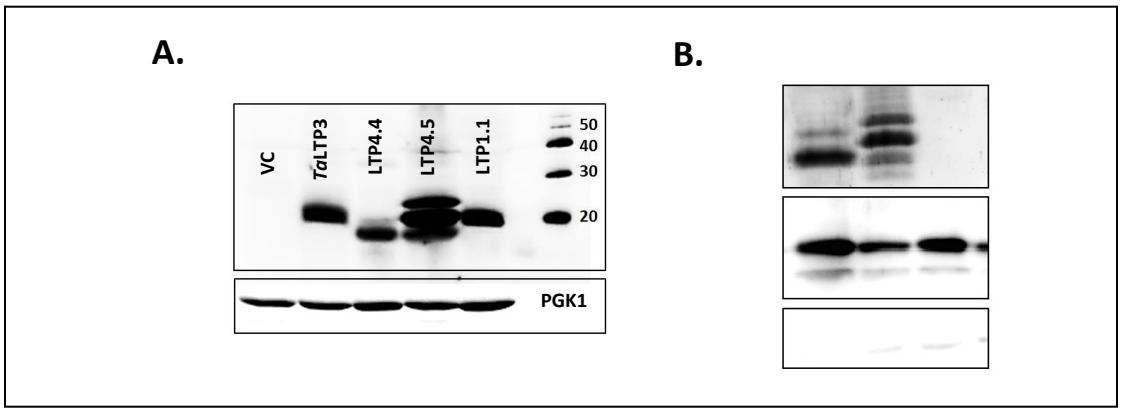

Figure 5.2. Expression of plant nsLTPs in yeast. BY4743 cells transformed with HA-tagged LTPs were induced for expression prior to whole cell protein extraction. Total lysate from LTP overexpressing cells were isolated prior to separating on 12% SDS-PAGE gel and immunostaining with anti-HA antibody. Loading control is indicated by immunostaining with anti-PGK1 antibody (B). Mitochondria was isolated from LTP overexpressing cells following 6h induction and separated on 15% SDS-PAGE gel. Following transfer of proteins, the membrane was stained with HA antibody and loading control checked with COX SS antibody. Immunostaining with PGK1 antibody assessed contmination of cytosolic fraction.

Subcellular fractionation of nsLTP overexpressing cells revealed minor differences in the enrichment of the nsLTPs in the different fractions. LTP4.4 was enriched in the cytosolic fraction (Fig. 5.3A) while LTP4.5 was enriched in the membrane fraction (Fig. 5.3B). Since the membrane fraction also contained mitochondrial membrane we looked at the possible localization of nsLTPs to mitochondria. When sucrose-gradient purified mitochondria, isolated from cells overexpressing LTP4.4 and LTP4.5, were immunostained with HA antibody, both LTP4.4 and LTP4.5 were found to be associated with the organelle (Fig. 5.2B).

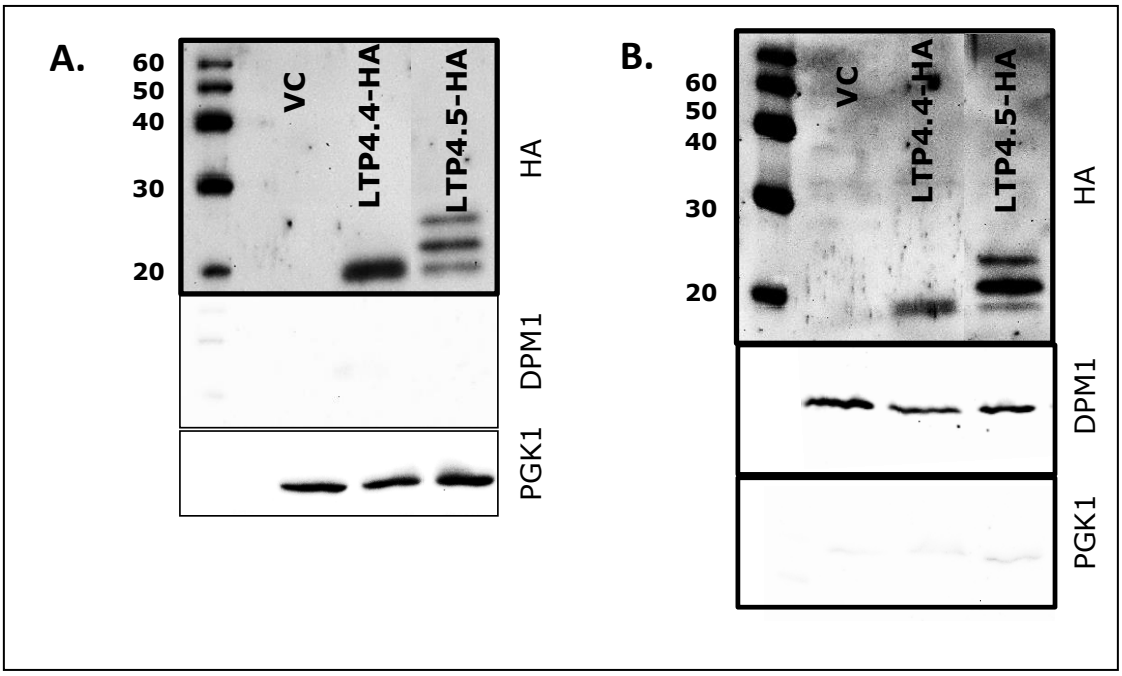

Figure 5.3. Protein expression and localization of type IV *At*LTPs in yeast. BY4743 cells overexpressing HA-tagged LTP4.4, LTP4.4ΔN, and LTP4.5 were induced for 6h. 1 OD_{600} were collected for whole cell protein extraction (A) and 5 OD_{600} cells were collected prior to isolation and separation of cytosolic (B), and membrane (C) fractions. Following SDS-PAGE (12%) and transfer, membranes were immunostained with HA mAb and then with either Pgk1 (44.74 KDa), Dpm1 (30.36 KDa) or both antibodies. Membranes stained with HA mAB were photographed after exposing for 120s while all other immunostains were exposed for 30s prior to photography.

5.2.2 nsLTP-mediated resistance is a specific response to trichothecenes in which mitochondrial translation is selectively protected

Trichothecenes are potent inhibitors of protein synthesis, among other cellular targets, which in turn affects the growth of cells. However, the observed resistance could be part of a general response of the cell due to the overexpression of nsLTPs which in turn affect the toxins entry into the cell. To investigate this we looked at the effect of

LTP4.4 and LTP4.5 overexpression on the growth of yeast against various inhibitors of translation and growth, namely cycloheximide, anisomycin and chloramphenicol. No significant shift in growth was observed, relative to the vector control, when nsLTP overexpressing cells were grown against 0.25µg/mL cycloheximide (Fig. 5.4A), 7.5µg/mL anisomycin (Fig. 5.4B) or 5mg/mL chloramphenicol (Fig. 5.4C). Thus the enhanced resistance, observed in cells overexpressing the two type IV nsLTPs, is a specific response to trichothecene toxicity.

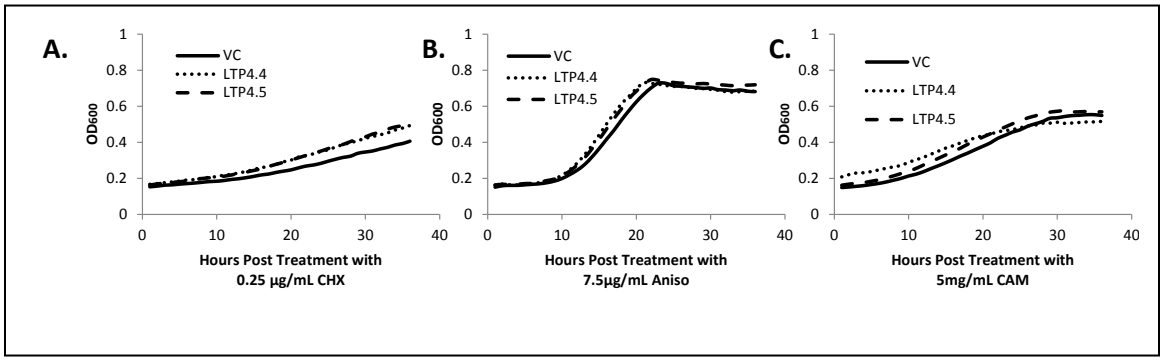

Figure 5.4. Growth of BY4743 overexpressing type IV *At*LTPs against inhibitors of translation and yeast growth. BY4743 cells overexpressing HA-tagged LTP4.4 and LTP4.5 were treated with CHX, cycloheximide (A), Aniso, anisomycin (B), and CAM, chloramphenicol (C). OD_{600} readings were recorded at every 30min. with continous shaking at 30°C in a BioTek (Synergy) plate reader.

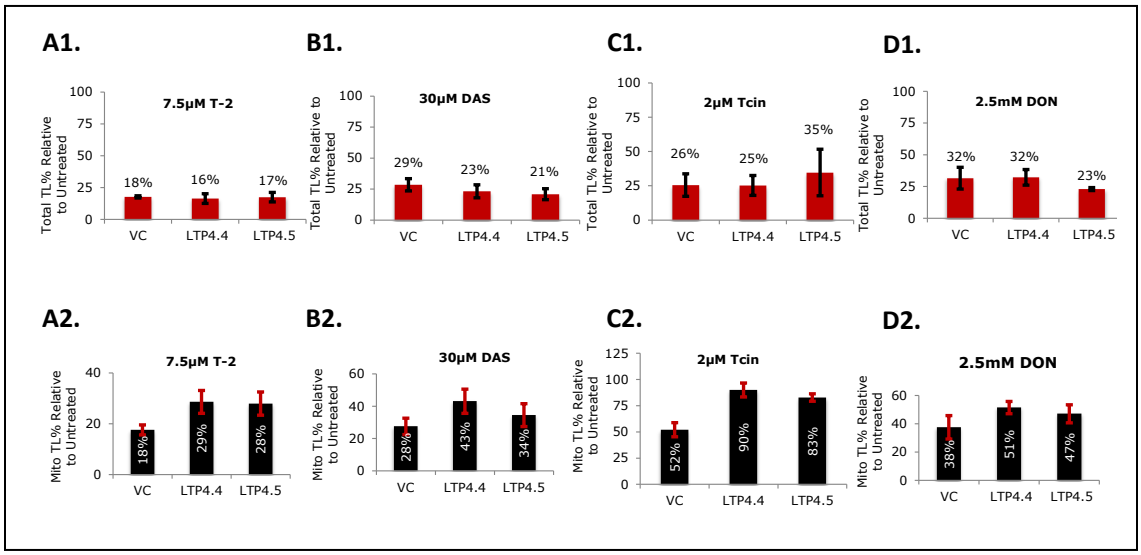

Figure 5.5. Total and mitochondrial translation in yeast cells overexpressing type IV *At*LTPs. BY4743 overexpressing LTP4.4 and LTP4.5 genes were treated with 7.5µM T-2 (A) and 30µM DAS (B) 2µM Tcin (C), and 2.5mM DON (D). For total translation (*upper panel*) following the 1h treatment with trichothecenes, [^{35}S]-methionine incorporation was measured for 20min. and rate of translation calculated as described in Materials and Methods. For mitochondrial translation (*lower panel*) prior to [^{35}S]-methionine incorporation, cytosolic translation was stopped by addition of cycloheximide. Final counts (CPM) for all experiments were normalized to the OD_{600} of each sample. Translation levels of trichothecene-treated samples were expressed as a percentage of the control (untreated) samples set to 100%. Error bars indicate S.E. where n = 3 independent replicates.

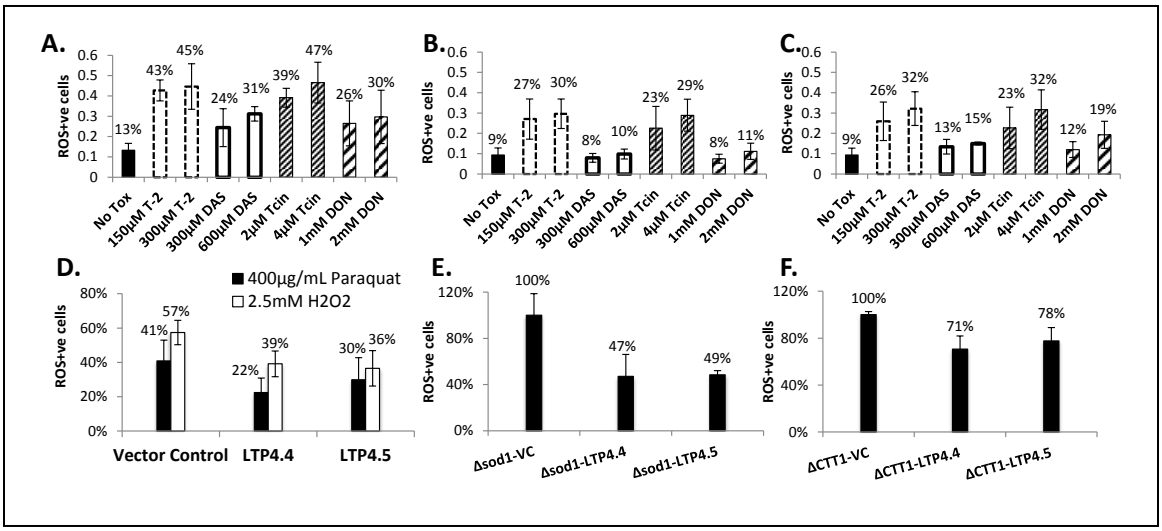

Figure 5.6. ROS levels in nsLTP overexpressing wild-type cells treated with trichothecenes and oxidants and in antioxidant-deficient sod1 and ctt1 deletion mutants. Trichothecene treated or untreated wild-type cells carrying the empty vector (A) or overexpressing LTP4.4 (B) or LTP4.5 (C) were stained for ROS. Wild type cells carrying the empty vector or overxpressing LTP4.4 or LTP4.5 treated with oxidants were stained for ROS. Δsod1 (E) and Δctt1(F) mutants overexpressing LTP4.4, LTP4.5 or the empty vector were stained for ROS. For each sample, 0.1 OD_{600} cells were stained with DCFH-DA for 20min post treatment. 15000 events were counted, live cells gated using forward and side scatter and DCFH fluorescence detected using the FL1 channel as described in Materials and Methods. Error bars indicate S.E. where n = 3 independent replicates.

Both cytosolic (Cundliffe and Davies, 1977) and mitochondrial protein synthesis (McLaughlin et al., 2009) are inhibited by trichothecenes with mitochondrial translation serving as a primary target (Bin-Umer et al., 2011). We therefore asked how the efficiency of cytosolic and mitochondrial translation is altered in trichothecene-treated yeast cells overexpressing LTP4.4 and LTP4.5. When treated with T-2 toxin, total translation dropped in VC and nsLTP overexpressing cells by more than 82% (Fig. 5.5 A1) but the drop in mitochondrial translation was less for nsLTP overexpressing cells (72%) relative to VC (82%) (Fig. 5.5 A2). When treated with 30µM DAS total translation was inhibited by greater than 71% in both VC and nsLTP overexpressing cells (Fig. 5.5 B1). However mitochondrial translation dropped only by 57-66% in nsLTP overexpressing cells relative to 72% for VC (Fig. 5.5 B2). Similarly, with 2µM Tcin total translation dropped by more than 65% in VC and nsLTP overexpressing cells but mitochondrial translation was inhibited to a lesser degree with 10-17% inhibition in nsLTP overexpressing cells as opposed to 48% in VC. Total translation was also inhibited by more than 68% with 2.5mM DON in nsLTP overexpressing cells and VC but only 49-53% inhibition of mitochondrial translation was observed in nsLTP

overexpressing cells compared to 62% in VC. Taken together, we find cytosolic translation is significantly inhibited in nsLTP overexpressing cells but mitochondrial translation is protected.

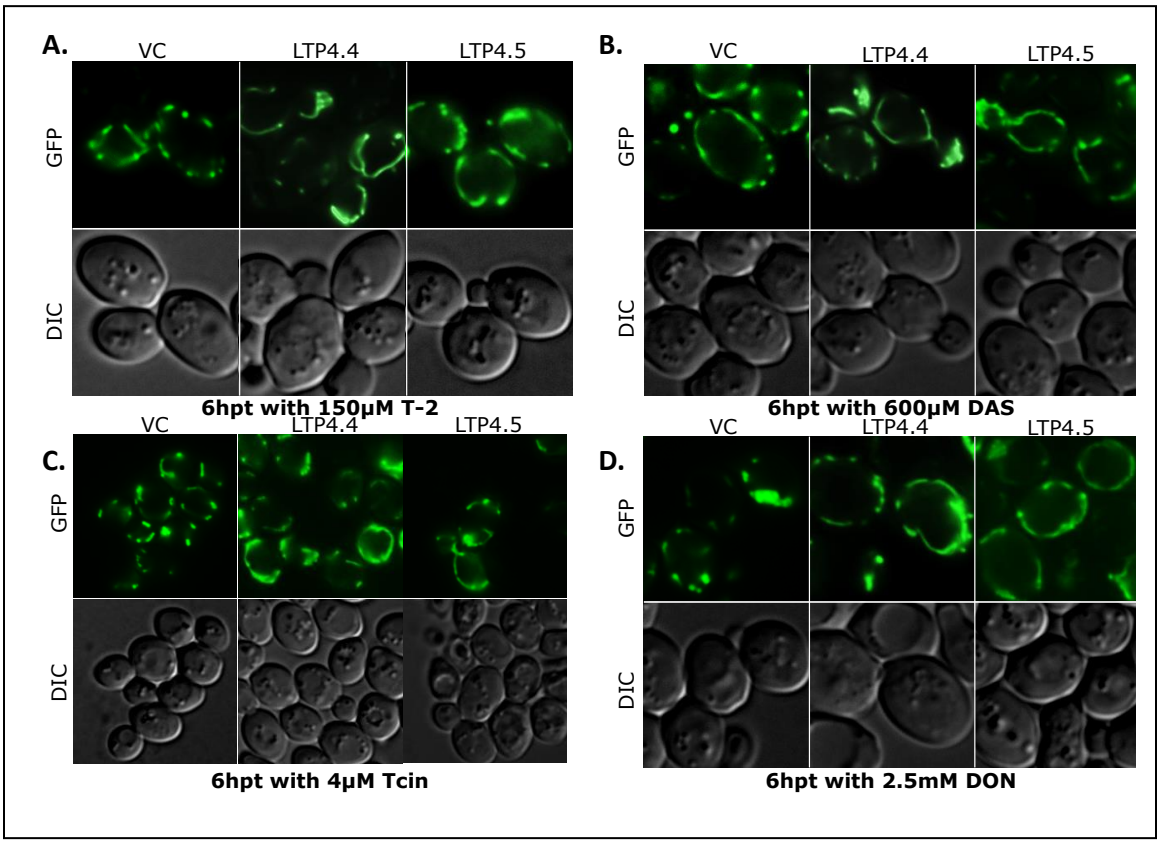

Figure 5.7. Mitochondrial membrane morphology of yeast cells overexpressing AtLTPs treated with trichothecenes. BY4743 constitutively expressing mitochondrial matrix targeted GFP (mTGFP) and carrying the empty vector (VC), or overexpressing LTP4.4 or LTP4.5 were treated with 4μM Tcin (A). 2.5mM DON (B), 150μM T-2 (C), and 600μM DAS (D) for 6h. Cells were then analyzed using epifluorescence microscopy at 100X magnification. Differential interference contrast (DIC) images of each cell are presented along with GFP images.

5.2.3 Trichothecenes elicit ROS production leading to mitochondrial membrane damage which is attenuated by the antioxidant nsLTPs

Thus far we find the two type IV nsLTPs associated with mitochondria (Fig. 5.2E) upon overexpression and mitochondrial translation selectively protected during nsLTP-mediated resistance to trichothecene toxicity (Fig. 5.5). These findings prompted us to explore two key biomarkers for mitochondrial membrane integrity, ROS generation and mitochondrial membrane fragmentation, in nsLTP overexpressing cells treated with trichothecenes.

ROS levels were measured using the ROS-sensitive stain DCFH-DA, which only fluoresces upon contact with ROS. While 13% of the untreated vector control cells stained positive for ROS (detected as DCF-positive by flow cytometer), this increased to 43-45% with T-2, 24-32% with DAS, 39-47% with Tcin and 26-30% with DON treatment (Fig. 5.6A). Hence trichothecenes significantly elicited ROS production in a dose dependent manner particularly with T-2 and Tcin.

In the untreated nsLTP overexpressing cells, we found less than 10% of the cells stained positive for ROS (Fig. 5.6B and 3C). Upon comparison, we find basal ROS levels to be lower in nsLTP overexpressing cells (10%) relative to the vector control (13%). This drop in ROS levels becomes more significant during trichothecene treatment. ROS positive cells dropped to 26-32% upon T-2 treatment, 8-15% upon DAS treatment, 23-32% upon Tcin treatment and 8-19% upon DON treatment in nsLTP overexpressing cells (Fig. 5.6B and 3C). Unlike cells carrying the empty vector (VC), we find ROS generation to be consistently lower in nsLTP overexpressing cells when treated with trichothecenes. Hence ROS generation triggered during trichothecene treatment is attenuated by the nsLTPs suggesting that they may act as antioxidants.

To investigate the antioxidant activity of the nsLTPs we treated nsLTP overexpressing cells with known oxidants such as paraquat and hydrogen peroxide. 41% and 57% vector control cells were ROS-positive within one hour treatment with 400µg/mL paraquat and 2.5mM hydrogen peroxide respectively (Fig. 5.6D). However, only 22-39% of nsLTP overexpressing cells were ROS-positive following similar treatment (Fig. 5.6D). nsLTP overexpression thus reduced ROS levels in cells treated with the oxidants suggesting that the two nsLTPs exhibited strong antioxidant activity.

Since nsLTPs exhibited strong antioxidant activity we investigated whether they can complement the ROS scavenging functions of the antioxidant enzymes superoxide dismutase and catalase. We therefore overexpressed LTP4.4 and LTP4.5 in Δsod1 and Δctt1 mutants which lack the antioxidant sod1 and ctt1 genes respectively. As expected, yeast mutants knocked out for sod1 and ctt1 genes exhibited very high levels of ROS (data not shown) relative to the wild type. However, upon nsLTP overexpression, a significant drop in the basal ROS levels was observed. Less than 50% of Δsod1cells stained positive for ROS (Fig. 5.6E.) while ROS levels dropped by 20-30% in Δctt1 (Fig. 5.6F) cells, relative to the vector control. The two type IV LTPs thus compensated for the antioxidant deficiency in cells lacking the sod1 and ctt1 enzymes further confirming their antioxidant capacity.

Significant alteration to the mitochondrial tubular morphology during the later stages of trichothecene toxicity (McLaughlin et al., 2009) is indicative of dysfunctional mitochondria and onset of apoptosis (Suen et al., 2008). To determine whether the integrity of mitochondrial membrane is affected in nsLTP overexpressing cells during

trichothecene toxicity we overexpressed LTP4.4 and LTP4.5 in yeast cells constitutively expressing GFP, targeted to the mitochondrial matrix. Severe fragmentation of the interconnected mitochondrial network is observed at six hours post treatment with either type A (Fig. 5.7A and 4B) or type B trichothecenes (Fig. 5.7C and 4D). However in LTP4.4 and LTP4.5 overexpressing cells, treated with the type A and type B trichothecenes, mitochondrial morphology was largely found to be fused and tubular with considerably less fragmentation (Fig. 5.7). Thus fragmentation of mitochondrial network is significantly alleviated in nsLTP overexpressing cells.

5.3 Discussion

5.3.1 LTP4.4 and LTP4.5 overexpression conferred resistance to trichothecenes

Our present work has focused on elucidating the mechanism of resistance to trichothecene toxicity and the role of two Arabidopsis type IV nsLTPs in yeast and by extension in higher eukaryotes including economically important cereal crops like wheat and barley. Only recently have nsLTPs been the focus of novel approaches to enhancing resistance to FHB and trichothecene toxicity. Earlier studies had identified the intrinsic antibacterial and antifungal properties of nsLTPs isolated from several different plants such as *Ace*-AMP1 (Cammue et al., 1995), *Hv*LTP2 (Molina and García-Olmedo, 2003) and *Ha*-AP10, which was shown to completely inhibit the germination of *F. solani* spores via membrane permeabilization (Regente et al., 2005). More recently, Zhu, X *et al*. showed that overexpression of *Ta.* LTP5 provided increased resistance to *F. graminearum* in transgenic wheat (Zhu et al., 2012). However, in all these and other

earlier studies, the nsLTPs were largely tested against the pathogens but not the toxins themselves. Furthermore, although these nsLTPs were shown to provide resistance not much has been investigated about their mechanism of action. Hence how these nsLTPs provide resistance to Fusarium pathogenesis or trichothecene toxicity is important and remains to be fully understood.

Earlier studies have identified the importance of nsLTPs in the plant's defense system against *Fusarium* infection (Foroud et al., 2011; Kruger et al., 2002; Petti et al., 2010) and phytotoxic effects of trichothecenes (Masuda et al., 2007). In our activation tagged screening of *A. thaliana* seeds for Tcin resistance, we identified two type IV nsLTP genes, LTP4.4 and LTP4.5, to be overexpressed (Manuscript in prep/press). When overexpressed LTP4.4 and LTP4.5 enhanced tolerance, in yeast, to otherwise lethal doses of type A and type B trichothecenes as suggested by their higher IC_{50} values relative to the vector control. Results from our yeast growth assays suggest that the observed resistance to type A (T-2 and DAS) and type B (Tcin and DON) trichothecene toxicity, associated with LTP4.4 and LTP4.5 overexpression, is not specific to plants. Either a conserved cellular mechanism is at play or a direct interaction between trichothecenes and the nsLTPs, leading to sequestration of the toxins, is involved in mediating resistance. However, not all nsLTPs have this property since overexpression of the type I LTP1.1 (IC_{50} lower than vector control) did not confer resistance to Tcin (Fig. 5.1C). Other *A. thaliana* derived nsLTPs, such as LTP1.5 (Masuda et al., 2007) and the remaining type IV nsLTP members (DIR1, LTP4.2 and LTP4.3) need to be investigated

to determine if their overexpression might also provide resistance, similar to LTP4.4 and LTP4.5, to trichothecene toxicity in yeast.

Despite the nsLTPs, investigated in this study, being of plant origin they were expressed optimally in yeast and at similar levels, albeit differently (Fig. 5.2A and 5.3). To what extent these differences in protein processing *in vivo* (Fig. 5.2) and their localization (Fig. 5.3) might play a role in mediating resistance to trichothecene toxicity is not yet fully understood. All nsLTPs, studied thus far, are known to be associated with cell wall in plants and are often secreted from the cell (Carvalho and Gomes, 2007). Secretion of the antifungal nsLTPs is likely to serve in the plant's first line of defense by inhibiting hyphal growth, as seen with *Ha*-AP10, and thereby prevent colonization of the fungal pathogen (Regente and De La Canal, 2001). However, unlike the toxin producing pathogen, during trichothecene toxicity, nsLTPs likely function inside the cell since the toxins target cellular processes like protein synthesis and mitochondrial functions. Since lipid transfer proteins are often secreted and found to be associated with the cell wall (Carvalho and Gomes, 2007), it is possible for the cell membranes to be altered upon overexpression of these proteins. For instance, in *A. thaliana* mutants with cuticular defects, expression of LTP genes were highly upregulated (Chassot et al., 2007). Hence the observed resistance to trichothecene toxicity in LTP4.4 and LTP4.5 overexpressing cells could be due to increased efflux pump activity, alterations to membrane permeability or other general cellular responses which affect the entry of the small molecule trichothecenes into the cell. However, this does not seem to be the case since growth of the nsLTP overexpressing cells were significantly inhibited by known

translation inhibitors, with varied modes of action, such as cycloheximide, anisomycin and chloramphenicol (Fig. 5.4). Therefore the resistance associated with the two type IV LTPs is specific to trichothecenes and nsLTP overexpression does not seem to affect the permeability of the yeast cell membrane.

5.3.2 LTP4.4 and LTP4.5 protected mitochondrial functions from trichothecene-induced oxidative stress

Several studies have previously indicated the critical role of mitochondria in trichothecene toxicity (McLaughlin et al., 2009; Pace et al., 1988; Zhou et al., 2005b). More recently we showed that mitochondrial translation is not only inhibited by trichothecenes but it is independent of cytosolic translation inhibition (Bin-Umer et al., 2011). Since neither nsLTPs have a mitochondrial targeting sequence, the role of mitochondria in nsLTP-mediated resistance to trichothecene toxicity was, however, not expected. Interestingly we found both LTP4.4 and LTP4.5 to be associated with the mitochondria (Fig. 5.2B) upon overexpression. Total translation was inhibited by both type A (T-2 and DAS) and type B (Tcin and DON) trichothecenes in the nsLTP overexpressing cells similar to that of cells carrying the vector alone (Fig. 5.5A). Contrast this with mitochondrial translation and we find that in all instances the drop in mitochondrial translation is significantly lower in the nsLTP overexpressing cells, relative to the vector control (Fig. 5.5B). However this cannot be attributed to inaccessibility to mitochondrial ribosomes for the trichothecenes due to altered mitochondrial membrane permeability in the nsLTP overexpressing cells. Firstly the mitochondrial translation inhibitor, chloramphenicol, inhibited growth in cells carrying

the empty vector as well as in cells overexpressing the nsLTPs (Fig. 5.4C). Secondly, mitochondrial membrane potential (ψ_{mito}) significantly dropped in these cells during FCCP treatment with significant changes in ψ_{mito} observed in cells treated with trichothecenes during the same time period (Fig. 5.4). Thus selectively protecting mitochondrial translation by the nsLTPs rendered the cells resistant to trichothecene toxicity.

ROS generation has been identified as a mechanism of trichothecene toxicity particularly in animal studies. T-2 treated mice showed a time dependent increase in ROS generation in the brain (Chaudhary and Rao, 2010) while intracellular ROS levels increased significantly in DON-treated HepG2 cells (Zhang et al., 2009). In wheat, Desmond et al. showed that DON elicited hydrogen peroxide production leading to programmed cell death (Desmond et al., 2008). Other studies in yeast and plants largely suggest a correlation as inferred from the upregulation of antioxidant genes during Fusarium infection (Geddes et al., 2008) or trichothecene treatment (Iwahashi et al., 2008). However a direct indication of ROS generation during trichothecene toxicity is lacking in yeast or plant. In our present work a dose dependent increase in ROS levels is evident in response to trichothecene treatment in yeast. We find both type A and type B trichothecenes promoted ROS levels in vector control cells within one hour of treatment (Fig. 5.6A) which suggests ROS generation to be an early time point event during trichothecene toxicity. We also find a correlation between cytotoxicity of trichothecenes and their ability to generate ROS. Hence T-2 and Tcin which are more toxic than their

congeners DAS and DON respectively promoted higher ROS levels, which further suggest that the role of ROS is a critical mechanism of trichothecene toxicity in yeast.

5.3.3 LTP4.4 and LTP4.5 exhibit antioxidant activity which protects yeast against trichothecene-induced oxidative stress

Recently Wu et al. identified a barley LTP with antioxidant activity that played a major role in stabilizing flavor in ageing beer (Wu et al., 2011). In the present work, we found basal and trichothecene promoted ROS levels to be lower in LTP4.4 and LTP4.5 overexpressing yeast relative to vector control (Fig. 5.6A-C), suggesting a similar activity for these two Arabidopsis nsLTPs. This is further confirmed when oxidant-treated nsLTP overexpressing cells exhibited significantly lower population of ROS positive cells unlike the vector control (Fig. 5.6D). The cell's antioxidant mechanism is mediated by several key enzymes including superoxide dismutases (SOD1 & SOD2) and the two isoforms of catalases (CTT1 and CTA1) (Herrero et al., 2008). The antioxidant activity of nsLTPs complemented, to some degree, the ROS scavenging functions of sod1 and ctt1 enzymes and hence ROS levels were attenuated in Δsod1and Δctt1 mutants upon nsLTP overexpression (Fig. 5.6E and 3F). However, the cell's capacity to scavenge ROS only partially rescues the cells during trichothecene toxicity since overexpression of sod1 or ctt1 in yeast did not render the cell significantly resistant to trichothecene toxicity (data not shown). Hence while ROS has a critical role other cellular targets particularly mitochondrial translation inhibition is also necessary for trichothecene toxicity.

Impaired expression of the mitochondrial encoded components of the electron transport chain (ETC) has been shown to promote ROS generation (Indo et al., 2007) and

render the cells sensitive to oxidative stress (Grant et al., 1997). Any inhibitory effect on mitochondrial translation which affects ETC will therefore trigger excess ROS production which initiates an oxidation cascade damaging proteins, mitochondrial membrane and other macromolecules leading to cell death (Avery, 2011). Thus inhibition of mitochondrial translation by trichothecenes, in the vector control, (Fig. 5.5B) led to increased generation of ROS (Fig. 5.6A) and the subsequent damage to the mitochondrial membrane indicated by the severely fragmented morphology (Fig. 5.7). However, through the association of the two nsLTPs to the mitochondria (Fig. 5.2F), the resulting selective protection of mitochondrial translation (Fig. 5.5B) and further scavenging of ROS due to their antioxidant property, trichothecene-mediated ROS generation is significantly limited (Fig. 5.6B and 3C) in the LTP4.4 and LTP4.5 overexpressing cells. This in turn prevents any subsequent damage, particularly to the mitochondrial membrane. Thus mitochondrial membrane fragmentation is considerably less severe in the nsLTP-overexpressing cells relative to the vector control (Fig. 5.7). It is, however, possible for the nsLTPs to have a direct effect on the toxins by sequestering trichothecenes and preventing it from targeting mitochondria and other cellular targets to induce cell death. Investigating direct interactions between the two nsLTPs and trichothecenes would likely answer these questions.

In our attempt to delineate the underlying mechanisms of trichothecene toxicity our current work has determined mitochondrial ROS generation to be a key event and identified the ability of two novel antioxidant Arabidopsis nsLTPs to selectively protect mitochondrial translation and scavenge ROS during trichothecene toxicity. nsLTPs

present a promising alternative and a highly effective solution to current approaches in engineering resistance to FHB and reducing trichothecene contamination. Unlike other defense proteins, nsLTPs are not phytotoxic and hence they can be overexpressed without affecting the plant physiology(Blein et al., 2002; Carvalho and Gomes, 2007) . To date, several nsLTPs have been implicated, albeit a correlation, in providing resistance to plants from Arabidopsis to wheat against different pathogens including *F. graminearum* (Molina et al., 1993; Zhu et al., 2012). Our work presents yeast as a powerful tool to rapidly identify nsLTPs and other plant genes with anti-Fusarium and trichothecene resistance properties and to study the resulting toxicity at the single cell level. Furthermore, findings from this study should provide an impetus to further explore mitochondrial ROS as a critical factor during trichothecene toxicity and the overexpression of nsLTPs as a method for generating FHB resistance in cereal plants like wheat and barley.

5.4 Materials and Methods

Yeast Strains and Plasmids. Yeast strain BY4743 (MATa/α, his3Δ1/his3Δ1, leu2Δ0/leu2Δ0, LYS2/lys2Δ0, met15Δ0/MET15, ura3Δ0/ura3Δ0) was used as the background for all experiments. Gateway® entry vector pDONR™221 was purchased from Invitrogen while the destination vector pAG425-GAL1-ccdB-HA (plasmid# 14249) was purchased from Addgene® (www.addgene.com).

*Nonspecific Lipid Transfr Proteins (nsLTPs) used in this study. At*LTP4.4 (At5g55450.1), *At*LTP4.5 (At5g55460.1), *At*LTP1.1 (At2g15050.2), and *Ta*LTP3 (AY226580.1).

Gateway Cloning and Yeast transformation. Standard gateway® cloning procedure was followed to clone the LTP genes into the destination vector, pAG425-GAL1-ccdB-HA. Gateway®-compatible primers were designed to amplify the LTP coding sequences without the stop codon. Using standard PCR protocol, the two nsLTPs were amplified from genomic DNA isolated from Arabidopsis seeds. The resulting LTP amplicons with flanking attB1 and attB2 sequences were then cloned into a pDONR™221 vector (Invitrogen) with Gateway® BP Clonase® II Enzyme mix according to manufacturer's protocol. Using Gateway® LR Clonase® II Enzyme mix, LTP4.4 and LTP4.5 genes were shuttled from the pDONR™221 entry vector into pAG425-GAL1-ccdB-HA, the destination vector. At the end of BP and LR reactions the resulting product was transformed into DH5-α cells for propagation and verified. Yeast cells were transformed with the final destination vectors carrying the LTP genes using a standard transformation protocol. The empty backbone vector, pAG425-GAL1-ccdB-HA, was used to transform yeast cells and used as vector control for further experiments.

Growth Assay. Yeast cells carrying the different overexpression vectors were initially grown in synthetic leucine dropout (SD-Leu) media supplemented with 2% dextrose and later shifted to SD-Leu media with 2% galactose for induction of the LTP4.4 and LTP4.5 genes. Following induction of the nsLTP genes for (3 to 6h) equal amounts of cells were added to standard microplates (24-well or 96-well) containing SD-Leu with 2% galactose. Tcin, DON, T-2, DAS, cycloheximide, anisomycin, and chloramphenicol were added to the final concentrations as specified. The plates were sealed with breathable

strips and growth at OD_{600} was recorded every 30-60 minutes for a period of 36-48 hours shaking constantly at 30°C in a BioTek® plate reader.

Whole Cell Protein Extraction. Total protein were isolated from the different cells using a previously described rapid protocol (Zhang et al., 2011) with some modifications. Briefly, 1 OD_{600} cells were collected following induction spun down and washed with water. The pellet was resuspended in 2M LiAc and kept in ice for 5 min. The pellet was then resuspended in 0.4M NaOH and kept in ice for 5 min. The pellet was then resuspended in 100µL 2X sample buffer, heated at 90°C for 5 min. After a 2 min. quick spin samples were loaded onto an SDS-PAGE gel.

Subcellular Fractionation. 5 OD_{600} cells of yeast transformants overexpressing the different LTP genes or the vector alone were collected after induction, washed with H_2O and resuspended in 600µL lysis buffer (50mM Tris-HCl, pH 8.0, 5mM EDTA, 1% (v/v) Triton X-100, 1mM PMSF). Equal volume of glass beads were added and vortexed at maximum speed in a bead beater for 2 min. The suspension was spun down at 3000 g (10min., 4°C) to precipitate the nucleus and cell debris. The supernatant was then centrifuged at 18,000 g (20min., 4°C) to precipitate the membrane and the supernatant was centrifuged further at 100,000 g (60min., 4°C) to precipitate the ribosomes. The supernatant containing the cytosolic fraction was then transferred to a separate tube. 2X SDS sample buffer was added to the membrane and cytosolic fractions, and heated before loading on a 12% SDS-PAGE gel.

Analysis of Protein Expression. The proteins from whole cell protein extraction and subcellular fraction were separated on a 12% SDS-PAGE gel, transferred to a nitrocellulose membrane. For dot blot assay, the proteins were directly applied to the membrane. The membrane was then probed with anti-HA (1:10,000) antibody (GenScript Cat#A01244-100). The blot was then stripped (8M Guanidine HCl) and reprobed using antibody against Pgk1p and Dpm1p and developed using ChemiDoc MP imaging system (Bio-Rad).

Analysis of Total Translation. Cells grown in SD-Leu (+2% Raffinose) were shifted to synthetic methionine dropout (SD-Met) media (Yeast Nitrogen Base w/o Amino Acids & Ammonium Sulfate, all amino acids except methionine) containing MSG as the nitrogen source and 2% galactose for 3 hours. Cultures grown to an OD600 of 0.2-0.3 were then split into two: one-half was treated with a range of increasing concentrations of Tcin, DON, T-2, and DAS in ethanol and the other half was treated with an equivalent amount of ethanol. Following one hour treatment with Tcin at 30°C, 3 OD_{600} cells were washed with minimal media by a quick spin (10,000 g for 1 min) and resuspended in 500 µL SD-Met (+2% raffinose). To each sample, 1 µL [^{35}S]-Met (Perkin-Elmer, NEG-009A, >1000 Ci/mmol) was added. The reaction was stopped after 20 min by washing and resuspending cells in 500 µL (20 mM) cold methionine and 75 µL Rodel Mix (560 µL 5 M NaOH, 0.11 mL β-mercaptoethanol, 0.76 mL H2O, 0.075 mL 1 mM PMSF). An equal volume of 50% TCA (trichloroacetic acid) was added to the mix and filtered through 2.4 cm glass fiber filters (grade 691, VWR). Filters were then washed, twice each, with 5%

TCA and 95% ethanol and scintillation counts per minute (CPM) measured. CPM readings were finally normalized to OD600 to indicate total translation.

Analysis of Mitochondrial Translation. The mitochondrial translation assay was done as the total translation assay with the following exception: Prior to the addition of [^{35}S]-Met, 20 µL (7.5 mg/mL) freshly prepared cycloheximide was added to each sample to selectively inhibit cytosolic translation and incubated for 5 min.

Flow Cytometry. Treated and untreated cells were stained with 2',7'-dichlorfluorescein-diacetate (DCFH-DA) for ROS generation and MitoTracker Red CMXRos for mitochondrial membrane potential according to manufacturer's protocol. In all instances cells were stained with DCFH-DA for 30 minutes at 30°C while for MitoTracker Red staining was performed for 30 minutes at 37°C. Following staining with the appropriate dyes, cells were analyzed using the Accuri C6 Flow Cytometer® (Accuri Cytometers Inc., Ann Arbor, MI). For each sample 15,000 events were recorded. Live/Dead cells were gated using the forward (FSC) and side (SSC) scatter prior to assessing for fluorescence. Channel gating and histogram plots were made using the CFlow Plus Analysis software (Accuri Cytometers Inc., Ann Arbor, MI). Changes in MitoTracker Red and DCFH-DA fluorescence were detected using the FL1 and FL3 channel respectively.

Data Analysis & Graphing. Data from the growth and translation assays were plotted and IC_{50} values and translation inhibition calculated using Microsoft Excel.

CHAPTER 6

Conclusions

Plant diseases like FHB caused by the fungal pathogen *F. graminearum* have recently reemerged due to various economic and environmental factors (Goswami and Kistler, 2004). This has resulted in increased contamination of the global food and feed supply with Fusarium trichothecenes primarily type B trichothecenes (DON and NIV). Chronic exposure to trichothecenes, largely type A and type B, is a threat to human health while destruction of economically significant cereal crops by *F. graminearum* poses a serious threat to the global breadbasket (Windels, 2000). Current investigations have largely focused on molecular mapping of novel genes controlling FHB resistance and trichothecene accumulation and devising improved management strategies to limit, if not prevent, incidence rates of infection. While significant strides have been made, the progress has been painstakingly slow. This work, on the other hand, has focused on exploring the molecular mechanisms underlying trichothecene toxicity to gain insight into Fusarium pathogenesis and develop effective measures to enhance resistance against trichothecenes. Identifying cellular targets critical for trichothecene toxicity will also further aid in engineering transgenic plants resistant to fungal infection and trichothecene contamination.

Trichothecenes were originally identified with their potent ability to inhibit cytosolic translation which was then associated with the observed cellular toxicity (Ueno, 1983). However further investigations suggested that other cellular processes are adversely targeted by trichothecenes and that trichothecene toxicosis cannot be simply attributed to cytosolic translation inhibition. Following this line of reasoning we had applied tools of yeast genomics and used a genome-wide approach, for the first time, to

study trichothecene toxicity. The overwhelming evidence from our genomic screening pursued us to investigate further the role of mitochondria as a target during trichothecene cytotoxicity (McLaughlin et al., 2009). This was further supported by a few reports from the 1980s that identified some of the in vitro effects of trichothecenes on mitochondria (Pace, 1983; Pace et al., 1988; Schappert and Khachatourians, 1983).

We took advantage of yeast as an excellent model organism to study mitochondrial biology and attempted to isolate some of the inhibitory effects of trichothecenes on mitochondria. While we utilized the high toxicity of Tcin in yeast to study mechanism of action of DON and other type B trichothecenes we observed similar effects with members of type A trichothecenes (T-2 and DAS) as well (Bin-Umer et al., 2011). We thus identified that type A and B trichothecenes damaged mitochondrial functions *in vivo* by inhibiting mitochondrial translation and disrupting mitochondrial membrane integrity by promoting severe membrane fragmentation. Our *in organello* studies which showed trichothecenes to inhibit translation in isolated yeast mitochondria suggest these inhibitory effects were direct. Furthermore we separated the inhibitory effects of trichothecenes on mitochondrial functions from cytosolic translation suggesting that mitochondrial translation and membrane integrity are targeted directly and upstream of cytosolic protein synthesis. We also found that mitochondria rendered dysfunctional by the inhibitory effects of trichothecenes attributed to the observed increase in ROS-levels in trichothecene treated cells. While trichothecenes were previously suggested to induce oxidative stress (Chaudhary and Rao, 2010) our studies identified ROS to play a direct role in mediating trichothecene cytotoxicity by damaging mitochondrial

membranes. These novel findings further confirmed that mitochondria is more critical to trichothecene toxicity than originally thought. This led us to explore the role of autophagy and particularly mitophagy as an alternative cellular mechanism to alleviate cytotoxicity by selectively removing trichothecene-damaged mitochondria. This work not only identified rapamycin-induced mitophagy as an effective strategy for trichothecene resistance we also identified trichothecenes to have potential neurotoxic effects particularly involving mitophagy. This work also show for the first time that mitophagy is disrupted during trichothecene toxicity and this was further supported when the targeted gene knockdown of essential components of the mitophagy process result in increased sensitivity to trichothecenes.

Findings from this study are of importance to human health particularly because mitophagy is a key cellular process that is adversely affected during neurodegenerative diseases (Bhatia-Kiššová and Camougrand, 2012; Lin and Beal, 2006). *Fusarium spp.* that produce trichothecenes are widely encountered worldwide and trichothecenes are unavoidable natural contaminant of cereal grains. Thus the possible etiological link between trichothecenes and neurodegenerative diseases warrants investigation starting with confirming these inhibitory effects in higher eukaryotes like *D. melanogaster* and also in mammalian studies. Results from these studies should then provide the impetus to pursue epidemiological surveys investigating incidence of neurodegenerative disease and rate of Fusarium trichothecene contamination in the cereal crops of the selected region.

REFERENCES

Aerts, A.M., Zabrocki, P., Francois, I.E., Carmona-Gutierrez, D., Govaert, G., Mao, C., Smets, B., Madeo, F., Winderickx, J., Cammue, B.P., *et al.* (2008). Ydc1p ceramidase triggers organelle fragmentation, apoptosis and accelerated ageing in yeast. Cell Mol Life Sci *65*, 1933-1942.

Alvaro, D., Lisby, M., and Rothstein, R. (2007). Genome-wide analysis of Rad52 foci reveals diverse mechanisms impacting recombination. PLoS Genet *3*, e228.

Asada, K. (1992). Ascorbate peroxidase–a hydrogen peroxide-scavenging enzyme in plants. Physiologia Plantarum *85*, 235-241.

Avery, S.V. (2011). Molecular targets of oxidative stress. Biochem J *434*, 201-210.

Ayed-Boussema, I., Bouaziz, C., Rjiba, K., Valenti, K., Laporte, F., Bacha, H., and Hassen, W. (2008). The mycotoxin Zearalenone induces apoptosis in human hepatocytes (HepG2) via p53-dependent mitochondrial signaling pathway. Toxicology in vitro : an international journal published in association with BIBRA *22*, 1671-1680.

Bae, H.K., Shinozuka, J., Islam, Z., and Pestka, J.J. (2009). Satratoxin G interaction with 40S and 60S ribosomal subunits precedes apoptosis in the macrophage. Toxicol Appl Pharmacol *237*, 137-145.

Bandy, B., and Davison, A.J. (1990). Mitochondrial mutations may increase oxidative stress: implications for carcinogenesis and aging? Free Radical Biology and Medicine *8*, 523-539.

Barrientos, A., Korr, D., and Tzagoloff, A. (2002). Shy1p is necessary for full expression of mitochondrial COX1 in the yeast model of Leigh's syndrome. Embo J *21*, 43-52.

Betina, V. (1983). The chemistry and biology of antibiotics (Elsevier Scientific Publishing Company).

Betina, V. (1989). Mycotoxins. Chemical, biological and environmental aspects (Elsevier).

Bhatia-Kiššová, I., and Camougrand, N. (2012). Mitophagy: A process that adapts to the cell physiology. The International Journal of Biochemistry & Cell Biology.

Bin-Umer, M.A., McLaughlin, J.E., Basu, D., McCormick, S., and Tumer, N.E. (2011). Trichothecene mycotoxins inhibit mitochondrial translation—Implication for the mechanism of toxicity. Toxins *3*, 1484-1501.

Bjelland, S., and Seeberg, E. (2003). Mutagenicity, toxicity and repair of DNA base damage induced by oxidation. Mutation research *531*, 37-80.

Blein, J.P., Coutos-Thevenot, P., Marion, D., and Ponchet, M. (2002). From elicitins to lipid-transfer proteins: a new insight in cell signalling involved in plant defence mechanisms. Trends Plant Sci *7*, 293-296.

Bonawitz, N.D., Rodeheffer, M.S., and Shadel, G.S. (2006). Defective mitochondrial gene expression results in reactive oxygen species-mediated inhibition of respiration and reduction of yeast life span. Mol Cell Biol *26*, 4818-4829.

Bouaziz, C., Martel, C., Sharaf el dein, O., Abid-Essefi, S., Brenner, C., Lemaire, C., and Bacha, H. (2009). Fusarial toxin-induced toxicity in cultured cells and in isolated mitochondria involves PTPC-dependent activation of the mitochondrial pathway of apoptosis. Toxicol Sci *110*, 363-375.

Boutrot, F., Chantret, N., and Gautier, M.F. (2008). Genome-wide analysis of the rice and Arabidopsis non-specific lipid transfer protein (nsLtp) gene families and identification of wheat nsLtp genes by EST data mining. BMC Genomics *9*, 86.

Bryden, W.L. (2007). Mycotoxins in the food chain: human health implications. Asia Pac J Clin Nutr *16 Suppl 1*, 95-101.

Bu'Lock, J. (1980). Mycotoxins as secondary metabolites. The biosythesis of mycotoxins. Academic Press, Inc., New York, NY, 1-16.

Burmeister, H.R., and Hesseltine, C.W. (1970). Biological assays for two mycotoxins produced by *Fusarium tricinctum*. Appl Microbiol *20*, 437-440.

Bushnell, W., Hazen, B., Pritsch, C., and Leonard, K. (2003). Histology and physiology of Fusarium head blight. Fusarium head blight of wheat and barley, 44-83.

Cammue, B.P., Thevissen, K., Hendriks, M., Eggermont, K., Goderis, I.J., Proost, P., Van Damme, J., Osborn, R.W., Guerbette, F., Kader, J.C., *et al.* (1995). A potent antimicrobial protein from onion seeds showing sequence homology to plant lipid transfer proteins. Plant Physiol *109*, 445-455.

Cannon, M., Jimenez, A., and Vazquez, D. (1976). Competition between trichodermin and several other sesquiterpene antibiotics for binding to their receptor site(s) on eukaryotic ribosomes. Biochem J *160*, 137-145.

Caporael, L.R. (1976). Ergotism: the satan loosed in Salem? Science *192*, 21-26.

Cardwell, K., Desjardins, A., Henry, S., Munkvold, G., and Robens, J. (2001). Mycotoxins: The cost of achieving food security and food quality. APSnet. American Phytopathological Society. August.

Carvalho, A.O., and Gomes, V.M. (2007). Role of plant lipid transfer proteins in plant cell physiology—a concise review. Peptides *28*, 1144-1153.

CAST (2003). Potential economic costs of mycotoxins in the United States. Mycotoxins: Risks in plant, animal, and human systems, 136-142.

Chassot, C., Nawrath, C., and Metraux, J.P. (2007). Cuticular defects lead to full immunity to a major plant pathogen. The Plant journal : for cell and molecular biology *49*, 972-980.

Chaudhari, M., Jayaraj, R., Bhaskar, A.S., and Lakshmana Rao, P.V. (2009). Oxidative stress induction by T-2 toxin causes DNA damage and triggers apoptosis via caspase pathway in human cervical cancer cells. Toxicology *262*, 153-161.

Chaudhary, M., and Rao, P.V. (2010). Brain oxidative stress after dermal and subcutaneous exposure of T-2 toxin in mice. Food and chemical toxicology : an international journal published for the British Industrial Biological Research Association *48*, 3436-3442.

Chen, G.Q., He, X., and McKeon, T.A. (2005a). A simple and sensitive assay for distinguishing the expression of ricin and *Ricinus communis* agglutinin genes in developing castor seed (*R. communis L.*). J Agric Food Chem *53*, 2358-2361.

Chen, H., and Chan, D.C. (2009). Mitochondrial dynamics–fusion, fission, movement, and mitophagy–in neurodegenerative diseases. Human molecular genetics *18*, R169-R176.

Chen, H., Chomyn, A., and Chan, D.C. (2005b). Disruption of fusion results in mitochondrial heterogeneity and dysfunction. J Biol Chem *280*, 26185-26192.

Chen, H., Detmer, S.A., Ewald, A.J., Griffin, E.E., Fraser, S.E., and Chan, D.C. (2003a). Mitofusins Mfn1 and Mfn2 coordinately regulate mitochondrial fusion and are essential for embryonic development. J Cell Biol *160*, 189-200.

Chen, Q., Vazquez, E.J., Moghaddas, S., Hoppel, C.L., and Lesnefsky, E.J. (2003b). Production of reactive oxygen species by mitochondria: central role of complex III. J Biol Chem *278*, 36027-36031.

Chen, Y., and Gibson, S.B. (2008). Is mitochondrial generation of reactive oxygen species a trigger for autophagy? Autophagy *4*, 246-248.

Cheng, X., Qin, Y., and Ivessa, A.S. (2009). Loss of mitochondrial DNA under genotoxic stress conditions in the absence of the yeast DNA helicase Pif1p occurs independently of the DNA helicase Rrm3p. Mol Genet Genomics *281*, 635-645.

Collinge, D.B., Jorgensen, H.J., Lund, O.S., and Lyngkjaer, M.F. (2010). Engineering pathogen resistance in crop plants: current trends and future prospects. Annu Rev Phytopathol *48*, 269-291.

Contamine, V., and Picard, M. (2000). Maintenance and integrity of the mitochondrial genome: a plethora of nuclear genes in the budding yeast. Microbiology and molecular biology reviews : MMBR *64*, 281-315.

Cundliffe, E., Cannon, M., and Davies, J. (1974). Mechanism of inhibition of eukaryotic protein synthesis by trichothecene fungal toxins. Proc Natl Acad Sci U S A *71*, 30-34.

Cundliffe, E., and Davies, J.E. (1977). Inhibition of initiation, elongation, and termination of eukaryotic protein synthesis by trichothecene fungal toxins. Antimicrob Agents Chemother *11*, 491-499.

Davidson, J.F., and Schiestl, R.H. (2001). Mitochondrial respiratory electron carriers are involved in oxidative stress during heat stress in *Saccharomyces cerevisiae*. Molecular and cellular biology *21*, 8483-8489.

Desmond, O.J., Manners, J.M., Stephens, A.E., Maclean, D.J., Schenk, P.M., Gardiner, D.M., Munn, A.L., and Kazan, K. (2008). The Fusarium mycotoxin deoxynivalenol elicits hydrogen peroxide production, programmed cell death and defence responses in wheat. Mol Plant Pathol *9*, 435-445.

Diekert, K., de Kroon, A.I., Kispal, G., and Lill, R. (2001). Isolation and subfractionation of mitochondria from the yeast *Saccharomyces cerevisiae*. Methods Cell Biol *65*, 37-51.

Dumont, A., Hehner, S.P., Hofmann, T.G., Ueffing, M., Droege, W., and Schmitz, M.L. (1999). Hydrogen peroxide-induced apoptosis is CD95-independent, requires the release of mitochondria-derived reactive oxygen species and the activation of NF-kappaB. Oncogene *18*, 747.

Ehrlich, K.C., and Daigle, K.W. (1987). Protein synthesis inhibition by 8-oxo-12,13-epoxytrichothecenes. Biochim Biophys Acta *923*, 206-213.

Eisenberg, T., Buttner, S., Kroemer, G., and Madeo, F. (2007). The mitochondrial pathway in yeast apoptosis. Apoptosis *12*, 1011-1023.

Etzel, R. (2002). Mycotoxins. Journal of the American Medical Association (JAMA) *287*, 425-427.

Fanelli, C., Taddei, F., Nisini, P.T., Jestoi, M., Ricelli, A., Visconti, A., and Fabbri, A. (2003). Use of resveratrol and BHA to control fungal growth and mycotoxin production in wheat and maize seeds. Aspects of Applied Biology *68*, 63-72.

Fannjiang, Y., Cheng, W.C., Lee, S.J., Qi, B., Pevsner, J., McCaffery, J.M., Hill, R.B., Basanez, G., and Hardwick, J.M. (2004). Mitochondrial fission proteins regulate programmed cell death in yeast. Genes Dev *18*, 2785-2797.

Fleischer, T.C., Weaver, C.M., McAfee, K.J., Jennings, J.L., and Link, A.J. (2006). Systematic identification and functional screens of uncharacterized proteins associated with eukaryotic ribosomal complexes. Genes Dev *20*, 1294-1307.

Fontanesi, F. (2013). Mechanisms of mitochondrial translational regulation. IUBMB Life *65*, 397-408.

Foroud, N., Ouellet, T., Laroche, A., Oosterveen, B., Jordan, M., Ellis, B., and Eudes, F. (2011). Differential transcriptome analyses of three wheat genotypes reveal different host response pathways associated with Fusarium head blight and trichothecene resistance. Plant Pathology *61*, 296-314.

Foroud, N.A., and Eudes, F. (2009). Trichothecenes in cereal grains. Int J Mol Sci *10*, 147-173.

Fox, T.D. (2012). Mitochondrial protein synthesis, import, and assembly. Genetics *192*, 1203-1234.

Fox, T.D., Folley, L.S., Mulero, J.J., McMullin, T.W., Thorsness, P.E., Hedin, L.O., and Costanzo, M.C. (1991). Analysis and manipulation of yeast mitochondrial genes. Methods Enzymol *194*, 149-165.

Freeman, G.G., and Morrison, R.I. (1948). Trichothecin; an antifungal metabolic product of *Trichothecium roseum* Link. Nature *162*, 30.

Fried, H.M., and Warner, J.R. (1981). Cloning of yeast gene for trichodermin resistance and ribosomal protein L3. Proc Natl Acad Sci U S A *78*, 238-242.

Fryer, M. (1992). The antioxidant effects of thylakoid Vitamin E (α-tocopherol). Plant, Cell & Environment *15*, 381-392.

Funes, S., and Herrmann, J.M. (2007). Analysis of mitochondrial protein synthesis in yeast. In Mitochondria (Springer), pp. 255-263.

Gajdusek, D.C. (1953). Acute Infectious Hemorrha-gic Fevers and Mycotoxicoses in the Union of Soviet Socialist Republics. Med. Sci.

Gasperi-Campani, A., Brognara, I., Baiocchi, D., and Roncuzzi, L. (2005). Mitochondrial DNA D-loop as a new target of Saporin 6 nuclease activity. Toxicon *45*, 475-480.

Geddes, J., Eudes, F., Laroche, A., and Selinger, L.B. (2008). Differential expression of proteins in response to the interaction between the pathogen *Fusarium graminearum* and its host, *Hordeum vulgare*. Proteomics *8*, 545-554.

Gong, D.W., He, Y.F., Karas, M., and Reitman, M. (1997). Uncoupling protein-3 is a mediator of thermogenesis regulated by thyroid hormone, beta 3-adrenergic agonists, and leptin. Journal of Biological Chemistry *272*, 24129-24132.

Gonzalez, A., Jimenez, A., Vazquez, D., Davies, J.E., and Schindler, D. (1978). Studies on the mode of action of hygromycin B, an inhibitor of translocation in eukaryotes. Biochim Biophys Acta *521*, 459-469.

Goswami, R.S., and Kistler, H.C. (2004). Heading for disaster: *Fusarium graminearum* on cereal crops. Mol Plant Pathol *5*, 515-525.

Grant, C.M., MacIver, F.H., and Dawes, I.W. (1997). Mitochondrial function is required for resistance to oxidative stress in the yeast *Saccharomyces cerevisiae*. FEBS letters *410*, 219-222.

Grovey, J. (2007). The trichothecenes and their biosynthesis. In Progress in the Chemistry of Organic Natural Products (Springer), pp. 63-130.

Hallstrom, T.C., and Moye-Rowley, W.S. (2000). Multiple signals from dysfunctional mitochondria activate the pleiotropic drug resistance pathway in *Saccharomyces cerevisiae*. J Biol Chem *275*, 37347-37356.

Hansen, J.L., Moore, P.B., and Steitz, T.A. (2003). Structures of five antibiotics bound at the peptidyl transferase center of the large ribosomal subunit. J Mol Biol *330*, 1061-1075.

Hartley, M.R., and Lord, J.M. (2004). Cytotoxic ribosome-inactivating lectins from plants. Biochim Biophys Acta *1701*, 1-14.

Hermann, G.J., Thatcher, J.W., Mills, J.P., Hales, K.G., Fuller, M.T., Nunnari, J., and Shaw, J.M. (1998). Mitochondrial fusion in yeast requires the transmembrane GTPase Fzo1p. J Cell Biol *143*, 359-373.

Herrero, E., Ros, J., Belli, G., and Cabiscol, E. (2008). Redox control and oxidative stress in yeast cells. Biochim Biophys Acta *1780*, 1217-1235.

Higgins, V.J., Alic, N., Thorpe, G.W., Breitenbach, M., Larsson, V., and Dawes, I.W. (2002). Phenotypic analysis of gene deletant strains for sensitivity to oxidative stress. Yeast *19*, 203-214.

Hohn, T.M., McCormick, S.P., and Desjardins, A.E. (1993). Evidence for a gene cluster involving trichothecene-pathway biosynthetic genes in *Fusarium sporotrichioides*. Curr Genet *24*, 291-295.

Hoon, S., St Onge, R.P., Giaever, G., and Nislow, C. (2008). Yeast chemical genomics and drug discovery: an update. Trends Pharmacol Sci *29*, 499-504.

Huang, P., Akagawa, K., Yokoyama, Y., Nohara, K., Kano, K., and Morimoto, K. (2007). T-2 toxin initially activates caspase-2 and induces apoptosis in U937 cells. Toxicol Lett *170*, 1-10.

Ichinoe, M., and Kurata, H. (1983). Trichothecene-producing fungi. Developments in food science IV, Trichothecenes: Chemical, biological and toxicological aspects. Amsterdam: Elsevier, 73-82.

Iglesias, M., and Ballesta, J.P. (1994). Mechanism of resistance to the antibiotic trichothecin in the producing fungi. European journal of biochemistry / FEBS *223*, 447-453.

Indo, H.P., Davidson, M., Yen, H.C., Suenaga, S., Tomita, K., Nishii, T., Higuchi, M., Koga, Y., Ozawa, T., and Majima, H.J. (2007). Evidence of ROS generation by mitochondria in cells with impaired electron transport chain and mitochondrial DNA damage. Mitochondrion *7*, 106-118.

Inoue, I., Namiki, F., and Tsuge, T. (2002). Plant colonization by the vascular wilt fungus *Fusarium oxysporum* requires FOW1, a gene encoding a mitochondrial protein. The Plant cell *14*, 1869-1883.

Iordanov, M.S., Pribnow, D., Magun, J.L., Dinh, T.H., Pearson, J.A., Chen, S.L., and Magun, B.E. (1997). Ribotoxic stress response: activation of the stress-activated protein kinase JNK1 by inhibitors of the peptidyl transferase reaction and by sequence-specific RNA damage to the alpha-sarcin/ricin loop in the 28S rRNA. Mol Cell Biol *17*, 3373-3381.

Isaac Kirubakaran, S., Begum, S.M., Ulaganathan, K., and Sakthivel, N. (2008). Characterization of a new antifungal lipid transfer protein from wheat. Plant Physiology and Biochemistry *46*, 918-927.

Ishihara, N., Jofuku, A., Eura, Y., and Mihara, K. (2003). Regulation of mitochondrial morphology by membrane potential, and DRP1-dependent division and FZO1-dependent fusion reaction in mammalian cells. Biochem Biophys Res Commun *301*, 891-898.

Iwahashi, Y., Kitagawa, E., and Iwahashi, H. (2008). Analysis of mechanisms of T-2 toxin toxicity using yeast DNA microarrays. Int J Mol Sci *9*, 2585-2600.

Jossé, L., Li, X., Coker, R.D., Gourlay, C.W., and Evans, I.H. (2010). Transcriptomic and phenotypic analysis of the effects of T 2 toxin on Saccharomyces cerevisiae: evidence of mitochondrial involvement. FEMS yeast research.

Kader, J.C., Julienne, M., and Vergnolle, C. (2005). Purification and characterization of a spinach-leaf protein capable of transferring phospholipids from liposomes to mitochondria or chloroplasts. European Journal of Biochemistry *139*, 411-416.

Kang, Z., and Buchenauer, H. (1999). Immunocytochemical localization of fusarium toxins in infected wheat spikes by *Fusarium culmorum*. Physiol Mol Plant P *55*, 275-288.

Kanki, T., Kang, D., and Klionsky, D.J. (2009). Monitoring mitophagy in yeast: the Om45-GFP processing assay. Autophagy *5*, 1186-1189.

Knorre, D.A., Popadin, K.Y., Sokolov, S.S., and Severin, F.F. (2013). Roles of mitochondrial dynamics under stressful and normal conditions in yeast cells. Oxid Med Cell Longev *2013*, 139491.

Kornmann, B., Currie, E., Collins, S.R., Schuldiner, M., Nunnari, J., Weissman, J.S., and Walter, P. (2009). An ER-mitochondria tethering complex revealed by a synthetic biology screen. Science *325*, 477-481.

Kralj, A., Gurgui, M., Konig, G.M., and van Echten-Deckert, G. (2007). Trichothecenes induce accumulation of glucosylceramide in neural cells by interfering with lactosylceramide synthase activity. Toxicol Appl Pharmacol *225*, 113-122.

Kruger, N. (2002). The Bradford method for protein quantitation. The protein protocols handbook, 15-21.

Kruger, W.M., Pritsch, C., Chao, S., and Muehlbauer, G.J. (2002). Functional and comparative bioinformatic analysis of expressed genes from wheat spikes infected with *Fusarium graminearum*. Molecular plant-microbe interactions : MPMI *15*, 445-455.

Kruglov, A.G., Andersson, M.A., Mikkola, R., Roivainen, M., Kredics, L., Saris, N.E.L., and Salkinoja-Salonen, M.S. (2009). Novel Mycotoxin from Acremonium exuviarum Is a Powerful Inhibitor of the Mitochondrial Respiratory Chain Complex III. Chemical Research in Toxicology *22*, 565-573.

Kurihara, Y., Kanki, T., Aoki, Y., Hirota, Y., Saigusa, T., Uchiumi, T., and Kang, D. (2012). Mitophagy plays an essential role in reducing mitochondrial production of reactive oxygen species and mutation of mitochondrial DNA by maintaining mitochondrial quantity and quality in yeast. J Biol Chem *287*, 3265-3272.

Kuzmenko, A.V., Levitskii, S.A., Vinogradova, E.N., Atkinson, G.C., Hauryliuk, V., Zenkin, N., and Kamenski, P.A. (2013). Protein biosynthesis in mitochondria. Biochemistry. Biokhimiia *78*, 855-866.

Langevin, F., Eudes, F., and Comeau, A. (2004). Effect of trichothecenes produced by *Fusarium graminearum* during Fusarium head blight development in six cereal species. European Journal of Plant Pathology *110*, 735-746.

Legros, F., Lombes, A., Frachon, P., and Rojo, M. (2002). Mitochondrial fusion in human cells is efficient, requires the inner membrane potential, and is mediated by mitofusins. Molecular Biology of the Cell *13*, 4343-4354.

Lemasters, J.J. (2005). Perspective - Selective mitochondrial autophagy, or mitophagy, as a targeted defense against oxidative stress, mitochondrial dysfunction, and aging. Rejuvenation Research *8*, 3-5.

Li, M., and Pestka, J.J. (2008). Comparative induction of 28S ribosomal RNA cleavage by ricin and the trichothecenes deoxynivalenol and T-2 toxin in the macrophage. Toxicol Sci *105*, 67-78.

Lin, M.T., and Beal, M.F. (2006). Mitochondrial dysfunction and oxidative stress in neurodegenerative diseases. Nature *443*, 787-795.

Ludovico, P., Rodrigues, F., Almeida, A., Silva, M.T., Barrientos, A., and Corte-Real, M. (2002). Cytochrome c release and mitochondria involvement in programmed cell death induced by acetic acid in *Saccharomyces cerevisiae*. Mol Biol Cell *13*, 2598-2606.

Ludovico, P., Sousa, M.J., Silva, M.T., Leao, C., and Corte-Real, M. (2001). Saccharomyces cerevisiae commits to a programmed cell death process in response to acetic acid. Microbiology *147*, 2409-2415.

Machida, K., Tanaka, T., Fujita, K., and Taniguchi, M. (1998). Farnesol-induced generation of reactive oxygen species via indirect inhibition of the mitochondrial electron transport chain in the yeast *Saccharomyces cerevisiae*. J Bacteriol *180*, 4460-4465.

Maldonado, A.M., Doerner, P., Dixon, R.A., Lamb, C.J., and Cameron, R.K. (2002). A putative lipid transfer protein involved in systemic resistance signalling in Arabidopsis. Nature *419*, 399-403.

Mao, K., Wang, K., Liu, X., and Klionsky, D.J. (2013). The scaffold protein Atg11 recruits fission machinery to drive selective mitochondria degradation by autophagy. Dev Cell *26*, 9-18.

Marobbio, C.M., Pisano, I., Porcelli, V., Lasorsa, F.M., and Palmieri, L. (2012). Rapamycin reduces oxidative stress in frataxin-deficient yeast cells. Mitochondrion *12*, 156-161.

Masuda, D., Ishida, M., Yamaguchi, K., Yamaguchi, I., Kimura, M., and Nishiuchi, T. (2007). Phytotoxic effects of trichothecenes on the growth and morphology of *Arabidopsis thaliana*. J Exp Bot *58*, 1617-1626.

McCormick, S.P., Stanley, A.M., Stover, N.A., and Alexander, N.J. (2011). Trichothecenes: from simple to complex mycotoxins. Toxins (Basel) *3*, 802-814.

McLaughlin, C., Vaughan, M., Campbell, I., Wei, C.M., Stafford, M., and Hansen, B. (1977). Inhibition of protein synthesis by trichothecenes. Mycotoxins in Human and Animal Health. Park Forest South, Ill: Pathotox Publishers, 263–275.

McLaughlin, J.E., Bin-Umer, M.A., Tortora, A., Mendez, N., McCormick, S., and Tumer, N.E. (2009). A genome-wide screen in *Saccharomyces cerevisiae* reveals a critical role for the mitochondria in the toxicity of a trichothecene mycotoxin. Proc Natl Acad Sci U S A *106*, 21883-21888.

McMullen, M., Jones, R., and Gallenberg, D. (1997a). Scab of wheat and barley: A re-emerging disease of devastating impact. Plant Disease *81*, 1340-1348.

McMullen, M., Jones, R., and Gallenberg, D. (1997b). Scab of wheat and barley: A re-emerging disease of devasting impact. Plant disease (USA).

McQuibban, G.A., Saurya, S., and Freeman, M. (2003). Mitochondrial membrane remodelling regulated by a conserved rhomboid protease. Nature *423*, 537-541.

Mendl, N., Occhipinti, A., Müller, M., Wild, P., Dikic, I., and Reichert, A.S. (2011). Mitophagy in yeast is independent of mitochondrial fission and requires the stress response gene WHI2. Journal of cell science *124*, 1339-1350.

Merhej, J., Richard-Forget, F., and Barreau, C. (2011). Regulation of trichothecene biosynthesis in Fusarium: recent advances and new insights. Appl Microbiol Biotechnol *91*, 519-528.

Mirocha, C.J., Pawlosky, R.A., Chatterjee, K., Watson, S., and Hayes, W. (1983). Analysis for Fusarium toxins in various samples implicated in biological warfare in Southeast Asia. Journal-Association of Official Analytical Chemists *66*, 1485.

Molina, A., and García-Olmedo, F. (2003). Enhanced tolerance to bacterial pathogens caused by the transgenic expression of barley lipid transfer protein LTP2. The Plant Journal *12*, 669-675.

Molina, A., Segura, A., and Garcia-Olmedo, F. (1993). Lipid transfer proteins (nsLTPs) from barley and maize leaves are potent inhibitors of bacterial and fungal plant pathogens. FEBS Lett *316*, 119-122.

Morton, C.O., Dos Santos, S.C., and Coote, P. (2007). An amphibian-derived, cationic, alpha-helical antimicrobial peptide kills yeast by caspase-independent but AIF-dependent programmed cell death. Mol Microbiol *65*, 494-507.

Murphy, P.A., Hendrich, S., Landgren, C., and Bryant, C.M. (2006). Food mycotoxins: An update. Journal of Food Science *71*, R51-R65.

Nasri, T., Bosch, R.R., Voorde, S., and Fink-Gremmels, J. (2006). Differential induction of apoptosis by type A and B trichothecenes in Jurkat T-lymphocytes. Toxicology in vitro : an international journal published in association with BIBRA *20*, 832-840.

Niki, E., Yamamoto, Y., Komuro, E., and Sato, K. (1991). Membrane Damage Due to Lipid Oxidation. Am J Clin Nutr *53*, S201-S205.

Obeid, L.M., Okamoto, Y., and Mao, C. (2002). Yeast sphingolipids: metabolism and biology. Biochim Biophys Acta *1585*, 163-171.

Orrenius, S., Gogvadze, V., and Zhivotovsky, B. (2007). Mitochondrial oxidative stress: implications for cell death. Annual review of pharmacology and toxicology *47*, 143-183.

Pace, J.G. (1983). Effect of T-2 mycotoxin on rat liver mitochondria electron transport system. Toxicon *21*, 675-680.

Pace, J.G., Watts, M.R., and Canterbury, W.J. (1988). T-2 mycotoxin inhibits mitochondrial protein synthesis. Toxicon *26*, 77-85.

Pan, T., Rawal, P., Wu, Y., Xie, W., Jankovic, J., and Le, W. (2009). Rapamycin protects against rotenone-induced apoptosis through autophagy induction. Neuroscience *164*, 541-551.

Parikh, B.A., Coetzer, C., and Tumer, N.E. (2002). Pokeweed antiviral protein regulates the stability of its own mRNA by a mechanism that requires depurination but can be separated from depurination of the alpha-sarcin/ricin loop of rRNA. J Biol Chem *277*, 41428-41437.

Paterson, R.R.M., and Lima, N. (2010). How will climate change affect mycotoxins in food? Food Research International *43*, 1902-1914.

Peraica, M., Radic, B., Lucic, A., and Pavlovic, M. (1999). Toxic effects of mycotoxins in humans. Bull World Health Organ *77*, 754-766.

Pestka, J. (2009). Trichothecene mycotoxins and the ribotoxic stress response.

Pestka, J.J. (2008). Mechanisms of deoxynivalenol-induced gene expression and apoptosis. Food additives & contaminants. Part A, Chemistry, analysis, control, exposure & risk assessment *25*, 1128-1140.

Petti, C., Khan, M., and Doohan, F. (2010). Lipid transfer proteins and protease inhibitors as key factors in the priming of barley responses to Fusarium head blight disease by a biocontrol strain of *Pseudomonas fluorescens*. Functional & Integrative Genomics *10*, 619-627.

Ponts, N., Pinson-Gadais, L., Barreau, C., Richard-Forget, F., and Ouellet, T. (2007). Exogenous H_2O_2 and catalase treatments interfere with *Tri* genes expression in liquid cultures of *Fusarium graminearum*. FEBS letters *581*, 443-447.

Pozniakovsky, A.I., Knorre, D.A., Markova, O.V., Hyman, A.A., Skulachev, V.P., and Severin, F.F. (2005). Role of mitochondria in the pheromone- and amiodarone-induced programmed death of yeast. Journal of Cell Biology *168*, 257-269.

Rao, S.S., and Grollman, A.P. (1967). Cycloheximide resistance in yeast: a property of the 60s ribosomal subunit. Biochem Biophys Res Commun *29*, 696-704.

Rapaport, D., Brunner, M., Neupert, W., and Westermann, B. (1998). Fzo1p is a mitochondrial outer membrane protein essential for the biogenesis of functional mitochondria in *Saccharomyces cerevisiae*. J Biol Chem *273*, 20150-20155.

Rasmussen, A.K., Chatterjee, A., Rasmussen, L.J., and Singh, K.K. (2003). Mitochondria-mediated nuclear mutator phenotype in *Saccharomyces cerevisiae*. Nucleic Acids Res *31*, 3909-3917.

Ravikumar, B., Berger, Z., Vacher, C., O'Kane, C.J., and Rubinsztein, D.C. (2006). Rapamycin pre-treatment protects against apoptosis. Hum Mol Genet *15*, 1209-1216.

Regente, M.C., and De La Canal, L. (2001). Purification, characterization and antifungal properties of a lipid-transfer protein from sunflower (*Helianthus annuus*) seeds. Physiologia Plantarum *110*, 158-163.

Regente, M.C., Giudici, A.M., Villalain, J., and de la Canal, L. (2005). The cytotoxic properties of a plant lipid transfer protein involve membrane permeabilization of target cells. Lett Appl Microbiol *40*, 183-189.

Rizzo, A.F., Atroshi, F., Ahotupa, M., Sankari, S., and Elovaara, E. (1994). Protective effect of antioxidants against free radical-mediated lipid peroxidation induced by DON or T-2 toxin. Zentralblatt fur Veterinarmedizin. Reihe A *41*, 81-90.

Rocha, O., Ansari, K., and Doohan, F.M. (2005). Effects of trichothecene mycotoxins on eukaryotic cells: a review. Food Addit Contam *22*, 369-378.

Sanchez, A., Alvarez, A.M., Benito, M., and Fabregat, I. (1997). Cycloheximide prevents apoptosis, reactive oxygen species production, and glutathione depletion induced by transforming growth factor beta in fetal rat hepatocytes in primary culture. Hepatology *26*, 935-943.

Schappert, K.T., and Khachatourians, G.G. (1983). Effects of Fusariotoxin T-2 on *Saccharomyces cerevisiae* and *Saccharomyces carlsbergensis*. Appl Environ Microbiol *45*, 862-867.

Schappert, K.T., and Khachatourians, G.G. (1984). Influence of the membrane on T-2 toxin toxicity in *Saccharomyces spp*. Appl Environ Microbiol *47*, 681-684.

Schappert, K.T., and Khachatourians, G.G. (1986). Effects of T-2 toxin on induction of petite mutants and mitochondrial function in S*accharomyces cerevisiae*. Curr Genet *10*, 671-676.

Schappert, K.T., Koshinsky, H.A., and Khachatourians, G.G. (1986). Growth-Inhibition of Yeast by T-2, Ht-2, T-2 Triol, T-2 Tetraol, Diacetoxyscirpenol, Verrucarol, Verrucarin-a, and Roridin-a Mycotoxins. J Am Coll Toxicol *5*, 181-187.

Scherz-Shouval, R., and Elazar, Z. (2011). Regulation of autophagy by ROS: physiology and pathology. Trends Biochem Sci *36*, 30-38.

Schindler, D., Grant, P., and Davies, J. (1974). Trichodermin resistance--mutation affecting eukaryotic ribosomes. Nature *248*, 535-536.

Schlunzen, F., Zarivach, R., Harms, J., Bashan, A., Tocilj, A., Albrecht, R., Yonath, A., and Franceschi, F. (2001). Structural basis for the interaction of antibiotics with the peptidyl transferase centre in eubacteria. Nature *413*, 814-821.

Schmale, D.G., and Munkvold, G.P. (2009). Mycotoxins in crops: A threat to human and domestic animal health. The Plant Health Instructor *3*, 340-353.

Sesaki, H., Dunn, C.D., Iijima, M., Shepard, K.A., Yaffe, M.P., Machamer, C.E., and Jensen, R.E. (2006). Ups1p, a conserved intermembrane space protein, regulates mitochondrial shape and alternative topogenesis of Mgm1p. J Cell Biol *173*, 651-658.

Sherif, S.O., Salama, E.E., and Abdel-Wahhab, M.A. (2009). Mycotoxins and child health: the need for health risk assessment. Int J Hyg Environ Health *212*, 347-368.

Shifrin, V., and Anderson, P. (1999). Trichothecene mycotoxins trigger a ribotoxic stress response that activates c-Jun N-terminal kinase and p38 mitogen-activated protein kinase and induces apoptosis. Journal of Biological Chemistry *274*, 13985.

Sikriwal, D., Ghosh, P., and Batra, J.K. (2008). Ribosome inactivating protein saporin induces apoptosis through mitochondrial cascade, independent of translation inhibition. Int J Biochem Cell B *40*, 2880-2888.

Sudakin, D.L. (2003). Trichothecenes in the environment: relevance to human health. Toxicol Lett *143*, 97-107.

Suen, D.F., Norris, K.L., and Youle, R.J. (2008). Mitochondrial dynamics and apoptosis. Genes Dev *22*, 1577-1590.

Summerell, B.A., and Leslie, J.F. (2011). Fifty years of Fusarium: how could nine species have ever been enough? Fungal Diversity *50*, 135-144.

Suzuki, S.W., Onodera, J., and Ohsumi, Y. (2011). Starvation Induced Cell Death in Autophagy-Defective Yeast Mutants Is Caused by Mitochondria Dysfunction. Plos One *6*, e17412.

Tainsh, A.R. (1981). Hunger in India: the human factor. International Relations *7*, 1053-1062.

Tamura, Y., Endo, T., Iijima, M., and Sesaki, H. (2009). Ups1p and Ups2p antagonistically regulate cardiolipin metabolism in mitochondria. J Cell Biol *185*, 1029-1045.

Tonshin, A.A., Teplova, V.V., Andersson, M.A., and Salkinoja-Salonen, M.S. (2010). The Fusarium mycotoxins enniatins and beauvericin cause mitochondrial dysfunction by affecting the mitochondrial volume regulation, oxidative phosphorylation and ion homeostasis. Toxicology *276*, 49-57.

Ueno, Y. (1983). Trichothecenes. Chemical, biological and toxicological aspects (Elsevier).

Ueno, Y. (1985). The toxicology of mycotoxins. Crit Rev Toxicol *14*, 99-132.

Ueno, Y., Nakajima, M., Sakai, K., Ishii, K., and Sato, N. (1973). Comparative toxicology of trichothec mycotoxins: inhibition of protein synthesis in animal cells. J Biochem *74*, 285-296.

van Dongen, P.W., and de Groot, A.N. (1995). History of ergot alkaloids from ergotism to ergometrine. European journal of obstetrics, gynecology, and reproductive biology *60*, 109-116.

Visconti, A., Minervini, F., Lucivero, G., and Gambatesa, V. (1991). Cytotoxic and Immunotoxic Effects of Fusarium Mycotoxins Using a Rapid Colorimetric Bioassay. Mycopathologia *113*, 181-186.

Wang, S.Y., Wu, J.H., Ng, T.B., Ye, X.Y., and Rao, P.F. (2004). A non-specific lipid transfer protein with antifungal and antibacterial activities from the mung bean. Peptides *25*, 1235-1242.

Wang, X., Zuo, X., Kucejova, B., and Chen, X.J. (2008). Reduced cytosolic protein synthesis suppresses mitochondrial degeneration. Nat Cell Biol *10*, 1090-1097.

Wang, Z.G., Feng, J.N., and Tong, Z. (1993). Human toxicosis caused by moldy rice contaminated with fusarium and T-2 toxin. Biomedical and environmental sciences : BES *6*, 65-70.

Wannemacher, R., and Wiener, S. (1997). Trichothecene mycotoxins. Medical aspects of chemical and biological warfare, 655–676.

Weigel, D., Ahn, J.H., Blazquez, M.A., Borevitz, J.O., Christensen, S.K., Fankhauser, C., Ferrandiz, C., Kardailsky, I., Malancharuvil, E.J., Neff, M.M., *et al.* (2000). Activation tagging in Arabidopsis. Plant Physiol *122*, 1003-1013.

Westermann, B., and Neupert, W. (2000). Mitochondria-targeted green fluorescent proteins: convenient tools for the study of organelle biogenesis in *Saccharomyces cerevisiae*. Yeast *16*, 1421-1427.

Whittemore, E.R., Loo, D.T., Watt, J.A., and Cotman, C.W. (1995). A detailed analysis of hydrogen peroxide-induced cell death in primary neuronal culture. Neuroscience *67*, 921-932.

Windels, C.E. (2000). Economic and social impacts of fusarium head blight: changing farms and rural communities in the northern great plains. Phytopathology *90*, 17-21.

Wu, M.J., Clarke, F.M., Rogers, P.J., Young, P., Sales, N., O'Doherty, P.J., and Higgins, V.J. (2011). Identification of a Protein with Antioxidant Activity that is Important for the Protection against Beer Ageing. International Journal of Molecular Sciences *12*, 6089-6103.

Yazar, S., and Omurtag, G.Z. (2008). Fumonisins, trichothecenes and zearalenone in cereals. Int J Mol Sci *9*, 2062-2090.

Youle, R.J., and van der Bliek, A.M. (2012). Mitochondrial fission, fusion, and stress. Science *337*, 1062-1065.

Zhang, T., Lei, J., Yang, H., Xu, K., Wang, R., and Zhang, Z. (2011). An improved method for whole protein extraction from yeast *Saccharomyces cerevisiae*. Yeast *28*, 795-798.

Zhang, X., Jiang, L., Geng, C., Cao, J., and Zhong, L. (2009). The role of oxidative stress in deoxynivalenol-induced DNA damage in HepG2 cells. Toxicon *54*, 513-518.

Zhou, H.R., Islam, Z., and Pestka, J.J. (2005a). Induction of competing apoptotic and survival signaling pathways in the macrophage by the ribotoxic trichothecene deoxynivalenol. Toxicol Sci *87*, 113-122.

Zhou, H.R., Jia, Q., and Pestka, J.J. (2005b). Ribotoxic stress response to the trichothecene deoxynivalenol in the macrophage involves the SRC family kinase Hck. Toxicol Sci *85*, 916-926.

Zhu, X., Li, Z., Xu, H., Zhou, M., Du, L., and Zhang, Z. (2012). Overexpression of wheat lipid transfer protein gene TaLTP5 increases resistances to Cochliobolus sativus and *Fusarium graminearum* in transgenic wheat. Functional & integrative genomics *12*, 481-488.